Functional characterization of the *extra petals* mutant in *Cardamine hirsuta*

I n a u g u r a l - D i s s e r t a t i o n

zur

Erlangung des Doktorgrades

der Mathematisch-Naturwissenschaftlichen Fakultät

der Universität zu Köln

vorgelegt von

Evangelos Kouklas

aus Thessaloniki, Griechenland

Köln Juli 2017

Functional characterization of the *extra petals* mutant in *Cardamine hirsuta*

I n a u g u r a l - D i s s e r t a t i o n

zur

Erlangung des Doktorgrades

der Mathematisch-Naturwissenschaftlichen Fakultät

der Universität zu Köln

vorgelegt von

Evangelos Kouklas

aus Thessaloniki, Griechenland

Köln Juli 2017

Berichterstatter: Prof. Dr. Miltos Tsiantis

Prof. Dr. Martin Hülskamp

Prüfungsvorsitz: Prof. Dr. Kay Hofmann

Tag der letzten mündlichen Prüfung:

26.06.2017

Die vorliegende Arbeit wurde am Max-Planck-Institut für Pflanzenzüchtungsforschung in Köln in der Abteilung für

Vergleichende Entwicklungsgenetik (Direktor Prof. Dr. Miltos Tsiantis) angefertigt.

Abstract

A fixed number of petals characterizes the flowers of different plant families. For example, species in the Brassicaceae have four petals, such as the model plant *Arabidopsis thaliana*. An exception to this is the *A. thaliana* relative *Cardamine hirsuta*, which has a variable number of petals between zero and four. To understand which genes control petal number in *C. hirsuta*, a genetic screen was performed for mutants with altered petal number. The *extra petals* (*exp*) mutant was identified as a recessive allele that caused an increase in petal number above four. In addition, *exp* flowers exhibited chimeric floral organs and unfused carpel tips. I found that all petals and petal/sepal chimeras arose from whorl 2 in *exp* flowers. Also, I showed that a mutation in the *C. hirsuta* orthologue of *SPLAYED* (*SYD*) caused the *exp* mutant phenotype. Most importantly, I showed that an artificial microRNA that silenced *SYD* gene expression caused an *exp* phenotype, whereas reintroducing the wild-type *SYD* locus into *exp* mutants rescued the phenotype. *SYD* encodes an ATP-dependent chromatin remodeling factor that activates different pathways during floral development in *A. thaliana*. Similarities between the phenotypes of *syd* mutants in *A. thaliana* and *exp*, suggest that SYD function may be conserved between these two species. In summary, I identified a function for SYD chromatin remodeling complexes in petal number control in *C. hirsuta*, and suggest that this type of regulation is a common component of floral development pathways in the Brassicaceae family.

Zusammenfassung

Eine feste Anzahl von Blütenblättern charakterisiert die Blüten von verschiedenen Pflanzenfamilien. Viele Arten in der Familie von Kreuzblütlern (Brassicaceae) haben vier Blütenblätter, wie die Modellpflanze *Arabidopsis thaliana*. Eine Ausnahme hiervon ist das behaartes Schaumkraut (*Cardamine hirsuta*). *C. hirsuta* ist sehr nah mit *A. thaliana* assoziiert und hat eine variable Anzahl von Blütenblättern zwischen null und vier. Um zu verstehen, welche Gene die Blütenblattzahl in *C. hirsuta* kontrollieren, wurden genetische Screens für Mutanten mit veränderter Blütenblattzahl durchgeführt. Die *extra petals* (*exp*) Mutante wurde als ein rezessives Allel identifiziert, das zu einer Erhöhung der Blütenblattzahl führte. Darüber hinaus zeigten *exp* Blüten chimäre Blumenorgane und unfusionierte Karpellspitzen. Meine Experimente hatten dann gezeigt, dass alle Blütenblätter und Blütenblatt / Sepal-Chimären aus Wirtel 2 in exp Blüten entstanden sind. Außerdem, eine Mutation von *SPLAYED* (*SYD*) ortholog in *C. hirsuta* hatte den exp Phänotyp erzeugt. Weiterhin eine künstliche microRNA (amiRNA) reduzierte die *SYD*-Genexpression und hatte einen ähnlichen Phänotyp erzeugt, während die Wiederherstellung vom Wildtyp-*SYD*-Locus in *exp*-Mutanten den Phänotyp rettete. *SYD* kodiert für einen ATP-abhängigen Chromatin-Remodeling-Faktor, der verschiedene Pathways in Blütenentwicklung von *A. thaliana* aktiviert. Ähnlichkeiten zwischen den Phänotypen von *syd*-Mutanten in *A. thaliana* und *exp*, deuten darauf hin, dass die SYD-Funktion zwischen diesen beiden Spezies konserviert werden kann. Zusammenfassend hatte ich eine Funktion für SYD-Chromatin-Remodeling-Komplexe in der Kontrolle von Blütenblattanzahl in *C. hirsuta* identifiziert und erkannt, dass diese Art von Regulation ein essentieller Bestandteil der floralen Entwicklungswege in der Familie von Kreuzblütlern ist.

Table of contents

Chapter 1

Introduction

1.1 Flowers

Flowers are often the most noticeable part of flowering plants (Angiosperms) due to their visual attraction related to flower shape, size and colour. Flowers were also a key innovation during land plant evolution by creating the opportunity to attract animal pollinators to plants, thus increasing the chances of successful pollen dispersal and cross-pollination (Zhang, L. et al., 2004). The scientific interest in explaining the variability in flowers and their structures started very early, as Goethe in 1790 sought a unity of form in diverse structures (Goethe, 1790). Successively, Sprengel in 1793 reported for the first time that flower parts, like petals, may play roles in multiple functions, such as protecting floral nectar from dilution by rain water, in addition to attracting pollinators (Sprengel, 1793). Angiosperms include at least 260.000 species (Takhtajan, 1997), making it by far the largest and most diverse clade of all land plants. Flowering plants had a great impact in shaping the Earth's biosphere, dominating in most terrestrial ecosystems and human agriculture, creating multiple commercial and industrial food sources for people and livestock. Although the exact age of the Angiosperm clade is still uncertain, significant fossil findings combined with multidisciplinary approaches using phylogenetics and developmental genetics have helped to understand angiosperm origins. Pollen fossils have provided evidence of early angiosperms around 136 million years ago (Frohlich et al., 2007), whereas a combined approach of fossils and molecular data estimate that the angiosperm clade diversified between 150 and 190 million years ago (Magallón et al., 2015). Most angiosperms have floral organs that enclose their reproductive organs called a "perianth". The perianth can be found in diverse forms, colours and shapes, including morphologically similar organs called tepals or distinct perianth organs comprising an outer calyx (sepals) and an inner corolla (petals) (Ronse De Craene, 2007). Petals often are

described as thin, pigmented organs with a single vascular trace and a narrow base; like all floral organs they are evolutionarily derived from leaves (Goto et al., 2001; Pelaz et al., 2000; Ronse De Craene, 2007, 2010). The distinction between sepals and petals is usually functional rather than morphological (Endress, 1994), since sepals protect young buds, while petals function mainly as attractive organs for pollinators. The appearance of flowers and the increased complexity of their reproductive system created a suite of floral traits such as floral architecture, petal colour and shape, scent and nectar associated with the attraction and utilization of a specific group of animals as pollinators by many plant species (Fenster et al., 2004). These floral traits often co-evolved together with the animal species through directional selection towards a phenotypical "match" between them that enhances reproductive success of the plants (Galliot et al., 2006). The transition from abiotic to animal pollination is associated with higher species richness, promoting significantly higher diversification (Dodd et al., 1999; Kay et al., 2006). Diversification of species may be accelerated by coevolution (Thompson, 2005), but since both pollinators and flowers must evolve, this process is often slower than unilateral evolution or pollinator shifts (Harder et al., 2009). An outstanding example of co-evolution is the development of petal nectar spurs in the genus *Aquilegia*, which has been shown to be adaptive for different pollinators, creating abundant inter-and intraspecific petal spur variation (Kramer et al., 2010). A significant evolutionary trend of increasing nectar spur length is observed during directional shifts from bee to bird to hawkmoth pollination, with longer spur length associated with pollinators with longer tongues (Whittall et al., 2007).

The origin of flowers remains an open question since Darwin's time (Darwin, 1859). Despite the constant enrichment of fossil records and rapid technological advances in biological research, several constraints hinder the reconstruction of hypothetical ancestors:

missing links between fossil records and extant angiosperm species, as well as extinctions among early crown clade angiosperms (Angiospermae) (Bateman et al., 2006). Many theories have been presented on how the ancestral angiosperm flower took form, including (1) the Anthophyte theory (Crane, 1985; Doyle et al., 1986), which considers a close relationship between Angiosperms and Gnetales based on a flower-like ovule, although this relationship is not supported by molecular evidence; (2) *Caytonia* – glossopterid model for carpel origin (Doyle, 2008): here molecular data together with the homology of the angiosperm bitegmic ovule with the cupule of glossopterids and Caytonia are taken into account to argue for a common carpel origination; (3) Out-of-male/out-of female theory (Theissen et al., 2002): this theory supports that flowers originated from a male cone via a reduction of B-class gene expression in the upper region of the cone, leading to the development of female structures at the apex; (4) Mostly male model (Frohlich et al., 2000): the origin of the flower was caused by an ectopic translocation of the ovules to the adaxial side of laminar microsporophylls via loss of the LEAFY (*LFY*) homolog (*NEEDLY*); (5) Developmental genetic model (Baum D. A. et al., 2006): LFY is a major player in the origin of the flower, coordinating the expression of B (low LFY expression) and C genes (high LFY expression) along the apex. Although the evolutionary theory of flower origin is still debated, the molecular phylogeny of flowers is well resolved. Molecular phylogenies have placed the base of the angiosperms at *Amborella*, Nymphaeales and Austrobaileyales (ANITA) lines (Barkman et al., 2000; Graham et al., 2000; Mathews, 1999; Parkinson et al., 1999; Qiu et al., 1999; Renner, 1999; Soltis et al., 2000; Soltis, P. S. et al., 1999; Zanis et al., 2002); many characteristics present in these lines, such as the thecal anther organization, ovule organization and to some extent the carpel organization are highly conserved and present in modern angiosperms as well (Endress, 2011).

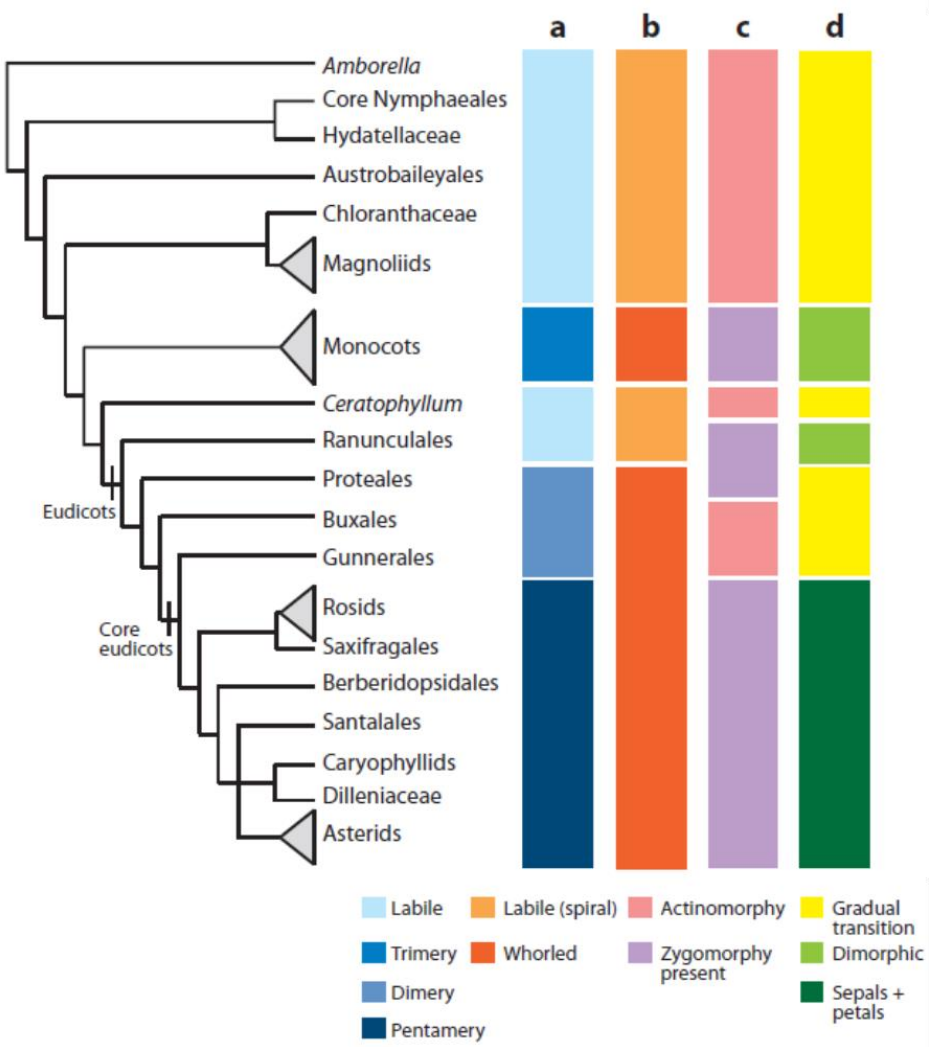

Figure 1: Trends present in angiosperm floral evolution. The dominant characteristics per family are colored in (a) merism, (b) phyllotaxis, (c) symmetry, and (d) dimorphic perianth. In basal angiosperms, it is clear that floral characteristics are more unstable, as seen in (a) and (b). In terms of symmetry (c), zygomorphy is present in monocots and core eudicots, whereas actinomorphy is found more often in basal angiosperms. Flowers with clearly defined petals and sepals (d) are found in core eudicots, but monocots and Ranunculales show a dimorphic perianth; moreover, basal eudicots and basal angiosperms have perianths with a gradual transition between sepals and petals. Figure adapted and edited from Specht et al. (2009). Angiosperm phylogeny from Soltis, D. E. et al. (2008), summarizing Jansen (2007); Moore (2007).

Throughout the evolution of floral form there was an underlying connection between a stable merosity (number of each type of floral organ) and a whorled phyllotaxis (Specht & Bartlett, 2009). For example, comparing a primitive and advanced plant group, Magnoliidae and Asteridae, reveals an evolutionary shift from an unstable organ number arranged in a spiral phyllotaxy towards a fixed, whorled merosity with few organs per whorl (Specht & Bartlett, 2009). In Magnoliidae, the organ number is variable, especially in the stamens and carpels, whereas in Asteridae, floral organ number usually shows a pentamerous pattern (e.g. five sepals, five petals, five stamens and two carpels) (Endress, 1990). Stable merosity is a derived trait of both eudicot and monocot flowers, with the majority of core eudicots displaying fixed pentamerous merosity and the majority of monocots fixed trimerous merosity (Figure 1) (Specht & Bartlett, 2009). Major angiosperm families are often characterized based on key features that include floral organ number. For example, in the Brassicaceae family, the perianth consists of a calyx of 4 distinct sepals and a corolla of 4 distinct petals that are commonly clawed and diagonally disposed. The androecium is tetradynamous, consisting of 4 long inner stamens and 2 short outer stamens.

The life cycle of a plant is divided in two phases: vegetative and reproductive. In order for a plant to produce flowers, it must pass through a vegetative phase of growth, where it maximizes photosynthetic capacity by producing leaves, thus increasing in size. During the transition to reproductive phase, the shoot apical meristem (SAM) that was giving rise to leaves becomes an inflorescence meristem (IM), producing floral meristems (FM) and flowering shoots instead. A predictive, computational model has been proposed that explains the development of different inflorescence types, for example, panicles, which are branching shoots ending in flowers; racemes, which are shoots bearing flowers in lateral positions; and cymes, which are shoots that terminate in flowers and bear lateral branches (Prusinkiewicz et

al., 2007). A key aspect of this model is the continuous variable “vegetativeness”, that characterizes shoot meristem identity at one extreme - high levels of vegetativeness - and flower meristem identity at the other extreme - low levels of vegetativeness (Prusinkiewicz et al., 2007). Based on genetic studies of inflorescence mutants in *A. thaliana*, *LEAFY* is proposed to reduce “vegetativeness” and *TERMINAL FLOWER 1* to increase “vegetativeness”. Together with environmental inputs like variable season length, a plausible model was created that unified the way that genetics and the environment promote a limited range of inflorescence types in a defined ecosystem, giving rise to a variety of floral forms (Prusinkiewicz et al., 2007).

Phyllotaxy refers to the way that shoots and floral organs are placed as they arise from their respective meristems. The most common arrangement of organs in shoot meristems is the spiral phyllotactic pattern and is characterized by the placement of organs into conspicuous spirals. In floral meristems, the organization of floral organs within a flower throughout the angiosperm clade falls in one of the three conserved architectures: whorled, spiral and chaotic, with the majority of the families having a whorled phyllotaxy (Endress, 1987). The whorled phyllotaxy consists of four concentric rings, called whorls. The individual organs within a group arise in short time intervals with each other and therefore appear to be in the same whorl.

The number and positioning of floral organs was already studied extensively by ancient Greeks (Theophrastus, 350 BC- 287 BC). Plant anatomy, taxonomy, development and genetics were centrepiece disciplines of science in the 18th and 19th century (Linnaeus, Goethe, Darwin, Mendel, van Leeuwenhoek, Schleiden etc.); moreover, the term “homeosis”, used to describe the replacement of one organ type by another, was also introduced during this period (Masters, 1869). Modern molecular genetic studies of model plant species like *A. thaliana* and *Antirrhinum majus* allowed scientists to connect genotype to phenotype and define the

molecular genetic pathways that control flower formation. But comparisons between these model species also provided insights about flower evolution and various aspects of flower development. These species offer a variety of advantages, like small genome size, short life cycle of 8 weeks, easy manipulation and genetic transformation and generation of high number of offspring for *A. thaliana*; *A. majus*, on the other hand, is a diploid plant that is easy to cultivate, shows variation in morphology and flower colour, and has a big collection of transposon-induced mutants that was developed during the 20th century (Hudson et al., 2008).

1.2 Structural organization of the *Arabidopsis thaliana* floral meristem

In *A. thaliana*, a member of the Brassicaceae family, flowers were the first parts of the plant where significant molecular discoveries were published (Coen & Meyerowitz, 1990). Careful characterization of the floral growth stages and clonal analysis of floral organs helped to identify exactly how a flower is formed. The most important growth stages are: stage 1, when a flower buttress arises, stage 2 when the flower primordium is formed, stage 3 when sepal primordia appear, stage 5 when petal and stamen primordia start growing, stage 11 when stigmatic papillae arise and stage 13b, when the flower is fully open (Smyth et al., 1990). An *A. thaliana* flower has four sepals, four petals, six stamens and two fused carpels, following a pattern present in the majority of Brassicaceae (Endress, 1992).

The stable floral organ merosity of *A. thaliana* is representative of the Brassicaceae family, since the floral ground plan shows great similarities in uniformity and position of the floral organs between the 340 genera of the Brassicaceae (Al-Shehbaz, 2010; Endress, 1992). The most distinguishable characteristics of the family are a cruciform (cross-shaped) corolla, six

stamens (the outer two short, the inner four longer) and a capsule often with a septum (Franzke et al., 2011). Even so, several genera exhibit great variability in their floral organ number and/or identity (for example *Cardamine*, *Caulanthus*, *Lepidium*, *Streptanthus*) (Al-Shehbaz, 2010), mostly in whorls 2 and 3, where petals and stamens arise.

1.3 *Cardamine hirsuta*: An exception to the uniformity of Brassicaceae floral structure

A. thaliana has been studied extensively as a model species, but more recently several other Brassicaceae species have been used to address various research topics. For example: *Arabidopsis lyrata* and *A. suecica* for self-incompatibility and genome evolution (Josefsson et al., 2006; Kusaba et al., 2001), *Arabis alpina* for perennialism, (Bergonzi et al., 2013), *Capsella rubella* and *C. grandiflora* for self-incompatibility (SI) system (Guo et al., 2009; Sicard et al., 2011), *Capsella bursa–pastoris* for flowering time and floral architecture (Franzke et al., 2011; Hintz et al., 2006; Karley et al., 2008).

Cardamine hirsuta is related to *A. thaliana* and has been established as a genetic system to study comparative development (Barkoulas et al., 2008; Blein et al., 2008; Hay, A. et al., 2006; Hay, A. S. et al., 2014; Pieper et al., 2016; Vlad et al., 2014). It presents the same technical advantages as *A. thaliana*, since it is easy to transform, it is autogamous and has a life cycle of 8 weeks. Importantly, one can exchange genomic loci between the two species by transformation, in order to observe functional divergence of genes and investigate their role in the evolution of form between these related species. The flowers of *C. hirsuta* are very similar to those of *A. thaliana*, with a common floral ground plan of four organ types arranged in whorls in a radially symmetric flower (Hay, A. S. et al., 2014). Two major differences are the absence of lateral stamens and the variable petal number between 0 and 4 in *C. hirsuta*

flowers (Hay, A. S. et al., 2014). Additionally, *C. hirsuta* petals have a shorter base and are more spoon-shaped than *A. thaliana* petals (Hay, A. S. et al., 2014). *A. thaliana* and *C. hirsuta* petals are useful organs to use for genetic studies, since they have a simple morphology and are dispensable for fertility.

The quantitative variation in *C. hirsuta* petal number provides an excellent opportunity to identify natural variation in this trait. QTL (Quantitative Trait Loci) that influence natural variation in *C. hirsuta* petal number have been identified using RIL (Recombinant Inbred Line) populations (Monniaux et al., 2016; Pieper et al., 2016). QTLs were identified that influence both average petal number and its stochastic variation in *C. hirsuta* RILs, showing that although both characteristics of petal number distribution are under genetic control, they remain uncanalized processes (Monniaux et al., 2016; Pieper et al., 2016). Furthermore, these results illustrate the advantage of using non-model species to explore the genetic basis of traits for which no natural variation exists in *A. thaliana*, for example, because of the stable floral organ merosity in *A. thaliana* (Hay, A. et al., 2016).

These studies have underlined that petal number variation is a heritable trait and that many genes affect the phenotype in both positive and negative directions (Monniaux et al., 2016; Pieper et al., 2016). The QTL analysis in both cases has shown that phenotypic variation is not due to developmental constraints inhibiting *C. hirsuta* flowers to have four petals but rather that a polygenic architecture maintains the variable petal number (Pieper et al., 2016). Moreover, QTLs have been found to affect not only the average petal number, but also its standard error between genotypes, either for the whole plant or for a particular time point in the plant's development (Monniaux et al., 2016). The change in phenotypic variability without a change in mean phenotype provides a powerful mechanism for increasing fitness in changing environments (Feinberg et al., 2010).

Interestingly, this trait is not only subject to genetic control, but seems to respond also to environmental cues, as differences in the growth conditions between separate experiments produced petal number variation (Pieper et al., 2016). Furthermore, *C. hirsuta* Ox plants reveal a pattern of elevated or decreased petal number depending on the plant age: the first flowers to open have a relatively high petal number; then, it decreases over time, and finally the last flowers produced show again elevated petal number (Pieper et al., 2016).

One example showcasing the lack of developmental constraints of *C. hirsuta* flowers towards building four petals is the discovery of a recessive allele, called *four petals 2* (*fp2*), that increases the average petal number by 2.0 over the wild-type value when homozygous without any additional changes in floral phenotype (Pieper et al., 2016). This phenotype is evidence that *C. hirsuta* could theoretically produce flowers with four petals and reduce phenotypic variability without influencing multiple physiological traits (Pieper et al., 2016).

The petal number variation occurring in different *C. hirsuta* ecotypes might indicate a relaxation in maintaining structures, like petals, that are not needed for pollination, since the species is predominantly selfing (Hay, A. S. et al., 2014). Hence, this shift may have evolved by neutral drift (Monniaux et al., 2016). Another scenario is that the shift may have been selected as part of the selfing syndrome in *C. hirsuta* to promote efficient selfing, possibly by eliminating petals to delay bud opening and encourage self-pollination (Monniaux et al., 2016).

1.4 Processes influencing petal number

Flower formation occurs through a series of sequential events. Once a flower primordium is initiated at stage 1, a rapid and coordinated cell expansion and division occurs in all three dimensions generating a concentric group of cells that forms the flower primordium, from which all floral tissues are derived (Bossinger et al., 1996; Reddy et al., 2004). This rapid growth over the primordium surface is succeeded by decreased and anisotropic growth in later stages of meristem development (Kwiatkowska, 2006). Floral meristem fate is specified at the flanks of the inflorescence meristem by activation of floral-meristem identity genes e.g. LEAFY (LFY), APETALA 1 (AP1) and simultaneous repression of inflorescence meristem genes e.g. TERMINAL FLOWER1 (TFL1). Then, floral organ identity is specified in four concentric whorls by the combinatorial activity of homeotic genes according to the 'ABC' model (Coen & Meyerowitz, 1990). Next, the homeotic genes activate downstream targets that specify tissue and cell types that constitute the four different floral organs – sepals, petals, stamens and carpels. In the end, the central pool of stem cells that maintains indeterminacy of the floral meristem is gradually reduced and at stage 6, when carpels in whorl four have formed, flower development becomes determinant (Lohmann et al., 2001; Sablowski, 2007). So far, no pathway was discovered to directly control petal number in *A. thaliana*. Instead, several studies show that petal number variation in *A. thaliana* is caused by pathways essential to floral development.

1.4.1 Meristem size

One of the pathways that influences petal number is the regulation of floral meristem (FM) size. Plant meristems are dynamic groups of cells that produce all plant parts. In flowers, a

group of pluripotent cells is responsible for both self-maintaining and setting the floral bauplan, creating the floral organs (Mayer et al., 1998; Steeves, 1989). Expansion or reduction of floral meristem size affects floral organ number, including petals. A core genetic network that regulates the stem cell population size in the shoot meristem involves the homeodomain transcription factor *WUSCHEL* (*WUS*) and the *CLAVATA1/3* (*CLV1/3*) ligand-receptor system (Clark et al., 1996; Laux et al., 1996; Mayer et al., 1998; Schoof et al., 2000).

WUS is expressed in a small central meristematic zone underneath the central zone (Mayer et al., 1998), called the organizing centre. *wus* mutants are characterized by failure to properly maintain meristems and result in defective shoot and flower development (for example, flowers with fewer organs) or no postembryonic growth in severe *wus* alleles (Mayer et al., 1998). The WUSCHEL protein positively regulates the expression of the CLAVATA3 (CLV3) gene in the central zone (CZ) of the meristem (Brand, 2000; Fletcher et al., 1999). CLV3 encodes a small extracellular protein that is processed into a secreted signalling peptide from superficial cell layers (L1 and L2) in the central region (Fletcher et al., 1999; Ni et al., 2006), which binds to the ectodomain of the leucine-rich receptor (LRR) kinase CLAVATA1 (CLV1) in underlying cells (L3 region) (Ogawa et al., 2008). Activation of CLV1 and other related receptor kinases (Kinoshita et al., 2010; Müller, R., Borghi, L., Kwiatkowska, D., Laufs, P., Simon, R., 2006) triggers an intracellular signalling cascade that creates a negative feedback loop by repressing WUS transcription from the CZ of the meristem, restricting its expression to the OC, where continued stem cell and meristem activity is required (Lenhard et al., 2003). Overexpressing *CLV3* or knocking out *WUS* present a similar phenotype, where the stem cell population cannot be maintained, causing the SAM and floral meristems to terminate prematurely (Brand, 2000). In comparison, mutations in any of the *CLAVATA* genes result in stem cells accumulating in the centre of the meristems, failing to restrict *WUS* expression; moreover,

inflorescences grow noticeably larger and flowers form additional organs, in all four whorls (Brand, 2000; Clark et al., 1996; Schoof et al., 2000).

The role of *WUS* in floral meristems is not restricted to regulating the stem cell population, as indicated by the occasional formation of flowers missing stamens and carpels in *wus* mutants (Laux et al., 1996). It was discovered that the region-specific activation of the AGAMOUS (AG) protein is regulated by WUS, inducing formation of stamens and carpels (Lenhard et al., 2001; Lohmann et al., 2001). At the same time, *AG* represses the expression of *WUS* to reduce the size of stem cell populations in floral meristems, creating a double role of *AG*: specification of floral organ identity and determinacy of the floral meristem (Lenhard et al., 2001; Lohmann et al., 2001). Moreover, *WUS* is positively regulated by *SPLAYED* (*SYD*), a SNF2 (Sucrose Non-Fermenting2) class ATPase, by binding to the proximal promoter region of the *WUS* locus, maintaining proper *WUS* transcript levels in its normal expression domain (Kwon et al., 2005). These interactions show that regulating the spatial and/or temporal expression of key transcription-factor-encoding genes like *WUS* is important for SAM maintenance. Additionally, it was demonstrated that *WUS* migrates through plasmodesmata laterally into the differentiating progeny of stem cells rather than via secretion, suggesting that transient *WUS* expression is essential in regulating stem cell number emanating from the niche (Daum et al., 2014; Yadav et al., 2011).

1.4.2 Acquisition of floral organ identity

Floral meristem fate requires the activation of flowering time genes, followed by IM identity genes. Flowering time genes function in four major promotion pathways: long-day photoperiod, gibberellin, autonomous, and vernalisation (Andrés et al., 2012; Jack, 2004;

Pajoro et al., 2014). Ultimately, the flowering time genes control the activity of two mutually repressive types of genes (Ratcliffe et al., 1999): those that specify IM identity and those that specify floral meristem identity. During the plant's switch to reproductive phase, the developmental potential of the SAM acquires the identity of the inflorescence meristem that then gives rise only to floral meristems and flowering branches (Pajoro et al., 2014; Shannon et al., 1991). The maintenance of inflorescence development and repression of the formation of floral meristems is controlled by the IM genes *TERMINAL FLOWER1* (*TFL1*) and *EMBRYONIC FLOWER 1* and *2* (*EMF1*, *2*) that are expressed in the centre of the shoot apex and axillary shoot meristems (Bradley, 1997). Their function is to maintain inflorescence development and at the same time to repress the formation of floral meristems (Bradley, 1997; Chen, L. et al., 1997). In *tfl1* and *emf* loss of function mutants, the inflorescence meristem precociously acquires floral identity, which leads to the production of a terminal flower (Alvarez, J. et al., 1992; Chen, L. et al., 1997; Shannon & Meeks-Wagner, 1991).

Subsequently, two of the floral meristem identity genes, *LEAFY* (*LFY*) and *APETALA1* (*AP1*), specify the lateral primordia to develop as flowers rather than shoots (Jack, 2004). *LFY* is one of the first genes active upon floral transition and its activation is necessary and sufficient to specify floral meristem identity (Weigel et al., 1992; Weigel et al., 1995). It was shown that *lfy* null mutations cause a transformation of the first few flowers into leaves with associated shoots which do not express any of the floral homeotic genes simply because these structures never acquired any floral identity (Huala et al., 1992; Schultz et al., 1991; Weigel et al., 1992). The LFY protein requires several co-factors to set the spatial expression of the floral organ identity genes *APETALA3* (*AP3*), *PISTILLATA* (*PI*) and *AGAMOUS* (*AG*) (Huala & Sussex, 1992; Liljegren et al., 1999; Parcy et al., 1998; Wagner et al., 1999; Weigel et al., 1992). *AP1*, one of the homeotic genes that encodes a MADS-box protein, has an important role in specifying the

floral meristem as well. Strong *ap1* mutants have sepals transformed into bract-like structures that bear ectopic flowers in their axils, making the whole flower a branched inflorescence-like structure (Bowman et al., 1993; Irish et al., 1990).

LFY and *AP1* have partially overlapping roles in specifying floral meristem fate, as *lfy ap1* double mutants show a more complete conversion of flowers into shoots than either single mutant (Bowman et al., 1993; Irish & Sussex, 1990; Schultz & Haughn, 1991; Weigel et al., 1992). These two genes have also overlapping expression patterns, with both being strongly expressed in floral meristems initiating on the periphery of the inflorescence meristem (Mandel et al., 1992; Weigel et al., 1992). LFY protein has been shown to move to adjacent cells, where it activates homeotic target genes, whereas AP1 acts cell-autonomously to activate downstream genes (Sessions et al., 2000). On the contrary, ectopic expression of *LFY* or *AP1* converts the inflorescence meristem to a flower; *35S::AP1* and *35S::LFY* flowers exhibit a terminal flower phenotype similar to that of *tfl1* mutants (Mandel et al., 1995; Weigel & Nilsson, 1995). Finally, it has been shown that *LFY* and *AP1* act redundantly and positively to regulate each other (Liljegren et al., 1999), with LFY directly activating *AP1* to establish floral meristem identity (Kaufmann et al., 2010; Wagner et al., 1999). Although *AP1* and *LFY* are the major floral meristem identity genes, other genes such as *CAULIFLOWER* (Bowman et al., 1993; Kempin et al., 1995), *FRUITFULL* (Ferrandiz et al., 2000; Gu et al., 1998) play secondary roles in specifying floral meristem identity.

After floral meristem initiation, the next step of flower formation is the patterning of concentric rings of different organ identity through activation of the floral homeotic genes. It has been established that floral organ initiation and growth happens in different developmental stages of the flower. Sepal primordia become visible at stage 3, stamen and petal primordia at stage 4, and carpel primordia at stage 5. From stage 6–8, the floral organ

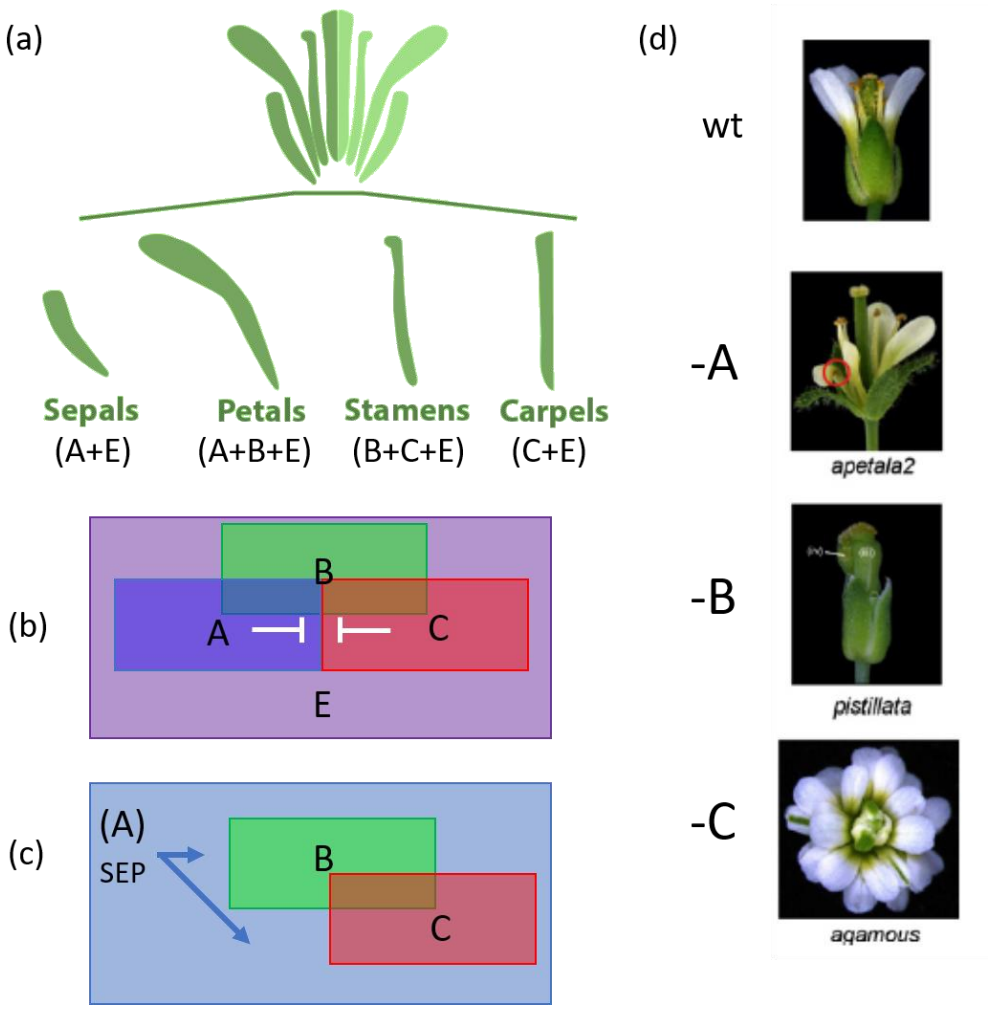

Figure 2: An overview of the ABCE model and its variations. The combinations of ABCE genes that provide the identity of each organ type is depicted in (a), with the addition of the SEPALLATA genes according to Ditta et al. (2004); Pelaz et al. (2000), extending the ABC model of Coen et al. (1990). Class A and class E genes give rise to sepals, A, B and E to petals, the classes B, C and E together provide the stamen identity in whorl 3; finally, C and E class genes give rise to carpels. A schematic overview of the ABCE model is presented in (b). A can either interact E to give rise to sepals or BE and is mutually exclusive with C, whereas B acts only combined with either AE or CE for petals or stamens, respectively. CE gives rise to carpels. An alternative ABC model was presented by Causier et al. (2010) in (c). (A) class genes are placed above B and C genes, since they have multiple functions not directly related to the floral organs, like establishing floral meristem identity and the transition to flowering. The activation of B and C genes and regulation of their domain of expression adds an extra level of functionality for (A) genes and together with the SEP genes control floral organ identity. Section (d) highlights the phenotypes of floral homeotic mutants. On the top panel is a wt *A. thaliana* flower. The apetala2 mutant below lacks A gene function, therefore sepals are converted to carpel-like organs and petals to stamen-like organs (circled in red). The *pistillata* mutant in the third picture has reduced B function, and the organs in whorls 1 and 2 have sepal identity, whereas whorls 3 and 4 have carpels, with organs in whorl 3 encircling those in whorl 4. The *agamous* mutant in the bottom panel lacks expression of the C class gene, resulting to expression of A genes in all whorls, creating sequentially sepals and petals, together with loss of meristem determinacy. Bars in (b) represent repression, and arrows in (c) activation. Panel (a) edited from Illustrations (2017). Panel (d) edited from Causier et al. (2010).

primordia enlarge and begin to differentiate. From that stage on, rate and orientation of cell division of each organ type seems to be controlled by the homeotic genes, creating a distinct histological and morphological profile (Bowman, 1994; Jenik et al., 2000; Smyth et al., 1990).

The floral homeotic mutants *agamous* (*ag*), *pistillata* (*pi*), *apetala1* (*ap1*), *apetala2* (*ap2*) and *apetala3* (*ap3*) in *Arabidopsis* and *plena (ple)*, *globosa (glo)*, *squamosa (squa)*, *deficiens (def)* in *Antirrhinum* were among the first mutants to be characterized in detail in these model plant species. The flowers of *ap2* plants contain carpels in the positions of sepals and stamens in the positions of petals (Figure 2d), *ap3* and *pi* flowers show homeotic transformations of petals into sepals and stamens into carpels (Figure 2d). *ag* flowers form petals in place of stamens and sepals in place of carpels but also are indeterminate and continue to produce new sepals and petals from the centre of the meristem, where carpels arise (Figure 2d). These complementary mutant phenotypes were interpreted by the ABC model of floral organ identity (Coen & Meyerowitz, 1990). It was proposed that there are three regulatory groups of genes: A class is AP1 and AP2, B is AP3 and PI and C is AG. The combination of those groups defines the organ identity in each whorl. For example, A group function is responsible for sepal initiation in whorl 1, A and B are responsible for petal initiation in whorl 2, B and C genes are responsible for stamen initiation in whorl 3 and C function alone is responsible for carpel initiation in whorl 4 (Figure 2a). The initial model was based on genetic experiments of single and higher order mutants, but new findings are constantly improving the regulatory network of floral organ identity. For example, one important aspect of the model is the mutual antagonism between class A and C gene activity (Gustafson-Brown et al., 1994). In the absence of C class gene expression, A class gene expression expands into the domain of C. The initial model had laid down the foundations to understand the genetic network of floral organ identity. Initially, several questions have been raised and therefore alternative theories were

proposed about the order of interactions between ABC genes. One of them, the (A)BC model, stated that A-genes have multiple functions in the flower; they activate B and C function genes and regulate their expression domains, but also have roles in establishing floral meristem identity (Figure 2c) (Causier et al., 2010; Schwarz-Sommer et al., 1990). Therefore, B and C genes do not have any functional consequences when expressed outside of their native domain (Krizek, B. A. et al., 1996; Mizukami et al., 1992; Pelaz et al., 2000), because they lack the floral meristem environment (provided by A genes) to putatively convert shoots into flowers (Causier et al., 2010). Nevertheless, although the partial functional redundancy of AP1 with CAL and FUL in determining floral meristem identity is probably conserved over long evolutionary time (Smaczniak et al., 2012a), AP1 has transcriptional activation domains that are absent in PI, AP3 and AG (Honma et al., 2001), allowing the creation of higher order complexes, confirming the ABC model hypothesis.

During the 1990s, ABC class genes were cloned and functionally characterized (Goto et al., 1994; Jack et al., 1992; Jofuku et al., 1994; Mandel et al., 1992; Yanofsky et al., 1990). In the 2000s, the model was revised and expanded by adding another class of MADS-box genes, the SEPALLATA (SEP) 1/2/3/4 (class E) genes, creating the ABCE model (Figure 2b). Although this family of genes was identified to have sequence similarity with AG and was named AGAMOUS-LIKE (AGL) very early (Ma et al., 1991), their functional characterization came almost a decade after (Pelaz et al., 2000). On the one hand, single or double mutants for *SEP1*, *SEP2*, *SEP3* yield flowers indistinguishable from wild type. On the other hand, *sep1*;*sep2*;*sep3* triple mutant phenotype is strikingly similar to *bc* (*ap3*;*ag*/*pi*;*ag*) double mutants (Bowman et al., 1991), thus suggesting that the three SEP genes are functionally redundant and important in determining three of the four floral organs: petals, stamens, and carpels (Honma & Goto, 2001; Pelaz et al., 2000). The outlier of the *AGL* family, *AGL3* (*SEP4*), which is expressed in

vegetative as well as flower tissues (Ma et al., 1991) was considered as a good candidate to act redundantly with the rest of the *SEP* genes, based on their high sequence similarity in the MADS box domain and their similar expression patterns in the floral meristem (Ditta et al., 2004; Ma et al., 1991). Indeed, the conversion of sepals into leaf-like organs in the *sep1*;*sep2*;*sep3*;*sep4* quadruple mutant indicates that *SEP4* contributes to sepal identity (Ditta et al., 2004).

Four out of five genes that constitute the initial ABC model (*AP1*, *AP3*, *PI* and *AG*) have been characterized as MADS box (name coming from founding members: MCM1, AGAMOUS, DEFICIENS and SRF, in yeast, *A. thaliana*, *Antirrhinum* and humans, respectively) family of transcription factors and are expressed in spatially restricted domains (Goto & Meyerowitz, 1994; Jack et al., 1992; Mandel et al., 1992; Yanofsky et al., 1990). All four genes belong to the MIKC type of MADS box family, which have a characteristic modular structure. From the N to the C terminus of the protein, four characteristic domains can be identified: the MADS-box (M), intervening (I), keratin-like (K), and C-terminal (C) domains (Parenicova, 2003). The MADS-box is a DNA binding domain of 58 amino acids that binds DNA at consensus recognition sequences known as CArG boxes [CC(A/T)6GG] (Hayes, T. E. et al., 1988; Riechmann et al., 1996). Experiments in yeast two-hybrid assays have already shown that MADS transcription factors in both *Antirrhinum* (Davies et al., 1996), and *A. thaliana* (Fan et al., 1997) can form heterodimers *in vivo*. In both cases, it was proposed that the K domain, which is characterized by a coiled-coil structure, facilitates the dimerization of MADS-box proteins (Parenicova, 2003). These findings agree with the “quartet” model, which was proposed in 2001 to explain how the ABCE gene products might function together (Theissen et al., 2000; Theissen et al., 2001). The model suggests that floral organs are specified by combinatorial protein interactions of ABCE-class MADS-domain transcription factors, which are thought to assemble

into organ-specific quaternary protein complexes in regulatory regions of target genes. Recent experiments have shown that MADS tetramers can bind to a DNA fragment that contains two CArG box sequences, creating heteromeric higher-order MADS-domain protein complexes that exist *in planta* (Melzer et al., 2009; Smaczniak et al., 2012b).

The second A class gene, *AP2*, is not a MADS box gene, but encodes a transcription factor of a plant-specific gene family (*AP2*/*EREBP*) with diverse functions (Riechmann et al., 1998). *AP2* contains two copies of a 68-amino acid direct repeat that is called AP2 domain (Jofuku et al., 1994). Normally, one would expect the expression pattern of an A class gene to be restricted to whorls 1 and 2. Surprisingly, *AP2* mRNA was initially found in all four floral whorls throughout flower development (Jofuku et al., 1994) although this was later revised and *AP2* expression was shown to be restricted to whorls 1 and 2 (Wollmann et al., 2010). In contrast to *ap1*, strong *ap2* mutants never produce petals, suggesting that *AP2* is necessary for the specification of petal identity, but also sometimes show defects in whorl 3 and 4 as well (Bowman et al., 1991). Moreover, in *ap2* mutant flowers, *AG* RNA is present in the organ primordia of all floral whorls which indicates that these AP2 functions to repress AG in whorls 1 and 2 (Drews et al., 1991). Interestingly, new evidence show that *AP2* is negatively regulated by the micro-RNA miR172 (Chen, X., 2004). Flowers from transgenic lines that overexpress miR172 resemble *ap2* flowers (Bowman et al., 1989; Drews et al., 1991); moreover, lines that overexpress micro-RNA resistant version of *AP2* resemble strongly *ag* mutant flowers, with petals in whorl 3 and loss of floral meristem determinacy (Chen, X., 2004). These findings, together with the transient overlap of *AP2* and miR172 RNAs support the theory that miR172 regulates AP2 targeting its mRNA for degradation and constrains its expression towards the outer whorls of the flower (Wollmann et al., 2010). The same model proposes that the

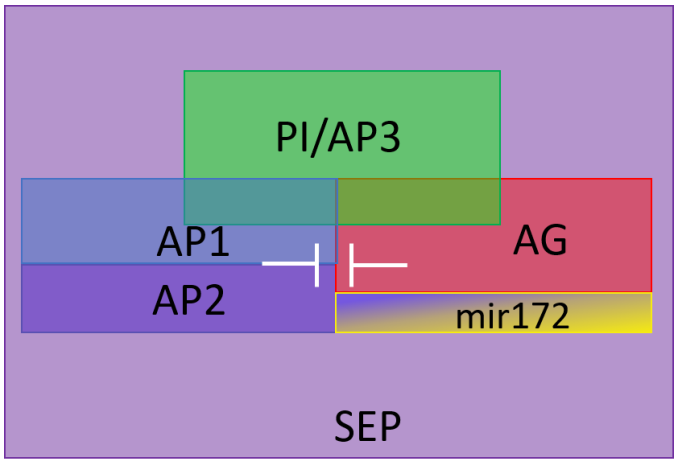

Figure 3: Schematic representation of the mir172 role in regulating floral organ identity. AP1 and AG repress one another, but AP2 and AG are expressed in balance within the flower, since mir172 targets AP2 mRNA for degradation in the inner whorls.

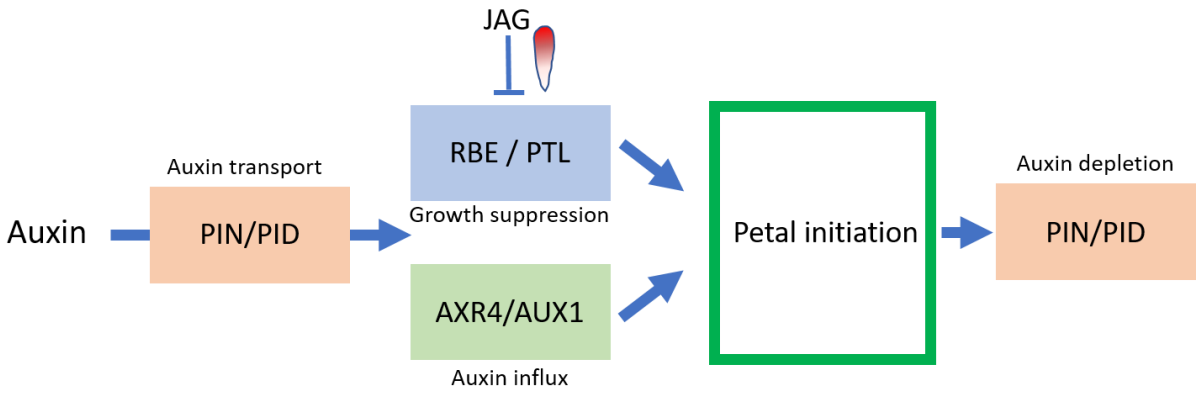

Figure 4: Model for petal initiation and growth based on Lampugnani et al. (2013). Three pathways are required for petal initiation: First, the auxin transport/auxin depletion pathway of PIN/PID that is responsible for transporting auxin to local auxin maxima and depleting auxin after organ initiation. Secondly, the partially complementing pathways of RBE/PTL that suppresses growth adjacent of the petal initiation zone and AXR/AUX1 pathway that is responsible for auxin influx to the local auxin maxima. JAGGED is repressing PTL in the distal petal area, highlighted in red, to create a second auxin maxima growth along the proximal-distal axis. Arrows represent activation, and bars represent repression.

decision whether stamens or petals develop is based on the balance between *AP2* and *AG* activities, rather than the two being mutually exclusive (Figure 3) (Wollmann et al., 2010).

Non-MADS proteins were also identified as interaction partners of plant ABC MADS proteins. *SEP3* was found to be a component of a ~670 kDa complex, much larger than the predicted size of a MADS tetramer (Smaczniak et al., 2012b). Amongst proteins that were consistently enriched in immunoprecipitation (IP) datasets of all MADS-domain proteins, several classes of nucleosome-remodelling factors have been found, including the histone demethylase RELATIVE OF EARLY FLOWERING 6 (REF6), the SWI/SNF (SWItch/Sucrose Non-Fermentable) ATPases BRAHMA (BRM) and SPLAYED (SYD), the CHD (Chromodomain/Helicase/DNA binding domain) remodeller PICKLE (PKL), as well as the ISWI (Imitation SWItch)-type remodellers CHROMATIN REMODELING 4 (CHR4), CHR11, and CHR17. The transcriptional corepressors SEUSS (SEU) and LEUNIG-HOMOLOG (LUH) were also identified as parts of MADS protein complexes (Smaczniak et al., 2012b). These findings support the hypothesis that floral MADS-domain proteins are part of large complexes or structures *in planta* and that probably the MADS tetramers act in combination with other transcription factors to regulate expression (Smaczniak et al., 2012b). This hypothesis suggests that MADS complexes can recruit multiple proteins for highly specific and dynamic targeting of various downstream genes. Moreover, constant enrichment of immunoprecipitations with chromatin remodelling factors supports the theory of mechanistic control of MADS-domain proteins target genes by modification of the chromatin states (Wagner et al., 2002).

1.4.3 Floral organ boundaries

In *A. thaliana* and in most Brassicaceae, each floral organ is distinctively separated from another. These zones of separation between organs are called boundary domains and are important for flower formation (Aida, M., Tasaka, M., 2006); for example, shifts in boundary size may cause an increase or decrease of floral organ numbers due to available space.

Sector boundary analysis of meristem surface cells has shown that sepals and carpels are initiated from eight cells, stamens from four cells, and petals from two cells (Bossinger & R., 1996). These cells are characterized as the founder cells of floral organs. Cell proliferation in the flower is divided into two stages: until floral stage 6, regulation of cell divisions is dependent on the position of cells in the FM, but later the patterns of cell proliferation are dictated by the identity of the developing organs (Jenik & Irish, 2000). In the end, the final fate of cells is dependent on their position, not their linage (Jenik & Irish, 2000). Despite that, the mechanism (or mechanisms) controlling how cells attain their fate in a morphologically undifferentiated floral meristem is an open question that has been difficult to address due to lack of molecular markers that label founder cells.

The major group that is involved in boundary formation in both shoot apical meristem and developing flowers is the *CUP-SHAPED COTYLEDON* (*CUC*) gene group, members of the NAC (NAM, ATAF1, -2, and CUC2) gene family. The three *CUC* genes, *CUC1*, *CUC2* and *CUC3*, have specific expression patterns and partially redundant functions in shoot meristem maintenance, lateral organ separation, and floral organ separation by repressing growth (Aida, M. et al., 1997; Vroemen, 2003). *cuc1*;*cuc2* double mutant seedlings completely lack an embryonic SAM and the two cotyledons are fused along both edges to form one cup-shaped structure (Aida, M. et al., 1997). In addition, adventitious shoots regenerated from mutant

calli form flowers in which sepals and stamens are severely fused (Aida, M. et al., 1997). *CUC1* and CUC2 mRNAs are degraded by miR164 (Baker et al., 2005; Laufs et al., 2004; Mallory et al., 2004). A mutant allele of MIR164C called *early extra petals1* (*eep1*) causes extra petals in approximately the first ten flowers on the inflorescence and smaller, more widely spaced petals, probably because of larger boundaries between organs of the same whorl (Baker et al., 2005). Overexpression of MIR164C results in flowers very similar to those of *cuc1*;*cuc2* double mutants; transgenic lines expressing miR164-resistant versions of *CUC1* and *CUC2* result in flowers resembling *eep1* mutants (Baker et al., 2005; Laufs et al., 2004; Sieber et al., 2007). These results highlight the importance of *CUC* genes and their negative regulator, miR164 to maintain boundaries between organs. As illustrated by the CUC-miR164 pathway, boundaries play a dual role in separating and maintaining meristem and organ domains, and cells in these regions express unique genes that reduce cell division (Rast et al., 2008).

Since boundaries between whorls and between organs are crucial for floral development, additional genes also control boundary formation. Cells in these boundaries are distinctly narrow and elongated with low proliferation rates (Aida, M., Tasaka, M., 2006). Several other genes have also been identified being active in inter-whorl and intra-whorl boundary regions of the floral meristems. One of the genes is called *PETAL LOSS* (*PTL*) and functions to restrain size of the inter-sepal zone during early flower development by repressing proliferation in the inter-sepal boundary regions. *ptl* flowers show reduced number of petals and basally fused sepals, a characteristic enhanced in *ptl;cuc* double mutants; additionally, the inter-sepal zones are enlarged compared to wild type (Griffith et al., 1999; Lampugnani et al., 2012). Accordingly, ectopic expression of *PTL* in the flower results in strong growth inhibition as evidenced by missing or dramatically reduced floral organs (Brewer et al., 2004). The sepal fusion phenotype of *ptl* mutant flowers may thus result from increased cell proliferation in the

inter-sepal zones. *PTL* influences petal development indirectly, perhaps through interference with a mobile petal-initiation signal or movement of the PTL protein (Brewer et al., 2004; Lampugnani et al., 2012). These findings, together with the fact that crosses of *ptl* with a B class mutants show no petal increase in comparison to *ptl* plants, support the hypothesis that the mechanism of *PTL* regulation is affecting the second whorl and not petals *per se* (Brewer et al., 2004). The discovery of *PTL* has led to understanding the enhanced role of boundary formation in petal number control. Firstly, it was shown that CUC1/2 act as suppressors of growth in the region between sepals, evident by the sepal fusion present in the mutant phenotype, thus reducing the size of available space for petal initiation(Lampugnani et al., 2012). The reverse effect of increased space is observed in *eep1-1* mutants, where more space between sepals leads to more petals, whereas in *ptl* mutants, the spatial constraint comes from the reduction of cells in the small area between the inter-sepal zone and the petal initiation zone (Baker et al., 2005; Lampugnani et al., 2012). The combination of the above-mentioned mutants leads to a widened inter-sepal zone due to increased CUC activity; also, the petal initiation zone is widened radially through loss of PTL function, so that multiple petals in a row can arise from the same corner, where normally one petal is positioned (Griffith et al., 1999; Lampugnani et al., 2012).

Likewise, the *RABBIT EARS* (*RBE*) gene encodes a C2H2-type (ERF, Ethylene Response Factor) zinc finger protein and is involved in defining second whorl boundaries. It is specifically expressed in petal primordia during early stages of petal development (Krizek, B. A. et al., 2006; Takeda et al., 2004). In *rbe* loss of function mutants, underdeveloped petals are formed in whorl 2, and sometimes petals are replaced by filaments or staminoid organs, and adjacent sepals occasionally fuse (Krizek, B. A. et al., 2006; Takeda et al., 2004). The defects observed in the second whorl of *rbe* mutants result from ectopic expression of AG in second-whorl cells

(Krizek, B. A. et al., 2006). Moreover, it has been established that *RBE* has another role in the inter-sepal boundary pathway by promoting the action of *CUC1* and *CUC2* boundary genes through direct repression of their negative regulator *EARLY EXTRA PETALS1* (*EEP1*) (Huang et al., 2012).

1.4.4 Organ polarity genes

Lateral organs that initiate on the flanks of shoot and floral meristems share many pathways that are crucial for their development. For example, all lateral organs, including petals, have axes of polarity that are patterned early in development. Mutations in organ polarity genes often influence the number and morphology of lateral organs such as petals.

Study of petal development combined with clonal analysis has shown that petals have anisotropic growth along the proximodistal axis, with a broad polarity organizer located at the distal part (Sauret-Güeto et al., 2013). *A. thaliana* petals have distinct adaxial/abaxial surfaces; the abaxial petal cells have wavy epicuticular ridges, whereas the adaxial cells have a conical shape and straight epicuticular ridges. The adaxial and abaxial polarity of lateral organs is regulated by three main gene families: the class III homeodomain/leucine zipper (HD-ZIP) genes *PHABULOSA* (*PHB*), *PHAVOLUTA* (*PHV*), *CORONA* (*CRN*), *ARABIDOPSIS THALIANA HOMEOBOX 8* (*ATHB8*) and *REVOLUTA* (*REV*), members of the *KANADI* (*KAN*) gene family and members of the *YABBY* (*YAB*) gene family (Eshed et al., 2001; McConnell et al., 2001; Prigge et al., 2005; Sawa et al., 1999a; Siegfried et al., 1999).

Class III HD-ZIP genes control the adaxial polarity of lateral organs; their expression pattern was analysed mainly in leaves, but phenotypical data suggest that may be expressed in the adaxial side of floral organs as well (McConnell et al., 2001; Otsuga et al., 2001; Prigge et al., 2005). Members of the family have different effects in floral organ number; 12% of the mutant

rev-6 flowers present limited set of flower organs and a defective flower meristem (Otsuga et al., 2001), whereas removing *PHV* in *rev;phv* double mutant results in tiny filamentous structures instead of flowers with no meristem activity (Prigge et al., 2005). The antagonistic relationship between PHB, PHV and REV with CRN and ATHB8 is highlighted in the quadruple *rev;phv;can;athb8* mutant, where flowers contain sepals, petals and stamens (Prigge et al., 2005). Besides their function in polarity, the increased number of floral organs in each whorl found in both *phb;phv;cna* triple mutant and *clv* mutants, indicates a putative correlation between stem cell maintenance and polarity in regulating meristem function (Prigge et al., 2005).

Next, the KANADI genes (KAN1-4) belong to a subclass of the plant-specific GARP (name originates from: GOLDEN protein, *Zea mays*; ARR proteins, *A. thaliana;* and the Psr1 protein, *Chlamydomonas*) family of transcription factors and is the main group of genes determining the abaxial side of all lateral organs, including petals (Eshed et al., 2001; Eshed et al., 2004; Kerstetter et al., 2001). Although single *kan1* mutants do not have a dramatic change in morphology, when combined with *kan2* the mutants reveal filamentous organs in both whorls 1 and 2, with petals showing conical cells on both sides, a characteristic of the adaxial petal side (Eshed et al., 1999; Eshed et al., 2001).

Members of the YABBY family also determine the abaxial side of lateral organs (Alvarez, J., Smyth, D. R., 1999; Bowman et al., 1999; Sawa et al., 1999a; Sawa et al., 1999b; Siegfried et al., 1999). *FILAMENTOUS FLOWER* (*FIL*), *YABBY2* (*YAB2*) and *YABBY3* (*YAB3*) are all expressed on the abaxial side of lateral organ primordia, although expression levels are different for each gene (Siegfried et al., 1999). Mutations in *FIL* result in a dramatic reduction in petal number (Sawa et al., 1999a), and construction of higher order mutants abolishes petal

development completely, due to high functional redundancy between *YABBY* gene family members (Siegfried et al., 1999).

These gene families regulate lateral organ polarity, and genetic interactions indicate that *KANADI* activity might act as a mediator between *PHB* and *YABBY* activities. In leaf development, the adjacent domains of adaxial and abaxial polarity are also required for lamina outgrowth (Waites et al., 1995). However, the precise relationships between these pathways in lateral organ development are unclear.

Apart from shared pathways expressed in both leaves and floral organs, additional flower-specific players have been identified. SEUSS (SEU) and LEUNIG (LUG) have been initially identified as transcriptional repressors of *AG* in developing sepals and petals for proper organ identity specification (Franks et al., 2002; Liu, Z. et al., 1995; Sridhar et al., 2004). Further investigation has extended SEUSS and LEUNIG function to regulating petal polarity along the adaxial/abaxial axis by enhancing the effects of *PHB* and *FIL*, thus influencing cellular growth of the petal blade (Franks et al., 2006). Another important factor in the interplay between floral organ polarity and number is the AP2/ERF-type transcription factor AINTEGUMENTA (ANT). In single *ant* mutants, petal number is reduced but organ polarity is not severly disrupted; however, additional mutations in one or more *YABBY* genes produce enhanced polarity defects (Nole-Wilson et al., 2006). A working model proposes that ANT acts in combination with FIL to promote organ polarity by upregulating *PHB*, but also to upregulate *AP3* (Nole-Wilson & Krizek, 2006). Furthermore, *ant* mutants fail to produce petals in an auxin-depleted background, connecting ANT with polar auxin transport and floral organ patterning (Krizek, B., 2009).

1.4.5 Auxin distribution

Many of the pathways mentioned in previous sections have been genetically connected with the mobile phytohormone auxin (the predominant form of which is indole-3-acetic acid; IAA). Auxin is a major coordinating signal in regulation of plant development as it triggers organ initiation at the periphery of the meristem (Vernoux et al., 2000). In *A. thaliana*, polar transport of auxin controls flower formation and differentiation, as shown by auxin-related mutants and their flower morphology (Bennett, S. R. M. et al., 1995; Oka et al., 1999; Okada et al., 1991; Reinhardt et al., 2000). Moreover, increased auxin levels mark the sites for positioning of floral organ primordia and local application of auxin is sufficient to initiate flower formation in the shoot apex (Heisler et al., 2005; Reinhardt et al., 2000). Various mutations in auxin biosynthesis, transport, and response have a noticeable effect on petal number (Cheng et al., 2006; Okada et al., 1991; Pekker et al., 2005; Sessions et al., 1997), but the initial signal driving auxin to establish petal founder cells is still an open question.

Mutations in the auxin signalling component *ARF3/ETTIN* (*ETT*) show elevated petal number in *A. thaliana*. The AUXIN RESPONSE FACTOR (ARF) gene family are transcriptional regulators of auxin response genes and interact with Aux-IAA genes, which are repressors of auxin-inducible genes (Vernoux et al., 2010). ARFs can be either activators (Q-rich ARFs) or repressors of transcription; they usually form homo- and heterodimers both within and between ARFs and Aux-IAAs (Leyser, 2006). *ett* mutants show increased number of both sepals and petals, a decrease in stamen number, partial loss of abaxial identity in petals, and apical-basal patterning defects in the gynoecium (Pekker et al., 2005; Sessions et al., 1997). Double *ett-1;arf4-1* mutants have a similar phenotype to single *ett* alleles, indicating that the genes are functionally redundant (Pekker et al., 2005). ETT seems to have diverse functions in flower development: initially, it serves as an essential intermediary for the gradual establishment of

abaxial identity initiated by KAN (Pekker et al., 2005). Secondly, ETT probably functions to impart regional identity in floral meristems that affects perianth organ number spacing, stamen formation, and regional differentiation in stamens and the gynoecium (Sessions et al., 1997), probably by mediating auxin responses at the promoters of auxin regulated genes (Kim et al., 1997; Ulmasov et al., 1997).

Mutations in the auxin synthesis pathway disrupt *A. thaliana* petal number as well. IAA biosynthesis occurs mostly through a tryptophan (Trp)-dependent pathway and consists of four parallel and partly interdependent pathways (Vernoux et al., 2010). The *YUCCA1* (*YUC1*) gene was identified as a mutant overproducing auxin and encodes a flavin monooxygenase-like enzyme that appears to oxidize tryptamine (TAM) to N-hydroxytryptamine (Zhao, 2001). Arabidopsis has 11 *YUC* genes, and *yuc* multiple knockout mutants cause local auxin deficiencies. Expression patterns of different *YUC* genes vary, but all show a spatiotemporal restriction within the flower rather being than ubiquitously expressed (Cheng et al., 2006). Triple and quadruple *yuc* mutants have a dramatic decrease in petal number together with abolishment of the reproductive organs (Cheng et al., 2006). The mutant traits signify the importance of local auxin biosynthesis for floral meristem establishment and floral organ initiation, since different *yuc* combinations result in different floral phenotypes (Cheng et al., 2006).

The first characterized gene involved in auxin signalling was the efflux carrier PIN1, a member of the *PIN* (*PIN-FORMED*) family, consisting of eight genes (Friml et al., 2002a; Friml et al., 2003; Friml et al., 2002b; Müller, A. et al., 1998; Okada et al., 1991). In *A. thaliana*, auxin transport is mediated by PIN auxin efflux proteins that transport auxin across membranes, as well as the auxin influx carriers AUXIN RESISTANT1 (AUX1) and its paralogs, that act to stabilize auxin gradients correlated to PINs (Bainbridge et al., 2008; Bennett, M. J. et al., 1996; Friml,

2003; Friml et al., 2003). When *PIN1* is mutated, plants sometimes carry pin-shaped inflorescence meristems without flowers, but the sporadical flowers initiated in various mutant alleles display an increase in petal number; conversely, auxin inhibition in wild-type *A. thaliana* plants results in *pin1*-like phenotypes (Bennett, S. R. M. et al., 1995; Oka et al., 1999; Okada et al., 1991). Additionally, *pin3* and *pin7* loss-of-function mutants have flowers with fused petals, no stamens, and occasionally no sepals (Benková et al., 2003). The importance of PIN1 is depicted by its central role in various computational models generated to explain shoot apex morphogenesis and phyllotactic patterning (Benková et al., 2003; Friml, 2003; Jönsson et al., 2006; Reinhardt et al., 2003; Smith et al., 2006). The molecular data and mathematical models show that PIN1-mediated transport generates localized auxin maxima that are responsible for outgrowth of leaf and other organ primordia (Vernoux et al., 2010; Vernoux et al., 2000).

While most computational models addressed auxin-based morphogenesis in shoot meristems, few addressed the role of auxin in floral meristems, specifically in floral organ initiation. One study used live imaging of auxin sensors and various genes involved in flower primordium development, to illustrate how auxin dynamics influence the specification of boundary domains, organ polarity axes, and sites of primordia initiation (Heisler et al., 2005). Establishment of floral primordia is correlated with PIN1 polarity in two stages: firstly, PIN1 drives auxin toward cells forming a primordium; secondly, PIN1 polarity is reversed in cells surrounding an older adjacent primordium (Heisler et al., 2005). Additionally, CUC2 at first activates SHOOT MERISTEMLESS (STM) expression, a gene required for meristem formation and maintenance (Edrizzi et al., 1996), and in later stages of primordia development is co-expressed with STM in a region of repressed growth and low auxin activity at the meristem boundary. Moreover, PIN1 expression is adaxially located from the STM expression domain,

directed toward the meristem and away from the primordium (Heisler et al., 2005). Finally, during primordium initiation, PIN1 expression also creates a domain between abaxial and adaxial cell identities, where REV and FIL are expressed asymmetrically relative to PIN1 (Heisler et al., 2005). This analysis of multiple pathways depicts the complexity of floral meristem initiation.

1.5 What limits petal number?

The number of petals per flower is a robust phenotype, compared to other phenotypes, like the number of leaves or branches produced per plant. *A. thaliana* flowers produce four petals in a manner that is robust to genetic or environmental variation. However, the genetic control of petal number is not as well understood as shown by the investigation of processes influencing petal organogenesis, identity and polarity that were described in the sections above.

First of all, a conceptual model has been proposed to explain how auxin controls petal initiation (Figure 4) (Lampugnani et al., 2013). The authors disrupted petal initiation using the *ptl* mutant and screened for enhancers that eliminated petals. In this way, they revealed an important role for the auxin influx gene *AUX1* in petal initiation. Genetic analysis of mutants involved in both auxin influx and auxin efflux, and the petal initiation mutants *ptl* and *rbe*, allowed the authors to place these components in a petal initiation pathway (Lampugnani et al., 2013). Moreover, study of the cross between the weak *pin1-5* allele and *aux1* showed a direct role for AUX1 in petal initiation, a role that is compromised by the loss of PIN1 function (Lampugnani et al., 2013). In summary, according to this model, petal initiation requires three different pathways: (a) PTL-RBE (regional growth suppression), (b) AXR4-AUX1 (auxin influx)

pathways are used to generate localized auxin maxima, partially complementing one another, and (c) PIN-PID pathway, transporting and depleting auxin to and from local petal initiation zones (Lampugnani et al., 2013). Even when two out of three pathways are knocked out, auxin is still -in part- circulating around the cells where petals initiate, resulting in petal number increase (Lampugnani et al., 2013). Recently, additional genes have been added to the existing model. JAGGED (JAG), a zinc finger transcription factor expressed during the emergence of all shoot organs (Dinneny et al., 2004; Ohno et al., 2004; Schiessl et al., 2012), promotes distal enhancement of petal growth (Sauret-Güeto et al., 2013). The direct repression of PTL by JAG in the distal petal area may increase distribution and activity of auxin in later stages of petal development (Sauret-Güeto et al., 2013). In conclusion, petal number can be limited by the local auxin distribution that is controlled by genes that are expressed at the petal initiation zones, thus making this auxin-based morphogenesis specific for petals.

A second category of genes include those that do not directly regulate petal organogenesis, but regulate floral meristem development, thus affecting petal number indirectly. One example is mutants of the bZIP transcription factor PERIANTHIA (PAN), which increases petal number but also other floral organs in whorls 1-3 (Chuang et al., 1999; Das et al., 2009; Maier et al., 2009; Running et al., 1996). The first mutant alleles, *pan-1* and *pan-2* came from a T-DNA mutagenized population and show elevated number of sepals, petals and stamens, transforming the flowers from tetramerous to pentamerous (Chuang et al., 1999; Running & Meyerowitz, 1996). Creation of double and triple mutants with the homeotic genes has shown that *PAN* acts independently of the petal identity genes to specify organ number and organ initiation patterns, placed downstream of *LFY* and *AP1* (Running & Meyerowitz, 1996). Its wide expression pattern extends to proliferating cells of the SAM, suggesting a more general (or dual) role of PAN that is not constricted to floral organ number control (Maier et

al., 2009). This hypothesis was strengthened by studies showing that PAN regulates stem cell fate by directly controlling *AG* expression and that WUS is able to ectopically activate *PAN* expression (Das et al., 2009; Maier et al., 2009). The results create a putative feed-forward loop, where WUS activates both *PAN* and *AG*; in later stages, accumulation of AG protein suppresses *WUS* transcription, which in turn leads to decreased PAN activation (Das et al., 2009; Maier et al., 2009). This hypothesis illustrates that control of petal number can be mediated through pathways that are not directly related to petal organogenesis, connecting petal number to various processes taking place within the dynamic environment of the floral meristem.

1.6 Chromatin remodelling ATPases: Connecting floral organ number and identity

Flower development has been extensively studied in *A. thaliana* and other plant species over the past decades. Understanding how many and varied pathways controlling floral development are coordinated is an interesting question, since it brings together multidisciplinary studies. The development of multicellular organisms relies on regulating chromatin, the structural templates of genetic information in eukaryotes. One way of modifying chromatin is through chromatin remodeling ATPases, which are important regulators of gene expression in eukaryotes. In plants, protein complexes containing SWI/SNF (SWItch/Sucrose Non-Fermenting)-type ATPases have been shown to regulate the transcriptional control of key developmental processes during all stages of plant growth. In this section, I will discuss how chromatin remodeling factors can interact with multiple pathways to orchestrate floral organ development.

In multicellular organisms, morphogenesis and growth relies upon genetically identical somatic cells; therefore, establishment of cell identities and maintenance of transcriptional programs within groups of cells is crucial for development and therefore must be strictly regulated by additional layers of gene regulation, spanning beyond primary DNA sequences (Hsieh et al., 2005). In eukaryotes, DNA is organized in a highly condensed, complex and repeated structure, called chromatin. The building block of chromatin is the nucleosome, consisting of two DNA windings wrapped around an octamer of histone proteins (two copies of each histones: H2A, H2B, H3, and H4) (Hayes, J. J. et al., 2001). Chromatin is a very dynamic structure and by exposing or impeding target DNA sequences to regulatory proteins, affects transcription. Chromatin regulation allows rapid cell identity changes by making cell-type specific sequences accessible to transcription factors and maintains cell identity by stabilizing transcriptional states within the genome (Morao et al., 2016). It is compacted in two different states at interphase: highly condensed heterochromatin and less condensed euchromatin (Heinz, 1928). Heterochromatin is often associated with telomeres and chromosomal pericentric regions, but also regions that are rich in repetitive sequences and low in gene density, as shown in plant genomes as well (Fransz et al., 2002; McClintock, 1951). These regions are enriched for transposable elements and tandemly repeated DNA, mediating gene silencing; interestingly, the sequences may be present in euchromatic regions as well, silencing genes specifically for one tissue type, while active in others (Crewal et al., 2002; Lippman et al., 2004). On the other hand, euchromatic regions show opposite characteristics: they are rich in genes, have fewer nucleosomes, with nuclease hypersensitive sites, indicating presence of transcriptionally active genes (Crewal & Elgin, 2002; Sun et al., 2001). The two different chromatin states can be achieved in two distinct ways: (i) through covalent modifications, like acetylation/methylation/phosphorylation of histone terminals, mediated

directly by histone modifying enzymes, or (ii) by changing the position or structure of the nucleosome with the use of ATP-dependent chromatin-remodelling factors, utilizing the energy of ATP hydrolysis (Tsukiyama, 2002; Varga-Weisz, 2001).

ATP-dependent chromatin-remodelling factors are currently classified into four different classes, based on the type of their central ATPase subunit: SWI2/SNF2-like, ISWI (Imitation SWItch), Mi-2 (CHD1), and INO80 (Mohrmann et al., 2005; Sarnowska et al., 2016). These classes are also characterized based on additional domains: ATPases of the Swi2 class usually contain a bromodomain, whereas the ISWI type have SANT (SWI3, ADA2, N-CoR, and TFIIIB) and SLIDE (SANT-like ISWI domain) domains (Grüne et al., 2003); INO80 are characterized by a split ATPase domain, a chromodomain and PHD fingers (Längst et al., 2004). All classes are an essential parts of multi-subunit protein complexes that enzymatically regulate chromosomal structure and activity, involved in processes like DNA replication, repair, recombination and transcription (Hogan et al., 2007; Tsukiyama, 2002). Several of these complexes are abundantly expressed; for example, each *Drosophila* cell nucleus has an estimated number of 100.000 ISWI molecules (Tsukiyama et al., 1995). The remodelling mechanisms implemented by these ATPases can vary; for example, the complexes could (a) unwrap DNA segments from the nucleosome surface and slide the DNA through, or (b) replace the histone with a variant histone (Hogan & Varga-Weisz, 2007; Mohrmann & Verrijzer, 2005). Research in animal models has uncovered the possibility of unique biological functions of each complex through distinct biochemical mechanisms in each subfamily (Hsieh & Fischer, 2005). Some SWI2/SNF2 subfamily members are responsible for unwinding DNA around the histone core, facilitating access of DNA to nuclease and restriction enzyme digestion , whereas ISWI factors relocate nucleosomes by sliding the histone octamers along the DNA template (Längst & Becker, 2004). All mechanisms of non-covalent modification are part of establishing a

transcriptional profile that is dependent on the tissue and developmental stage of the organism (Saha et al., 2006); conclusively, chromatin remodelling is an extremely specialized and well-coordinated mechanism of transcriptional regulation in eukaryotes.

In *A. thaliana*, there are 42 ATPases of the SWI2/SNF2 family but only four belong to the SWI2/SNF2 subfamily, based on phylogenetic analysis of the SNF2 ATPase catalytic domains (Sarnowski et al., 2005). The members of the SNF2 subclade are: SPLAYED (SYD), BRAHMA (BRM), MINU1 (MINUSCULE1) and MINU2 (Farrona et al., 2004; Sang, 2012; Wagner & Meyerowitz, 2002). SYD and BRM are the closest homologues of yeast and animal SWI/SNF ATPase subunits, with SYD lacking the bromodomain in the C-terminus (Jerzmanowski, 2007). The first chromatin remodelling factor in plants was discovered in a *lfy* enhancer screen, where the *syd* mutant enhanced the floral phenotype of a weak *lfy* allele (Wagner & Meyerowitz, 2002). Further investigation showed how SYD interacts with various developmental pathways; for example, double *syd;wus* and *syd;stm* mutants together findings that show recruitment of SYD to the *WUS* promoter indicated direct connections to SAM development and stem cell maintenance. (Kwon et al., 2005; Wagner & Meyerowitz, 2002). BRM plays also a role in flower development, since BRM-RNAi transgenic plants and *brm* loss of function mutants flower prematurely, have a reduced number of flowers, fused sepals, small deformed petals and stamens as well as sepaloid petals and reduced fertility (Farrona et al., 2004; Hurtado et al., 2006). Both *SYD* and *BRM* have broad expression patterns; *SYD* is expressed in all meristems, in young leaves, flower primordia and all floral whorls until stage 3 but in later stages of flower development *SYD* expression is visible only in petals, stamens and carpels (Wagner & Meyerowitz, 2002). On the other hand, *BRM* is expressed in the vegetative SAM, in the root meristem, in young leaves and young flower buds, but also in petals, stamens and carpels, showing a partial overlap with *SYD* expression (Hurtado et al., 2006). The domains of

expression for both genes and their pleiotropic phenotypes are indicative of their involvement in various developmental processes; overlap in their expression patterns may suggest partial functional redundancy. For example, both SYD and BRM regulate *CUC* gene expression, genes known as regulators of organ boundary formation. Genetic and molecular data show that BRM promotes expression of all three *CUC* genes, but SYD regulates only *CUC2* expression during cotyledon separation (Kwon et al., 2006). Moreover, the partial diversification of SYD and BRM functions may arise from their sequence difference, resulting in regulatory specificity for each ATPase, indicating that *SYD* may have been evolved from an ancestral *BRM* gene during an ancient duplication event before the split of monocots with eudicots (Bezhani et al., 2007; Su et al., 2006).

The importance of both ATP-dependent chromatin remodelling factors in flower development has been highlighted by their role in flower patterning. Conditional double *syd; aMIRBRM* mutants show severe floral homeotic defects, due to down-regulation of *AP3* and *AG* expression (Wu et al., 2012). Also, protein pull-down experiments have shown that SYD and BRM physically interact with LFY and SEP3, whereas chromatin immunoprecipitation (ChIP) experiments have shown that SYD, BRM and LFY bind to *AG* and *AP3* regulatory regions in a similar pattern during initiation of flower patterning, indicating possible recruitment of SYD and BRM by LFY and SEP3 (Wu et al., 2012). Interestingly, mutual antagonism between SYD and CURLY LEAF, a Polycomb Repressor Complex (PRC2) member and predicted H3K27 methyltranserase (Goodrich et al., 1997), together with increased H3K27 trimethylation levels at *AP3* and *AG* regulatory regions in *syd*-2 compared to wild-type plants, suggests that chromatin modifications in these loci are mediated by SYD (Wu et al., 2012). These findings, together with the hypothesis that MADS-box proteins act in large protein complexes that

include SYD and BRM, suggest a role for chromatin remodelling factors in flower initiation and differentiation (Smaczniak et al., 2012b).

Moreover, SYD may influence the transition to flowering as well, since it was found as an interaction partner with AP1, indicating that SYD and AP1 may act together to activate LFY prior to floral induction (Smaczniak et al., 2012b). Recently, auxin-controlled fate reprogramming has been connected with the acquisition of floral meristem identity to shed light on how auxin as a signal can make use of chromatin remodelling factors to initiate flower primordia. AUXIN RESPONSE FACTOR 5/MONOPTEROS (ARF5/MP) is an auxin-dependent transcription factor that when mutated, produces naked pin-like inflorescences (Przemeck et al., 1996). MP was found to interact physically with BRM and SYD in high auxin conditions, whereas this interaction is blocked in low auxin conditions due to the presence of BODENLOS (BDL) and AUXIN RESISTANT 3 (AXR3), Aux/IAA proteins known to associate with ARF5/MP (Ouellet et al., 2001; Weijers et al., 2006; Wu et al., 2015). Furthermore, decreased accessibility of loci targeted by ARF5/MP in *syd*;*brm* double mutants compared to wt leads to the assumption that MP recruits SYD and BRM to increase DNA accessibility for up-regulation of key regulators in flower primordia initiation (Wu et al., 2015). The results suggest that BRM and SYD are necessary for auxin-responsive gene expression; this is achieved by unlocking the repressed chromatin state at MP target loci that results in making accessible binding sites for additional transcription factors (Wu et al., 2015). These recent advances have led to a better functional understanding of the chromatin remodelling ATPases. Interestingly, their additional level of genetic regulation provides a framework connecting phytohormone signalling with cell identity and pattering processes, acting as a coordinator of different pathways to ensure floral meristem formation and floral organ initiation.

1.7 Aim of this work

The aim of this work is the functional characterization of the *extra petals* (*exp*) mutant in *C. hirsuta*. *C. hirsuta* is a crucifer exhibiting variable petal number between flowers of the same plant. This derived characteristic is influenced by genetic and environmental factors, as reviewed in section 1.3. Control of petal number has not been studied extensively, since it was shown to be influenced by several pathways, as discussed in section 1.4. The study of a mutant with increased petal number in a species with variable petal number may help towards understanding the evolution of petal number robustness and reveal species-specific or non-specific components that limit petal number.

In chapter 3, I characterize the floral phenotype of *exp*, including extra petals and additional floral defects caused by the *exp* mutation, showing that *exp* is a recessive, hypomorphic allele. Also, I present data showing that the extra petals and chimeric petal-sepals found in *exp* flowers originate from the second whorl. Furthermore, I discuss how the expression of floral organ identity genes is altered in *exp*, possibly explaining the appearance of chimeric organs in whorls 2 and 3. In chapter 4, I show that the causal mutation in *exp* resides in the *C. hirsuta SYD* gene, which encodes a chromatin remodeling factor. Moreover, I show that silencing *SYD* expression using artificial miRNAs is sufficient to phenocopy *exp*. Finally, I demonstrate that reintroducing various versions of *SYD* in the *exp* mutant, reverts the phenotype towards wild-type, meaning that *SYD* is the causal gene underlying the *exp* mutant phenotype. In chapter 5, I discuss connections between extra petal formation in the context of chromatin-mediated regulation of multiple pathways.

Chapter 2

Materials and methods

2.1 Materials used

2.1.1 Buffers and media

Buffers, solutions and media were prepared based on the protocols from Sambrook (2001).

2.1.2 Bacteria strains

The *E. coli* DH5α, DH10b and MFDpir ΔT IV lacIq (JKE201) strains were used for plasmid amplification. The *A. tumefaciens* GV3101 strain (Koncz, C. et al., 1986) and GV3101RK2 (Koncz, C. et al., 1994) were used for *C. hirsuta* plant transformations.

2.1.3 Plant material

A. thaliana plant material

A. thaliana plants of the ecotype Columbia (Col-0) and Landsberg (L.*er*) were grown on soil or 0.5x Murashige and Skoog medium (MS) (Murashige, 1962). The mutant line *syd-2* (L.*er*) was obtained from the Arabidopsis Biological Resource Center (ABRC).

C. hirsuta plant material

C. hirsuta reference accession Oxford (Ox) was used throughout (Hay, A. and Tsiantis (2006). The *exp* was backcrossed twice to Ox before being characterized here.

2.1.4 Plant growth conditions

Plants were grown in a greenhouse with supplemental lighting under conditions of 18-h, 20°C days and 6-h, 16°C nights.

2.1.5. Oligonucleotides

The following list of oligonucleotides were used in this project for sequencing or amplification via PCR or qRT-PCR. All oligonucleotides were ordered from Sigma Laboratories.

Primer name	Sequence	Use
amiR1_Pr1	gaTAGTATCGAATAATATCGCAGtctctcttttgtattcc	For amiRSYD1 construct
amiR1_Pr2	gaCTGCGATATTATTCGATACTAtcaaagagaatcaatga	For amiRSYD1 construct
amiR1_Pr3	gaCTACGATATTATTGGATACTTtcacaggtcgtgatatg	For amiRSYD1 construct
amiR1_Pr4	gaAAGTATCCAATAATATCGTAGtctacatatatattcct	For amiRSYD1 construct
amirR2_Pr1	gaTTACCTATTGAAACCCCTCAAtctctcttttgtattcc	For amiRSYD2 construct
amirR2_Pr2	gaTTGAGGGGTTTCAATAGGTAAtcaaagagaatcaatga	For amiRSYD2 construct
amirR2_Pr3	gaTTAAGGGGTTTCATTAGGTATtcacaggtcgtgatatg	For amiRSYD2 construct
amirR2_Pr4	gaATACCTAATGAAACCCCTTAAtctacatatatattcct	For amiRSYD2 construct
amirR3_Pr1	gaTGACATGTTTAGAACTCGCTGtctctcttttgtattcc	For amiRSYD3 construct
amirR3_Pr2	gaCAGCGAGTTCTAAACATGTCAtcaaagagaatcaatga	For amiRSYD3 construct
amirR3_Pr3	gaCAACGAGTTCTAATCATGTCTtcacaggtcgtgatatg	For amiRSYD3 construct
amirR3_Pr4	gaAGACATGATTAGAACTCGTTGtctacatatatattcct	For amiRSYD3 construct
dCAPS-SYD-Intron-Fw	CCTGGTTGGAATTCATGCCCTC	dCAPS SNP2
dCAPS-SYD-Intron-Rev	AAAATGACTACAAGAGGCTAGGAGT	dCAPS SNP2
QRT-AP3-Fw	GCTGGGGAACTAAGAGCTGAA	QRT AP3
QRT-AP3-Rev	AAGGGCATGGTTGGGGTAAT	QRT AP3
QRT-AG-Fw	TGATTTGCATAACGATAACCAGC	QRT AG
QRT-AG-Rev	GGTTGAGATTGCGTTTGAGG	QRT AG
dCAPS-SNP1-New2-F	CATCATTGGGCTCCATAACA	dCAPS SNP1
VK-v082dSNPEx3R	AAGAAGCCAGCAGTTATACTCTGG**C**TAG	dCAPS SNP1
QRT-SYDN-Fw	CCTCAAGCTGCTGGTACCCAAACGG	QRT SYD
QRT-SYDN-Rev	CCACCAAGCTGCCTACCAGAAGTG	QRT SYD
SYDcds1-SYDcds2-F	CATCCGGTGGAAACTCCAAGGC	SYD constructs
SYDcds1-SYDcds2-R	GCCTTGGAGTTTCCACCGGATG	SYD constructs
pSYD43-SalIFw	GGGACCGTCGACAATGAATGATGAAGTTAGG	SYD constructs
pSYD-XhoIRv	GGTCCCCTCGAGCTTTAATTTTAAATTACACC	SYD constructs
pSYD25-SalIFw	GGGACCGTCGACAATTTTAAATAATTATTCTTG	SYD constructs
SYDcds-XhoIFw	GGGACCCTCGAGATGGCACCTTCACATAATATTG	SYD constructs
pSYD43-SacIFw	GGGACCGAGCTCAATGAATGATGAAGTTAGG	SYD constructs
pSYD25-SacIFw	GGGACCGAGCTCAATTTTAAATAATTATTCTTG	SYD constructs
SYDStopDCSmaRv	GGTCCCCCCGGGCTAGCCTTGGAGTTTCCACCGGATG	SYD constructs
pSYD2.5-S1	CTTATGTATAATGGAACTTGTTAGATAG	Sequencing
pSYD2.5-S2	TTCATGTCATTCTTACAATG	Sequencing
pSYD2.5-S3	CCCAATTTTGCATAATCAAC	Sequencing
pSYD2.5-S4	CCACGGAATTTACCTATAAT	Sequencing
SYDcds-S1	GCTAAGTTTCTCCATAAGCTTA	Sequencing
SYDcds-S2	AAATGGAAATGCCTGGTAAT	Sequencing
SYDcds-S3	CAAACAAACTCCATCGGAGA	Sequencing

SYDcds-S4	GTGAAGGAGTTCCACAAGAG	Sequencing
SYDcds-S5	GCAGTCAGAAATTAACTTCT	Sequencing
SYDcds-S6	TAATTTGGGCTCGATTGGAA	Sequencing
SYDcds-S7	CAGAGTATAACTGCTGGCTT	Sequencing
SYDcds-S8	ATCTCCGGTACTGGCAATAC	Sequencing
SYDcds-S9	TGGTTTTGATTCTGCATCAC	Sequencing
SYDcds-S10	AACCCCACTTCAGCCAGCCA	Sequencing
SYDcds-S11	AAGAAGGTGATAGCACTCAT	Sequencing
SYDcds-S12	CTGAAGATGCAGAATTTCTAC	Sequencing
SYDcds-S13	AGAACGGATGAAGTTCCACA	Sequencing
SYDcds-S14	GCCATGCATCTTCTGAGAAG	Sequencing
SYDcds-S15	AGTGGTTGCTGAAGATACAA	Sequencing
SYDcds-S16	GTCAGATCCATTGGTCGCAG	Sequencing
OCS-S1	ACTGAAGGGAACTCCGGTTC	Sequencing
m13RR	GTTGTAAAACGACGGCCAGTG	Sequencing
m13FF1	TCCCATATCGACCTGCAGGC	Sequencing
pSYD4.3-S1	GAGCTAACTTCACTGGAGAA	Sequencing
pSYD4.3-S3	GTCTACATATAGGGGAAAAAC	Sequencing
pSYD4.3-S4	CCATAAAGTTATGATGAAGGGTG	Sequencing
pSYD4.3-S5	GGAAATTTTGTGAAAGGAAGGAG	Sequencing
pSYD4.3-S7	GGGTTGGGTGTTTCAAGTAG	Sequencing
SYDgen-S1	GCCAGTGTGCTGGAATTCAG	Sequencing
SYDgen-S2	GCTGATTCAGCTAGAATTTCTTCTG	Sequencing
SYDgen-S3	GTGGGATCAAAATATGGATAATGCT	Sequencing
SYDgen-S4	CTGCTTGAATTTCCCTTGAGATATT	Sequencing
SYDgen-S5	AGAATTGTTTGATCCGAAAGGG	Sequencing
SYDgen-S6	ACAGCAGAAAGCCGACCAGG	Sequencing
SYDgen-S7	GAATTGACCTTCACGTTTGATGTAA	Sequencing
SYDgen-S8	TCTTTGGAGGATTAGAAGTTCACAA	Sequencing
SYDgen-S9	GCGACCAAGCAAAGGTATTTTCT	Sequencing
SYDgen-S10	GGTATTTAATGCGACCCCATATG	Sequencing
SYDgen-S11	CCTTCTGACTCTCTTCTCATCTTGA	Sequencing
SYDgen-S12	AGAGGGTTGAGGATAATTTGGG	Sequencing
SYDgen-S13	AGCGTAATAGTTATTTCCACTGAAC	Sequencing
SYDgen-S14	TCTTCAAGCTGCTGATACTGTGATA	Sequencing
SYDgen-S15	AAACATCCCTGTTAGGCTTCAAC	Sequencing
SYDgen-S16	GAAAGAAAATGAGATGGTATGCTTG	Sequencing
SYDgen-S17	GGAAACTCCAAGGCCACAACAG	Sequencing
SYDgen-S18	CAGGCGCTAAATGTACTTGAGAATT	Sequencing
SYDgen-S19	CAAGCAGAGGAGAAGCTCCTAAAC	Sequencing
SYDgen-S20	GACATTGGGTCGTCTAAAGTTGC	Sequencing
SYDgen-S21	ACATGTGGATGGGGAATCTTTTGA	Sequencing
SYDgen-S22	GGCAGGTCCCTGATGTCTCAA	Sequencing
SYDgen-S23	TGCTGAAGACTGATGAATTGCC	Sequencing
SYDgen-S24	GAAGGTGGATGTGCCTGCAT	Sequencing
SYDgen-S25	CTTGGCAGTGAAGAACCCGA	Sequencing

SYDgen-S26	GGAGGCAGCTAAGTTTCTCCATAAG	Sequencing
SYDgen-S27R	GCAGCCAAAGCAATTAAATCAAGG	Sequencing
SYDgen-S28	CAAGTGGTTGGAGTTGGCAATGAGG	Sequencing
SYDgen-S29R	CCTCATTGCCAACTCCAACCACTTG	Sequencing
SYDgen-S30	GGTGCACGGTTCAATGAGTTGAAG	Sequencing
SYDgen-S31	GGATGGTCTCTATTCAGGTGAATTG	Sequencing
SYDgen-S32R	GCTTTCCAGATAGTGCTGTATAGC	Sequencing
SYDgen-S33	GCTGCGTCGGCTGAAACATAAG	Sequencing
SYDgen-S34	GGGCCCTGCTTAATTTCCTAC	Sequencing
SYDgen-S35	GCTGAAGACTGATGAATTGCC	Sequencing
SYDgen-S36R	CCACTGAGGCTTGTACCTTC	Sequencing
SYDgen-S37	GGCCTAAAGTTGGTACTCCCG	Sequencing
SYDgen-S38R	CGACTGTATAGGCGATGCAG	Sequencing
OCS-R	CGCTCGGTGTGTCGTAGATA	Sequencing
SYDgen-S39R	GGTTTGACCGGTTCTGCCGC	Sequencing
SYDgen-S40R	CGTCCTCTGTTACTGGGAGAG	Sequencing
SYDgen-S41R	CGGGAGTACCAACTTTAGGC	Sequencing
SYDgen-S42R	GGCTCAGATTGAACATAGCTCG	Sequencing
SYDgen-S43R	CATCCGTTCTACTGTCTTCAAG	Sequencing
SYDgen-S44R	GCACATTTGTTCTCGTTGCTGC	Sequencing
SYDgen-S45R	CATGCATGTTATAACTACACCTCCT	Sequencing
SYDgen-S46R	GGCCTCGTTTGACAGGTGGTGTTTC	Sequencing
SYDgen-S47R	GCATGGAAACATAAAGAGTGCC	Sequencing
SYDgen-S48R	CACAGATCGGTTGGAAAGAAAC	Sequencing
SYDgen-S49R	CCTCCATAACATCAAGAAGCC	Sequencing
SYDgen-S50R	GAGCATAAAACAACACCTTTGC	Sequencing
SYDgen-S51R	CCAGTTAACAGGAGTCGGTGGG	Sequencing
SYDgen-S52R	CCACCCCTTAGGCTTGCTGGCTGC	Sequencing
SYDgen-S53R	CCCTTCAACCTTTCTCTCCTAA	Sequencing
SYDgen-S54R	GGACACAAATATAACTAGTTCCTCG	Sequencing
SYDgen-S55R	CCTCTTGATCTGCTATGGGC	Sequencing
SYDgen-S56R	GAAATACAAGGCACTGGGCTC	Sequencing
SYDgen-S57R	GAGTCGTGTATGCATCTGATGAC	Sequencing
SYDgen-S58R	CGTGTTGATTGACTACAGTGTCC	Sequencing
SYDgen-S59R	GTAACTACTTGAAACACCCAACCC	Sequencing
OCSF1	GGCATGCAAGCTAGCTTACTAGTG	Sequencing
pPCV812-NewMCS-F	gggaccgcggccgcgtcgacctcgagcctgcaggcccggggcggccgcggga cc	pSYD::SYDgen construct
pPCV812-NewMCS-R	ggtcccgcggccgccccgggcctgcaggctcgaggtcgacgcggccgcggtcc c	pSYD::SYDgen construct
Amp-cPCR-F	GCTTAATCAGTGAGGCACCTATCTC	pSYD::SYDgen colony PCR
Amp-cPCR-R1	GAGATAGGTGCCTCACTGATTAAGC	pSYD::SYDgen colony PCR
Amp-cPCR-R2	GGATAAAGTTGCAGGACCACTTC	pSYD::SYDgen colony PCR

2.2 Genetic methods

2.2.1 Plant transformation

Plasmids containing T-DNA were introduced into *A. tumefaciens* strain GV3101 (for *pSYD2.6::amiRSYD-OCS, pSYD2.6::GUS, pSYD4.3::GUS* and *pSYD2.6::SYDΔC-OCS* constructs) by electroporation and for *pSYD2.6::SYDgen-OCS*, *A. tumefaciens* strain GV3011RK2 was used and the plasmids were introduced via conjugation, as described in Koncz, C. et al. (1994) . In both cases, a single colony was grown in 5 ml of Luria Broth (LB) medium together with the respective antibiotics overnight at 28°C, which was then used to inoculate a 1 L culture. These cultures were grown to an optical density of OD600nm = 0.7 - 1. Cells were re-suspended in transformation buffer (5% sucrose, 10 mM $MgCl_2$, 1X Gamborg's vitamins (Sigma Laboratories), 100 ng/ml BA (6-benzylaminopurine), 0.03% silwet-77). Plasmids were transformed via floral dip into plants. Inflorescences were submerged in the solution for 10 minutes, after which plants were laid on their side, in the dark, overnight at room temperature. The next day the plants were returned to the greenhouse and placed upright.

2.2.2 Selection of transgenic plants

Transgenic plants were selected by spraying with 400 µM BASTA herbicide (commercial name “Basta” from Bayer) or with hygromycin diluted in MS growth medium (50 mg/L). Seeds grown on MS plates were sterilised using 70% ethanol, 0.5% Triton X-100 for 10 minutes, followed by a wash with 99% ethanol for 10 minutes and left to dry overnight under a fume hood.

2.2.3 Genotyping

To genotype SYD-SNP1 I designed dCAPS markers using the dCAPS Finder 2.0 web tool (http://helix.wustl.edu/dcaps/dcaps.html). There, both wt and *exp* sequences were inserted and only one mismatch was allowed for the primer design. The primers used for genotyping were called dCAPS-SNP1-New2-F (V059, forward) and VK-v082dSNPEx3R (V082, reverse). The reverse primer carries a mismatch that allows only wt sequence to be digested by NheIHF (New England Biolabs). These primers were used to genotype a selfed F_2 population of 72 plants segregating for *exp* for co-segregation analysis, and also to genotype transgenic plants for complementation analysis. Since the forward primer (V059) anneals in an intron, a wt allele is not amplified from the truncated SYD transgene (pSYD2.6::SYD-OCS), allowing the *exp* genotype to be unambiguously determined, but is amplified from the genomic SYD transgene (*pSYD::SYDΔC-OCS*), meaning that the *exp* genotype of *pSYD::SYDΔC-OCS* transgenic plants could not be unambiguously determined. pSYD2.6::SYD-OCS transgenic plants were genotyped for the presence of the transgene with a sequencing primer from SYD (SYDgen-S35, primer list) and the reverse primer for OCS (OCS-R, primer list). *pSYD::SYDΔC-OCS* transgenic plants were genotyped for the presence of the transgene with primers spanning over the *SYDΔC* and OCS fragments (SYDcds-S14 and OCS-R).

2.3 Molecular biology methods

2.3.1 Transgenic plant construction

The amiRSYD vectors were constructed based on the design described in Schwab (2006) and Ossowski (2008). An overlapping PCR was designed based on primer pairs (presented in 2.1.5) created from the Web MicroRNA Designer (WMD) website (http://wmd3.weigelworld.org/cgi-bin/webapp.cgi). The oligonucleotide sequences (I to IV), were used to engineer the artificial microRNA into the endogenous miR319a precursor by site-directed mutagenesis. The PCR fragments generate an MIRNA precursor in which the endogenous miRNA and miRNA* (Ossowski, 2008) are replaced with an artificial sequence specific for SYD. The chimeric sequence was then transferred to the binary pGREEN (BASTA Resistance) vector (Hellens et al., 2000), as a NotI fragment and transformed into wildtype *C. hirsuta* plants. 10 independent T_1 lines were selected in *C. hirsuta*. The phenotypic analysis was performed in the T_2 generation, where four lines were selected for characterization.

The pSYD2.6::SYD-OCS cassette was generated by separate amplification of pSYD2.6 and SYD from a *C. hirsuta* BAC clone (Hay, A. S. et al., 2014). The pSYD2.6 fragment carried a SacI restriction site at the 5' end, and a XhoI restriction site at the 3' end. The genomic sequence of SYD carried a XhoI restriction site at the 5' end and a SmaI restriction site at the 3' end. Both fragments were subcloned in the pBJ97 vector and sequenced. Then, fragments were digested with the respective enzymes and ligated in the same vector. The cassette containing both fragments plus the OCS terminator was subsequently NotI digested and inserted into the binary pPCV812 vector (Koncz, C. S. J., 1986). The sequence was also checked with the primers V143-V145 primers to ensure that the gene was inserted into the vector. Then, it was inserted into the MFDpir ΔT IV lacIq (JKE201) *E. coli* strain provided by C. and Z.

Koncz, where it was grown on LB + DAP 0.3mM plates. A single colony was picked and grown in liquid LB+DAP, whilst growing in parallel the *A. tumefaciens* GV3101RK2 strain. 50 ul drops of both strains were put on top of each other on YEB plates and left to grow at 28^{o}C for three days in order for the plasmid to be transferred from *E. coli* to *A. tumefaciens* by conjugation. From the drops, bacteria were streaked again on fresh YEB plates so that single colonies would appear. Then, the single colonies were grown in liquid medium to be transformed into plants. Seeds of the transformed plants were grown on 0.5x MS plates together with 50mg/L hygromycin. Four T1 lines were generated and transferred to soil. Three lines showed an *exp* phenotype and one wt phenotype. All lines were genotyped for the presence of the transgene and the presence of the *exp* allele.

The *pSYD::SYDΔC-OCS* construct was created in a similar way. The same promoter was used as described above. The *SYDΔC* fragment was reverse transcribed to cDNA with Superscript IV RT (Thermo Fisher Scientific) from inflorescence RNA of wt plants according to the manufacturer's protocol. Then, the fragment was amplified with V125 and V131 as primers, adding a stop codon at the 3' of the sequence. The restriction sites added to the sequence were: XhoI at the 5' end, and SmaI at the 3' end. The same process was followed as described for the *pSYD::SYD-OCS* construct, but the binary vector that was used was pGREEN (BASTA Resistance). The construct was then electroporated into *A. tumefaciens* strain GV3101 and transformed into plants. Fifteen T_1 plants were identified, and six T_2 lines were analysed for single-copy insertions. Four T_2 lines were genotyped for the presence of the transgene and the presence of the *exp* allele.

The GUS constructs were generated using the amplified pSYD2.6 and pSYD4.3 promoters, digested by the combination of SacI/XhoI (New England Biolabs) and subcloned into the intermediate vector pBJ36 carrying the GUS gene. The promoters were sequenced

and then the NotI cassette of *pSYD2.6::GUS-OCS* and *pSYD4.3::GUS-OCS* were transferred into the binary pGREEN (BASTA Resistance) vector. Three and one T1 lines were identified for *pSYD2.6::GUS* and *pSYD4.3::GUS*, respectively. The presence of the transgene was verified by GUS staining as described below. Extraction of DNA fragments from agarose gels and PCR purification of digests / PCR products were performed using Macherey-Nagel kits, as described in the manufacturer's protocols.

2.3.2 Genomic DNA extraction

To extract plant genomic DNA for PCR analysis, one to three leaves were mechanically homogenised in 1.5 ml eppendorf tubes by adding 400 µL extraction buffer (250 mM Tris-Hcl pH 7.5, 250 mM NaCl, 25 mM EDTA, 0.5% SDS) and the tube was then vortexed for two minutes. Samples were spun afterwards at full speed in an Eppendorf microcentrifuge for 5 minutes, and 300 µL of the supernatant was removed to a fresh tube containing 300 µL isopropanol at room temperature. Tubes were vortexed and incubated at room temperature for around 5 minutes to precipitate DNA. Afterwards, tubes were spun at full speed for 10 minutes, supernatant was discarded, and DNA was air-dried. DNA was then re-dissolved by pipetting up and down carefully in 100 µL TE (10 mM Tris-HCl pH 8.0, 1 mM EDTA), kept at 4^{o}C overnight.

2.3.3 Quantitative RT-PCR analysis

1 µg total RNA extracted from inflorescences (Qiagen RNAeasy kit) was DNAse I treated (Turbo DNA-free kit, Ambion Life Technoogies) and used for cDNA synthesis with oligo (dT) primers and Superscript IV reverse transcriptase (Thermo Fischer Scientific). cDNA was

amplified on the AB ViiA7 Real-Time PCR system (Applied Biosystems, Thermo Fisher Scientific). Amplification reactions were prepared with the SYBR-Green PCR Master kit (Applied Biosystems) according to manufacturer's specifications with 0.4 µM of primers and with 10 µL of cDNA per reaction (from 1/10 dilution of the cDNA synthesized). Each reaction was made in technical triplicates, and three biological samples were used per genotype. The efficiency of each set of primers and calculation of the gene expression level was determined according to the manufacturer's protocol (Applied Biosystems, Thermo Fisher Scientific). The relative gene expression analysis was described in Livak et al. (2001). The error bar represents the standard error of mean calculated on biological experiment repetitions. Expression levels were normalized based on the values for the housekeeping CLATHRIN gene (CARHR174880) which was used as an internal reference gene as described in Cnops et al. (2004).

2.4 Microscopy, histology and histochemistry

2.4.1 Scanning electron microscopy (SEM)

Tissue was fixed overnight in 4% gluteraldehyde, in 1x PBS (Sigma) at 4°C, washed three times in PBS for 20 minutes and dehydrated in ethanol series from 10% to 100%. Samples were dried the next day in a Leica CPD300 critical point dryer, sputter coated with platinum using a Polaron Sputter Coater SC7600 and viewed on a Zeiss Supra 40VP SEM. For the Cryo-SEM, fresh material was used. The samples were then inserted in an Emitech K1250X cryo unit for cooling, sublimation and sputtering with gold/platinum and viewed on the same SEM.

2.4.2 Light microscopy/spectroscopy

Imaging of cross-sections was performed using a Zeiss Axiophot microscope. For binocular imaging, a Nikon SMZ 1270 with a Nikon DS-Fi2 camera head was used, and images were taken with the respective Nikon software. To enhance the contrast of the specimens, I used polarized filters provided by Nikon. Pictures were captured with a Nikon DS800 digital camera using the official Nikon software.

2.4.3 Toluidine blue staining of paraffin sections

Inflorescences were fixed overnight in 4% paraformaldehyde in PBS at 4°C, dehydrated in ethanol series on ice, paraffin infiltrated and embedded automatically in the Leica ASP300. Tissue was cut in 8 µm sections, rehydrated and stained with 0.05% toluidine blue O in 50 mM citrate buffer for 5 minutes. Sections were again dehydrated, de-paraffinized in Histoclear (HistoChoice, Sigma-Aldrich), and mounted with Entellan (Merck Millipore).

2.4.4 b-glucuronidase staining with X-Gluc substrate (GUS analysis)

Tissue was fixed in 90% acetone at -20°C for one hour, washed twice with water for Molecular Biology (Sigma Aldrich), and stained overnight at 37°C in the dark with freshly prepared 100 mM sodium phosphate buffer, 10 mM sodium EDTA, 2 mM 5-bromo-4-chloro-3-indolyl-ß-D-glucuronic acid supplied with ferrocyanide and ferricyanide salts (2 mM for all GUS lines). Reactions were terminated with methanol overnight at room temperature. Then, the solution was replaced with 99% EtOH and left overnight at room temperature. Inflorescences and seedlings were dissected and mounted in 50% glycerol and viewed with dark field microscopy.

Chapter 3

Identification of *extra petals* (*exp*)

3.1 Introduction

Floral architecture in the Brassicaceae family consists of four sepals, four petals, six stamens and two carpels fused together, as presented in characteristic crucifers, like *Arabidopsis thaliana, Arabidopsis lyrata* and *Capsella rubella*. Various pathways have been identified that control many aspects of petal formation, highlighted by: the ABC model, showing the genetic regulation of floral organ identity (Coen & Meyerowitz, 1990), the role of boundaries during floral organ initiation (Huang et al., 2012) and the influence of auxin in petal organogenesis (Lampugnani et al., 2013). The recent advances of discovering genetic networks regulating petal growth and petal cell differentiation (Huang et al., 2016) together with the advantages of using petals as a model experimental system, like their simple structure and their dispensable nature, provide a basis to identify mechanisms driving plant organogenesis (Irish, 2009).

Cardamine hirsuta, a genetically tractable relative to *Arabidopsis thaliana* does not follow the rule of four petals, since the plants show variable petal number per flower per plant. This characteristic, as an exception, creates an excellent opportunity to investigate genes that control natural variation in petal number (Pieper et al., 2016).

In the first results chapter I will present a phenotypic characterization of the mutant *exp* phenotype that spans beyond the formation of extra petals, showing also chimeric organs from adjacent whorls and unfused carpel tips. Moreover, I will show that *exp* is a recessive allele and that it is probably hypomorphic due to the nonsynonymous mutation that does not result in a stop codon. Also, I will present data of *exp* flower dissections and cross-sections showing that the origin of extra petals and of chimeric petals-sepals is the second whorl.

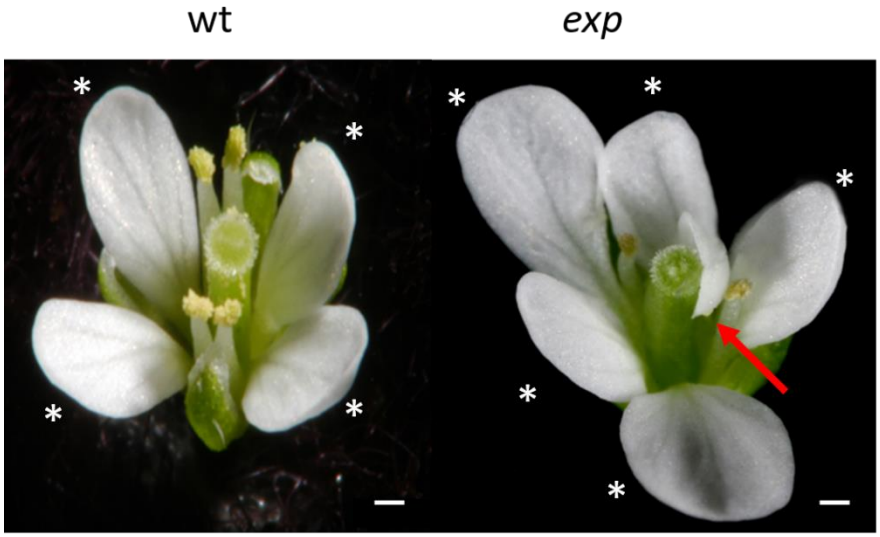

Figure 5: Comparison of *C. hirsuta* wt Ox (left panel) with *exp* flower (right panel). In both panels petals are indicated with asterisks (*). The Ox flower was selected to have four petals to show the maximum number of petals that can be observed in whorl 2. The *exp* flower has 5 petals and carries a petaloid stamen (red arrow). Scale bars: 100µm

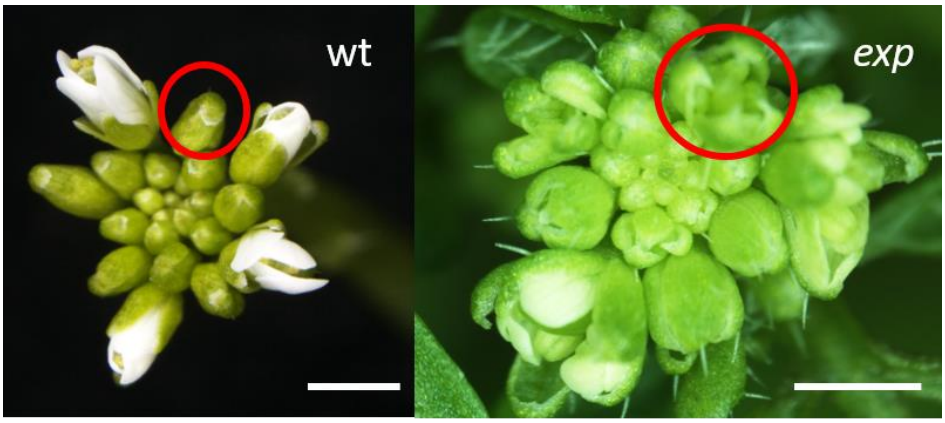

Figure 6: Depiction of C. hirsuta wt (left) and *exp* (right) inflorescences. The wt inflorescence follows a spiral pattern of flower initiation. On the right, the *exp* inflorescence appears bigger because the flowers open earlier than in wt. The red circles compare flowers of a similar stage, showing that sepals are already open in *exp* but closed in wt. Scale bar in both pictures is 1mm.

Finally, I will demonstrate that floral organ identity genes are mis-regulated in *exp*, thus providing a possible explanation for the appearance of chimeric organs in whorls 2 and 3.

3.2 Floral phenotype of *exp*

To identify novel pathways that control petal number variation in *C. hirsuta*, an unbiased forward genetics approach was used. We used ethyl methanesulfonate (EMS) to mutagenize wt Oxford seeds to screen for plants with alternate petal number. There, a mutant was identified that presented extra petals and therefore called *extra petals* (*exp*) (Figure 5). The phenotype is a result of a monogenic recessive mutation (chisq: $5{,}4938E^{-256}$) that has an effect on several floral characteristics, while the vegetative plant characteristics remain wild type-like.

Firstly, the main inflorescences of *exp* plants look bigger than wt, because the flowers open at an earlier stage (Figure 6). A closer look in the *exp* flowers showcases a variety of floral defects. Due to the increase in floral organ number, the flowers look bigger and of irregular shape (Figure 5). Starting from the first whorl, the sepals are wt-like, with no phenotypic variability and no increase in number. In the second whorl, I observed excess number of wt-like petals but also chimeric organs that are petal-sepal fusions (Figure 7a, 8a, 8b). The chimeric organs are smaller than normal petals, have a broader base and consist in most cases of two equal parts of petal and sepal, suggesting that they originated from an equal number of founder cells of each organ identity (Figure 8a). A few chimeras show only partial sepal identity, looking like petal sectors that have lost B-class gene expression. The sepaloid side of the chimera contains trichomes like all wt sepals and shows the same organ shape and range

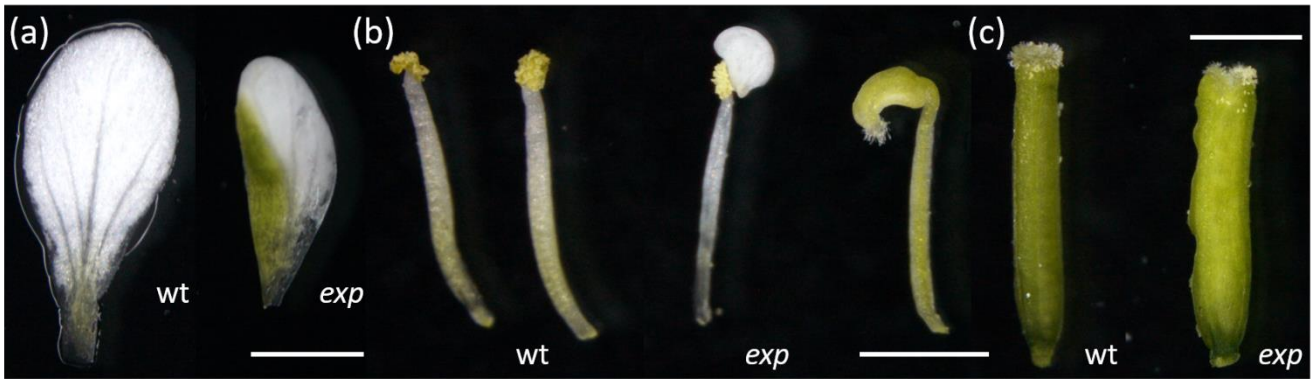

Figure 7: Floral organs of C. hirsuta wt and *exp* under light microscopy. The size of a wt petal is compared with the smaller-sized chimeric sepal-petal in (a). The sepal-like part of the chimera is variable and in this case, covers almost half of the total size. In (b) two wt anthers are shown next to two *exp* stamens, to show the phenotypic variability of floral organs in the third whorl of exp. In the left *exp* stamen, the anther is fused to a petal-like structure, whereas the right *exp* stamen is partially converted to a carpel. (c) exhibits the differences between a wt and a mutant carpel on the left and right, respectively. The *exp* carpel is shorter, thicker and is partially unfused at the top. Scale bars: 1mm.

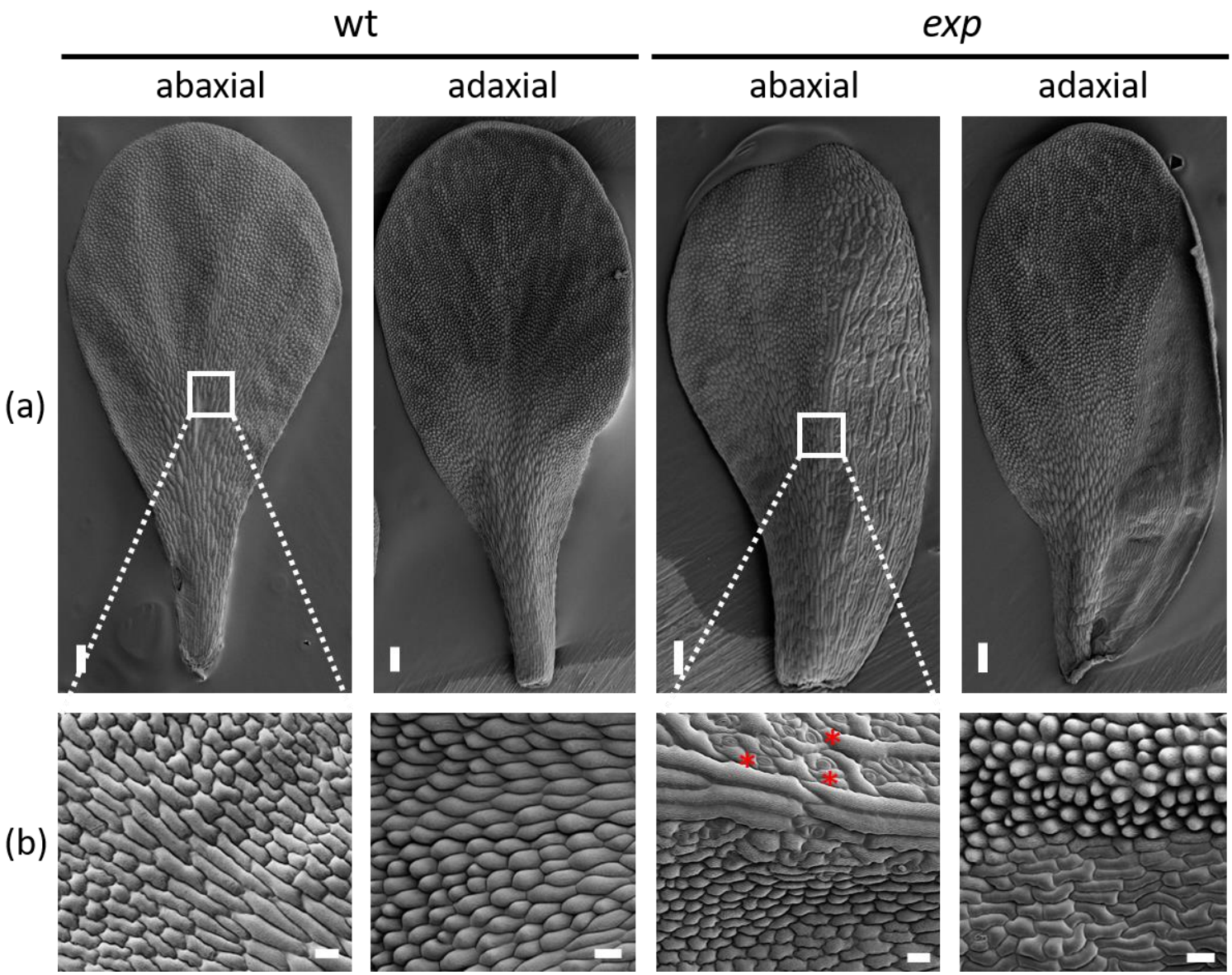

Figure 8: Scanning Electron Microscope (SEM) images of wt and *exp* sepal-petal chimeras. Whole-petal SEM images reveal the petal base difference in width between wt petals and *exp* chimeras in (a), together with the clonal-like growth of the chimera compared to wt. The petaloid side of *exp* petals is directly comparable to wt. The sepaloid side has a similar shape to a sepal, lacking the spoon-shape of a petal. In (b) the epidermis of both petal sides of wt and *exp* is shown. The sepaloid side of the chimera shows the same epidermal cell types found in sepals, including giant cells and stomata (red asterisks), whereas wt petal lacks both. The petaloid side has wt-like conical cells on the adaxial epidermal surface, making them indistinguishable from a normal petal. Scale bars in (a): 100µm, in (b): 20µm. Magnification in (a) 100x, in (b) 500x.

of epidermal cell types found in sepals, including giant cells and stomata on the dorsal side (Figure 8b). The petaloid side has a wt-like petal shape and the cells on the adaxial epidermal surface are conical, indistinguishable from a normal petal (Figure 8a, 8b). The average organ number in whorl 2 was 4.04, significantly higher than wt flowers (3.17) (Figure 9) (Wilcoxon test, p-value < $2.2e^{-16}$). Plants start with a petal number average above 4 in the first ten flowers, which then progressively stabilizes at 4 petals from flower 11 to flower 21, then petal number shows variability until no more flowers are produced. Flowers with 5 petals and more are found throughout aging of the inflorescence. Conversely, wt plants started with a petal number average around 3.5 that remains stable for the first ten flowers, with a drop to 2.5 for the next ten flowers, that slowly increases above 3 for flowers 20 and beyond till shoot meristem arrest. In the third whorl, apart from the four normal stamens that are present in a *C. hirsuta* flower, I observed also chimeric fusions between petals and stamens, but also between two stamens. Their occurrence was more frequent than these of whorl 2. Moreover, there was greater variability in organ shape, spanning from partial petal-stamen fusions to complete additions of petal tips on the anthers and staminoid carpels (Figure 7b). No statistical significance was observed between the average number of organs in whorl 3 between *extra petals* and wild-type plants (Wilcoxon test, p-value = 0.5141). In whorl 4, *exp* mutants present carpels that are shorter and most of them are unfused at the apex (Figure 7c), reminiscent of *spatula* and *splayed* mutants in *A. thaliana*, but also wt-like carpels with no obvious phenotypic differences. Both female and male reproductive organs in *exp* are fertile, so homozygous mutants can produce offspring.

There is a penetrance variability between the mutant traits observed in *exp* flowers. Some characteristics appear to be age-dependent; for example, the penetrance of extra organs is reduced from 3 in 10 flowers (for flowers 1-10) to 2 in 10 flowers (overall) (Figure

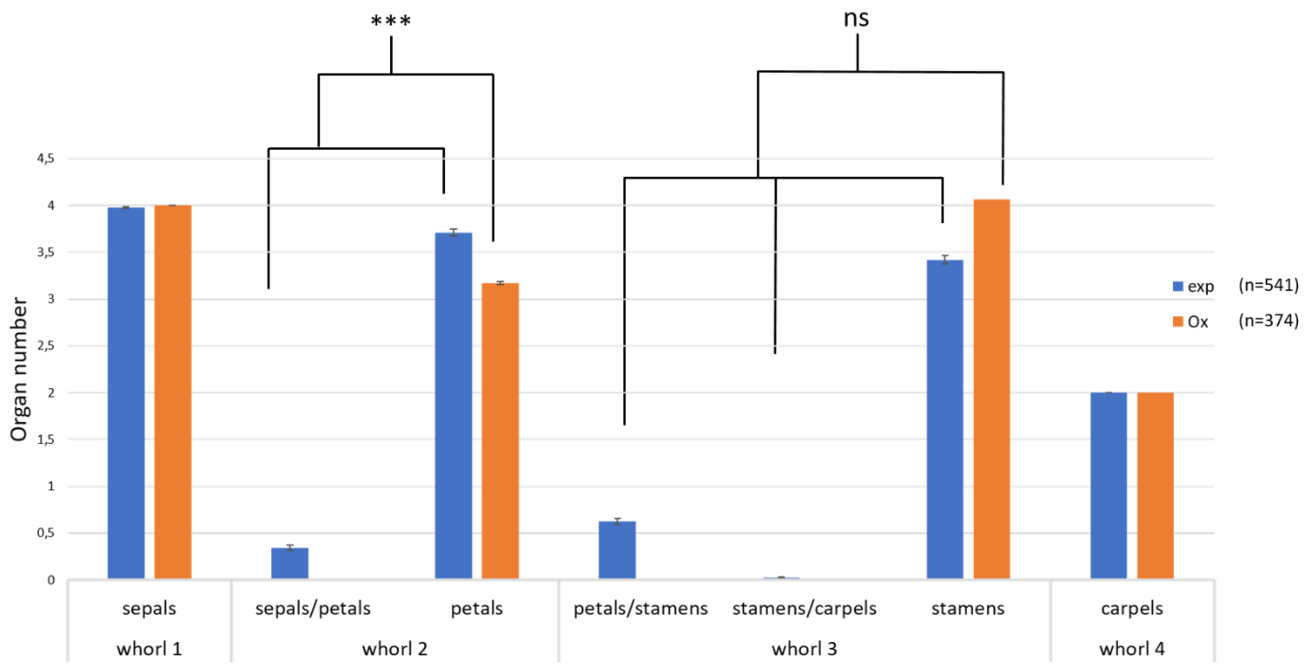

Figure 9: Organ number quantification between wt and *exp* per whorl. Sepal number average remains the same for both wt and *exp* plants. In whorl 2, chimeric sepals/petals and extra petals occur in *exp*, with the total number of floral organs in the second whorl increased significantly, from 3.17 (±0.08) in wt to 4.04 (±0.7) in *exp* (Wilcoxon test, p-value ≤ $2.2e^{-16}$). In whorl 3, chimeras between petals and stamens occur more often than stamen/carpel chimeras. The total number of floral organs in whorl 3 is not significantly different to wt. Also, there is no change in carpel number average in whorl 4. Number of flowers dissected in *exp*: 541, in wt: 374. Three asterisks: p-value ≤ 0.001, ns: no significance. Error bars represent SEM.

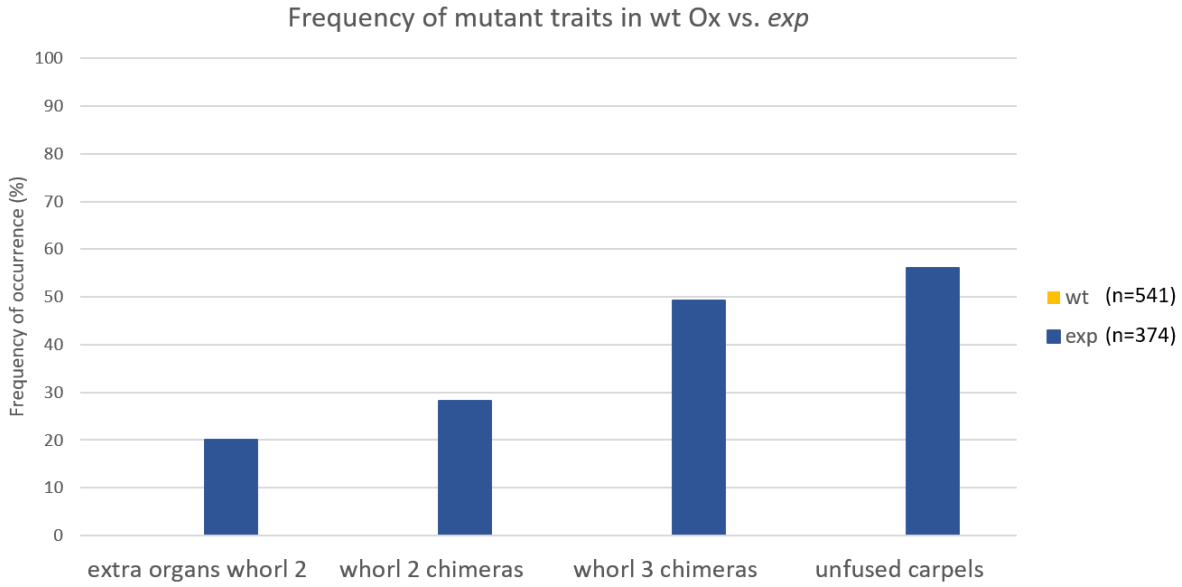

Figure 10: Frequency of *exp* floral organ phenotypes (in blue) compared to wt Ox (in yellow). In 374 flowers of *exp*, 20% exhibited extra organs in whorl 2, almost 30 % of them had chimeric petals/sepals, half of them developed chimeric stamens/petals or stamens/carpels in whorl 3, and 56% of *exp* flowers showed unfused carpel tips. Frequency of traits in %. In 541 flowers of wt, none of these phenotypes were observed.

10). Conversely, the presence of unfused carpels in *exp* flowers is more penetrant, since 6 in 10 *exp* flowers overall share this phenotype, present in early and late stage flowers (Figure 10). Finally, though no significant difference of organ numbers in whorl 3 was observed, almost half of the flowers had at least one stamen-petal/stamen-carpel chimera compared to wild-type (Figure 10).

3.3 Segregation analysis of *exp*

To understand the inheritance of the *exp* allele, I grew 72 F_2 progeny of a cross between *exp* and wild type plants under standard greenhouse conditions. From the total number of plants, I observed 15 *exp* mutants and 57 plants with a wild-type phenotype. The plants were segregating in a 3:1 ratio (chisq: $5{,}4938E^{-256}$), showing clearly that the *exp* allele is recessive. The wt *EXP* allele is complete dominant over *exp*, since the heterozygote phenotype was indistinguishable from homozygous wt plants.

3.4 *exp* phenotype is whorl 2 specific

The careful phenotypic characterization of *exp* flowers showed pleiotropy in the affected floral organ traits, indicating that the causal gene might be involved in multiple pathways. The significant increase in petal number, the floral organ that is highly variable in *C. hirsuta*, raises a question about the origin of extra petals. The hypothesis would be that petals arise from whorl two, where petals are normally produced, meaning there is a shift of organ boundaries within the whorl. Alternatively, if petals would arise from either whorl one of three, there would be a shift of A or C class gene expression between whorls.

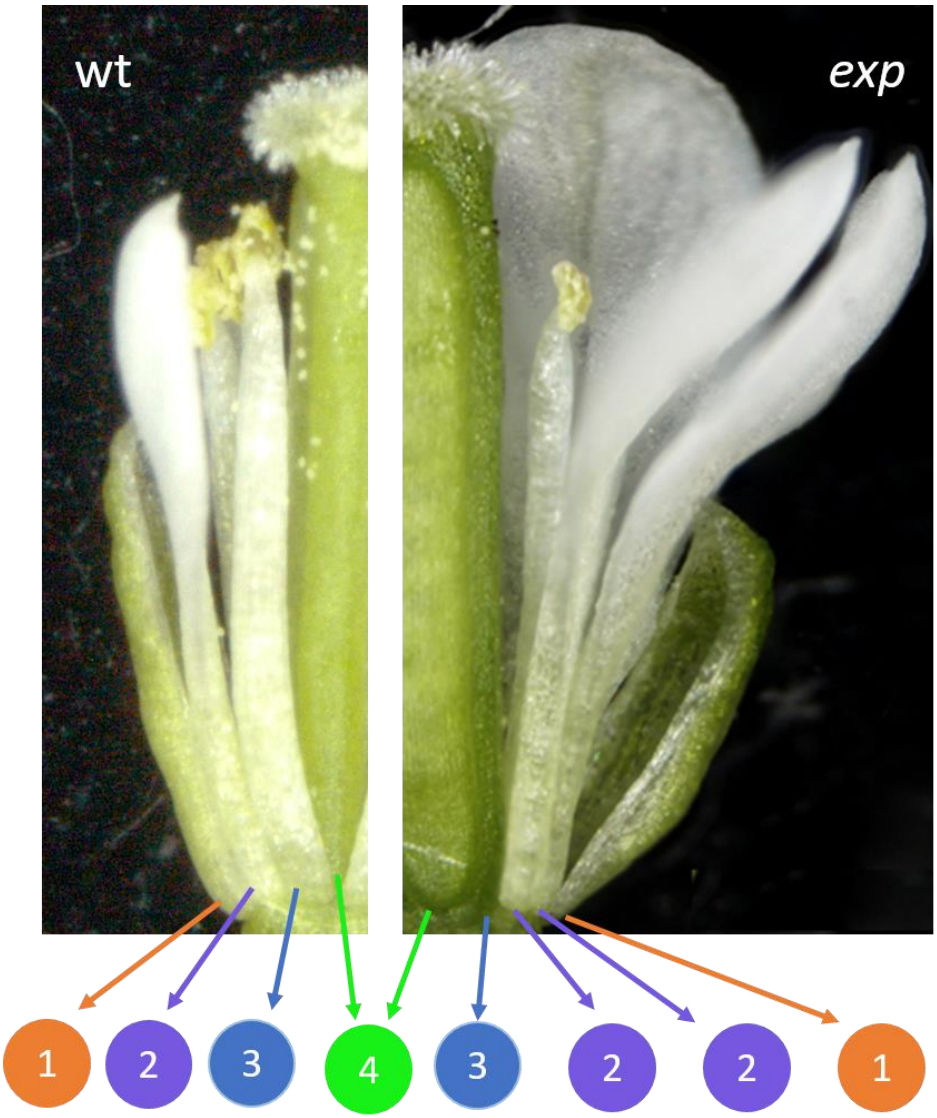

Figure 11: Floral organ positioning in wt (left panel) and *exp* (right panel). In C. hirsuta wt Ox, floral organs arise similar to *A. thaliana*: sepals from whorl 1, petals from whorl 2, stamens from whorl 3 and carpels in the central fourth whorl. On the other hand, *exp* flowers may seem deformed macroscopically due to the extra organs present. The floral organs arise from the same whorls as wt, with the additional petals and sepal-petal chimeras originating from whorl 2, whereas chimeric petal-stamens and stamen-carpels arise from whorl 3.

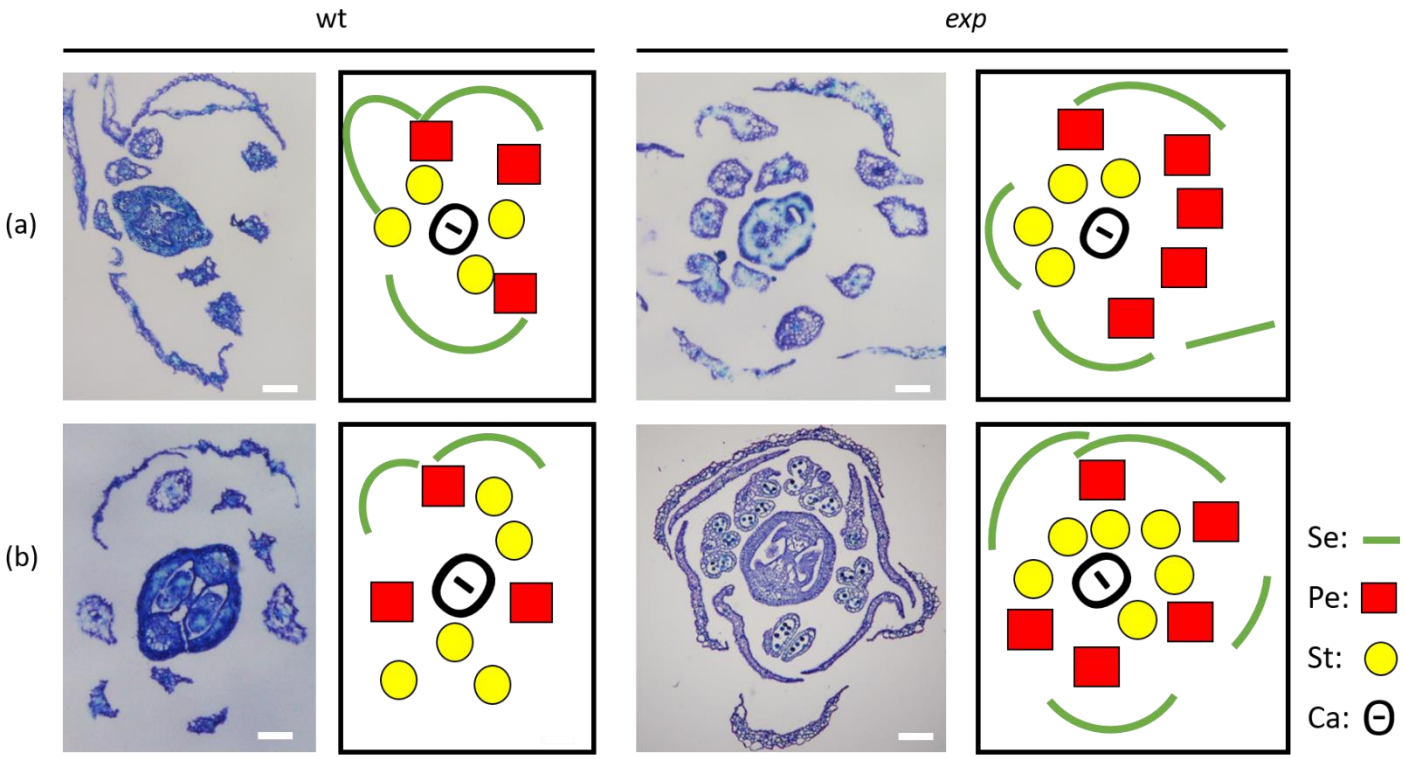

Figure 12: Cross sections of wt and *exp* mature flowers and their respective organ depictions. wt and *exp* cross sections in (a) are located proximal to the organ bases and in (b) the sections are towards the organ tips. Sepals are located in whorl 1 and are depicted with green lines. The petals (red squares) in both wt and *exp* sections are located in whorl 2 at the intersepal region and external to the stamens, shown in yellow circles. Carpels (Θ) are in the center of the flower. Sections in (a) and (b) were performed in different flowers. Legend: Se: Sepals, Pe: Petals, St: Stamens, Ca: Carpels. Scale bar in all four panels: 100µm.

To test this hypothesis, I dissected 542 *exp* flowers to pinpoint the origin of all floral organs from flower 1 until flower 25. I mapped the combination of organs present in each whorl in order to characterize the exact number and position of the components per flower.

In every flower the whorl 1 sepals encircled the extra petals, which means that these petals arise from whorl 2, including the petal-sepal chimeras (Figure 11). On the other hand, I observed that the stamens, together with all types of chimeric petals-stamens/stamen-carpel organs originate from whorl 3. The presence of extra organs in the limited space of whorl 2 pushes the sepals outwards, giving the impression that flowers are often deformed. To further support the origin of extra organs from whorl 2, fully open mature wt and *exp* flowers were sectioned (Figure 12). Cross-sections close to the flower base (Figure 12a), and further distal (Figure 12b), show extra organs with petal identity in whorl 2 (red squares) that are clearly distinct from adjacent whorls. Additionally, all organs with stamen identity arise from whorl 3 (Figure 12a, b). These two lines of evidence are certainly strong indications that extra organs originate from whorl 2.

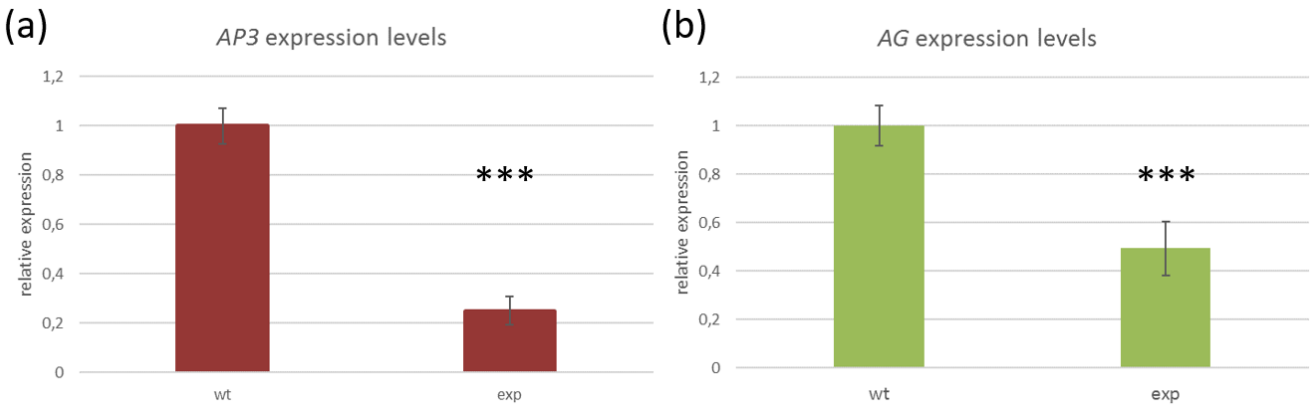

Figure 13: Relative expression levels of AP3 and AG in wt and *exp* background. In (a), the relative expression of *AP3* is compared between wt and exp. A significant 3-fold reduction in *AP3* transcript (Student's t-test, pval: $2.67e^{-5}$) is observed in the *exp* background. (b) shows the difference in relative expression of AG in wt and *exp*. *AG* expression is reduced significantly by 2-fold in the *exp* background compared to wt (Student's t-test, pval: 0.001). Statistical significance threshold for three asterisks: p-value ≤ 0.001. Error bars represent standard error in fold expression.

3.5 Floral organ identity genes show decreased levels of expression in *exp*

The floral phenotype of *exp* and particularly presence of chimeric organs in whorls 2 and 3 suggest that floral organ identity genes may be misregulated in *exp*. To investigate this idea, I analysed the expression of *AP3* and *AG*, genes involved in the formation of petals and stamens, in whole inflorescences of *exp*. Interestingly, there is a significant two-fold decrease in *AG* and a 3-fold decrease in *AP3* expression (*AP3, AG*: p-value ≤ 0.001) in the mutant background compared to wt (Figure 13a, b). This suggests that *EXP* function is required to maintain wild-type levels of *AP3* and *AG* expression.

In summary, we discovered a recessive, hypomorphic mutant called *exp* showing a pleiotropic floral phenotype, including extra organs, organ identity changes and unfused carpels. The extra petals, as well as the chimeric sepals/petals arise from the second whorl and may be a result of *EXP* regulating the floral organ identity genes *AP3* and *AG*.

Chapter 4

Molecular cloning of *exp*

4.1 Introduction

In chapter 3, I presented my characterization of the *exp* floral phenotype, which contains extra organs and chimeric organs in whorl 2, organ identity changes in whorls 2 and 3 and unfused carpels. In chapter 4, I will show how *SPLAYED* (*SYD*) was identified as a putative causal gene underlying the *exp* phenotype. Moreover, I will present that when artificial miRNAs against *SYD* are expressed *in planta*, their phenotype is *exp*-like. Finally, I will demonstrate that reintroducing various versions of *SYD* in *exp*, reverts the phenotype back to wild-type, meaning that indeed *SYD* is the causal gene.

4.2 NGS-mapping experiment reveals *SPLAYED* as putative causal gene for *exp*

The *exp* mutant was identified in a forward genetics screen using ethyl methanesulfonate (EMS) to mutagenize wild-type *C. hirsuta* seeds and screen for mutants with altered petal number. I followed a "mapping-by-sequencing" approach to identify the causal gene underlying the *exp* phenotype (Hartwig, 2012; James et al., 2013; Schneeberger et al., 2009). This approach takes advantage of bulk segregant analysis and whole-genome sequencing in order to speed up the process of mutant identification (Schneeberger et al., 2009).

DNA from 35 *exp* and 35 wt plants, segregating in a backcrossed F_2 population, was pooled into two samples and then sequenced by Illumina short read sequencing. By using a backcrossed population, we ensure that only mutagen-induced changes can serve as markers in the analysis (James et al., 2013). Subsequently, the short sequence reads were mapped to the annotated *C. hirsuta* genome (Gan et al., 2016) and analysed by a custom algorithm

Table 1: List of putative causal SNPs based on p-value. Almost all SNPs from the list are located on chromosome 4 (chr4). The two SNPs with the highest p-value (pvalue: 200, 175.56) are on the same gene, *SPLAYED* (*SYD*). The first SNP, in the position 12975531, is a nonsynonymous SNP on the exon 27 and causes a G to A mutation. The second-best SNP is located on an intron of SYD. The only mutation not on chromosome 4 is located on the mitochondrial DNA and causes a synonymous change. The rest SNPs from the list are located in intragenic regions between genes. Chrm: chromosome, position: position on chromosome, reference: reference sequence, alternate: mutated sequence, genes: genes annotated

chrm	position	reference	alternate	pvalue	mutation type	genes	Description
Chr4	12975531	G	A	200	nonsynonymous SNV	CARHR121200:CARHR121200.1:exon27:c.G3649A:p.A1217T	SPLAYED
Chr4	12969353	G	A	175,56	intronic	CARHR121200	SPLAYED
ChrM	106587	G	R	156,54	synonymous SNV	CARHR282770:CARHR282770.1:exon1:c.C384T:p.R128R	Ycf1
Chr4	13016749	C	T	149,33	upstream;downstream	CARHR121260,CARHR121270;CARHR121210,CARHR121220,CARHR121230,CARHR121240,	
Chr4	9651023	G	R	148,74	intergenic	CARHR118800(dist=39588),CARHR118810(dist=55706)	
Chr4	8291437	G	A	139,72	upstream	CARHR118460,CARHR118470,CARHR118480	
Chr4	11538780	G	R	137,35	upstream;downstream	CARHR119900,CARHR119910,CARHR119920,CARHR119930;CARHR119890	
Chr4	12632876	G	A	130,07	downstream	CARHR120790	
Chr4	13119164	G	R	123,09	upstream;downstream	CARHR121340,CARHR121350,CARHR121400,CARHR121410;CARHR121360,CARHR121370,CARHR121380,CARHR121390,	
Chr4	9956779	G	A	120,68	intergenic	CARHR119020(dist=24972),CARHR119030(dist=64950)	

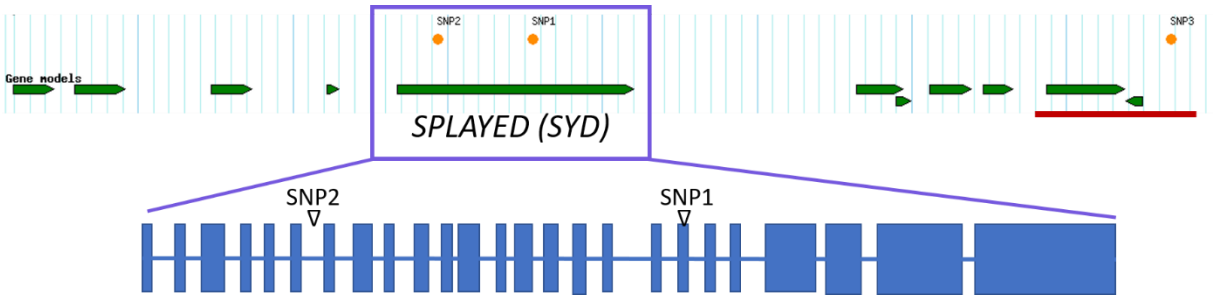

Figure 14: Map of the genomic region of chromosome 4 in *C. hirsuta*, showing the positions of the three SNPs (in yellow) most likely to be causal. SNP3 is located at an intergenic region, not related to any gene. Zoomed in is the genomic locus of *SYD* with the position of both SNP1 and SNP2 on the gene. SNP2 is located on an intron, whereas SNP1 is located on an exon. Blue boxes are exons, line between them is intronic region. Scale bar (in red) is 10kb.

developed by X. Gan, providing us with a list of putative causal single nucleotide polymorphisms (SNPs) for the *exp* mutation (Table 1).

Initially, observing Table 1 reveals that most of the SNPs are found on chromosome 4. Furthermore, two SNPs with the highest p-value are located in one gene: CARHR121200, the ortholog of *SPLAYED* (*SYD*) in *Arabidopsis*, which is an ATP-dependent chromatin remodelling factor (Wagner & Meyerowitz, 2002). The first SNP is a nonsynonymous mutation of G to A in exon 27, causing amino acid 1217 to change from an alanine (A) to a threonine (T), whereas the second SNP of *SYD* is in an intron, causing no apparent change (Figure 14). The next SNP is in the mitochondrial genome and is a synonymous change of G to A (or no change at all). The rest of the list is comprised of changes that appear in intergenic regions of chromosome 4 and do not seem to be putatively causal. Therefore, the gene most likely linked to the *exp* mutation is *SYD*.

4.3 dCAPS marker reveals causal SNP in *SYD* co-segregates with the *exp* phenotype

One of the most common classes of DNA sequence variation in nature is the single nucleotide polymorphism (SNP). These variants can be used as markers for various purposes, from mapping natural phenotypic variation to Marker Assisted Breeding (MAS). The biggest advantage of SNPs is that they exist in almost unlimited numbers, as differences of individual nucleotides between individuals and every polymorphism in a single cell containing DNA could actually be a potentially useful marker (Ganal, 2009). There are various ways of identifying SNPs in plants: for example, direct sequencing, Single Strand Conformation Polymorphism (SSCP), Chemical Cleavage of Mismatches (CCM) and Enzyme Mismatch Cleavage (EMC) (Edwards, 2001).

A relatively inexpensive way of using SNPs for genotyping is the Derived Cleaved Amplified Polymorphic Sequences (dCAPS) assay. This technique uses mismatches in PCR primers to create restriction endonuclease (RE)-sensitive polymorphism based on the target mutation. It is a derivative of the CAPS assay, but applied for SNPs that do not create a natural restriction site, so the mismatches modify the PCR product. Designing dCAPS markers is simplified by use of an online program (http://helix.wustl.edu/dcaps/dcaps.html) and these markers have been widely used for various purposes, spanning from associating genetic maps with diseases, to discovering polymorphisms highlighting the evolutionary significance of genes (Neff et al., 1998; Palomino et al., 2009; Yamanaka et al., 2004; Yanagisawa et al., 2003; Zhang, Y. et al., 2012).

In this project, I designed dCAPS markers to genotype a selfed F_2 segregating population for the *exp* mutation (that was analyzed phenotypically in 3.3) for SNP1 (exonic) of *SYD* (see Materials and Methods, 2.1.5). The primers for SNP1 were designed to create a

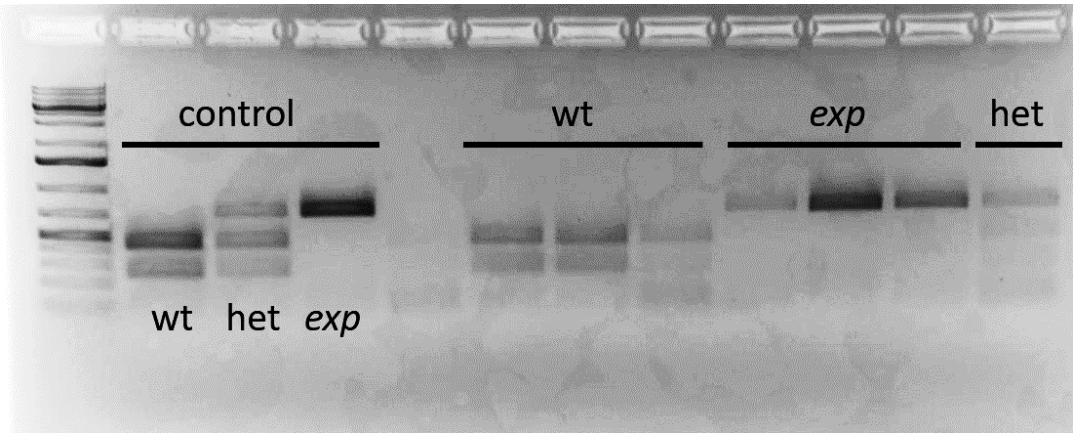

Figure 15: Genotyping for SNP1 in a population of selfed F_2 plants segregating for exp. Control group contains one plant sample per genotype investigated. Plant material was extracted and PCR amplified with custom dCAPS primers, producing a 330 bp product. Then, digestion with NheI-HF showed the difference between wt, heterozygotes and *exp*: wt sequence was digested (2 bands, 300bp and 30bp), whereas *exp* samples were not (1 band, 330bp), heterozygotes showed all 3 bands due to the presence of both alleles. wt= wild type, het= heterozygote, *exp* = extra petals sequence. Ladder: GeneRuler 50bp. Samples were loaded on a 3% low-melting agarose gel.

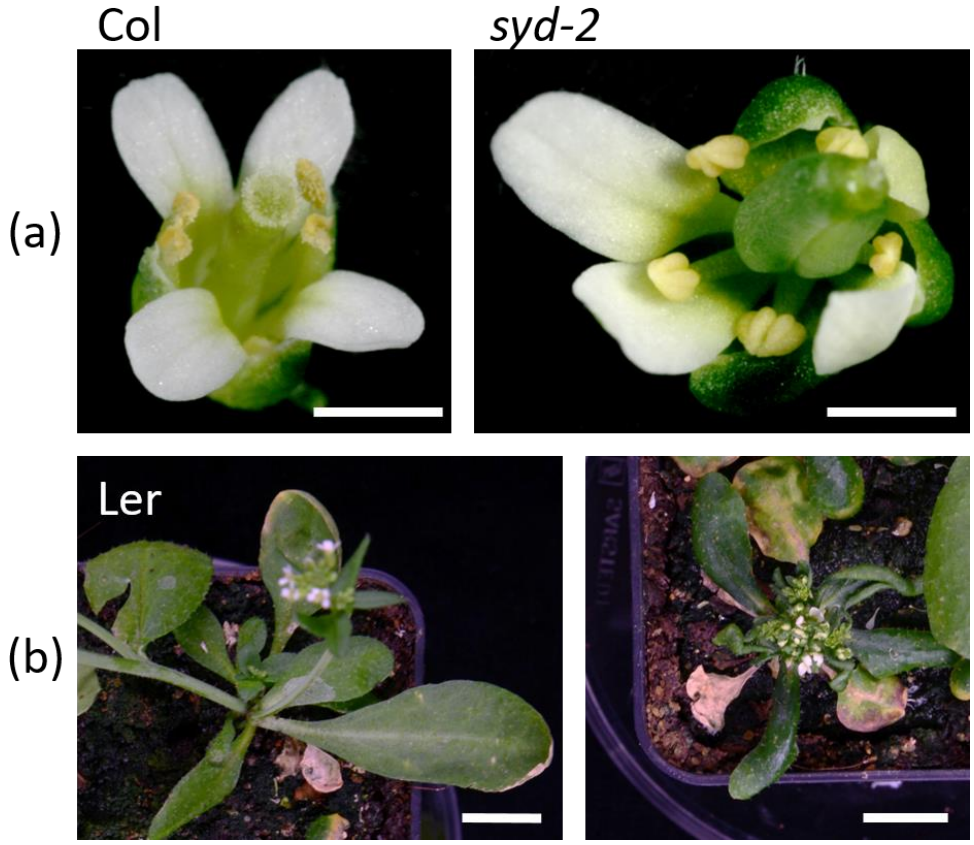

Figure 16: Floral and whole-plant phenotype of *syd-2* compared to *A. thaliana* Col (flower) and Ler (whole-plant). Wild-type flowers of *A. thaliana* have four sepals, four petals, six stamens and two fused carpels in the center (a), *syd-2* the flowers have increased number of splayed sepals, petals and reduced stamen number; carpels are unfused at the tip and broader. The mutant plants (b) show reduced growth and smaller leaves than Ler. Scale bar in (a): 100µm, in (b): 1cm

mismatch (underlined) of A (in the wt sequence) to G in the PCR product, where together with the wt G (that is mutated to A in *exp*) (in bold) creates a restriction site for the Nhe-HF enzyme (5'-**G**/CTAGC-3' in wt versus 5'-**A**CTAGC-3' in *exp*), resulting in a 30bp cleavage of the 330bp PCR amplicon (Figure 15). The mutated A in *exp* disrupts the restriction site and remains undigested (Figure 15). Finally, the heterozygote samples showed presence of both products, since they are carrying only one *exp* allele (Figure 15).

In the above-mentioned population of 72 plants, the mutant genotype for SNP1 was present in 15 samples, 33 plants were heterozygotes and 23 wild-types. Taken together with the phenotypic analysis performed in 3.3 (57 wt;like plants, 15 *exp* plants), it was observed that the genotype of SNP1 co-segregated completely with the *exp* phenotype. First, this creates a line of evidence to support the claim that *SYD* is the gene of interest. Secondly, it showcases as well a high possibility for the exonic SNP1 to be causal for the *exp* mutation.

4.4 *SPLAYED*: A chromatin remodelling factor that influences petal number in *A. thaliana*

Chromatin remodelling ATPases have been extensively studied in *A. thaliana* and their interactions with various pathways was discussed in 1.6. Although BRM and SYD mutant alleles have floral defects, their floral phenotype was not well characterized. Their putative function to act as coordinators between pathways controlling floral meristem formation and floral organ initiation may possibly extend to control of petal number as well, since SYD and BRM interact with genetic components that influence all aspects of flower development. In this subsection, I compare the floral phenotype of *exp* with *syd-2*, a null mutant of *SYD* in *A. thaliana* and also the genomic and protein sequences of SYD in both species.

Arabidopsis ATPases have been useful to study chromatin regulation dynamics, since null mutants in plants are not embryo lethal compared to other model organisms, as discussed in Wagner and Meyerowitz (2002). So far, it was shown that during reproductive development, SYD and its paralogues are crucial to both the transition to flowering and the expression of flower homeotic genes (Farrona et al., 2004; Hurtado et al., 2006; Su et al., 2006; Wagner & Meyerowitz, 2002; Wu et al., 2012). Moreover, it was reported that mutant alleles of *SYD* cause floral organ identity and floral organ merosity defects (Wagner & Meyerowitz, 2002). Recently, an interplay between auxin and chromatin remodelling complexes was discovered by the recruitment of SYD and its paralog BRM by the auxin response factor MONOPTEROS, increasing DNA accessibility to initiate floral primordia (Wu et al., 2015). The involvement of the SNF/SWI proteins in multiple pathways highlights the plasticity and pluripotency of the ubiquitously expressed ATPases, but also the possibility of direct control of floral organ number by chromatin remodelling factors.

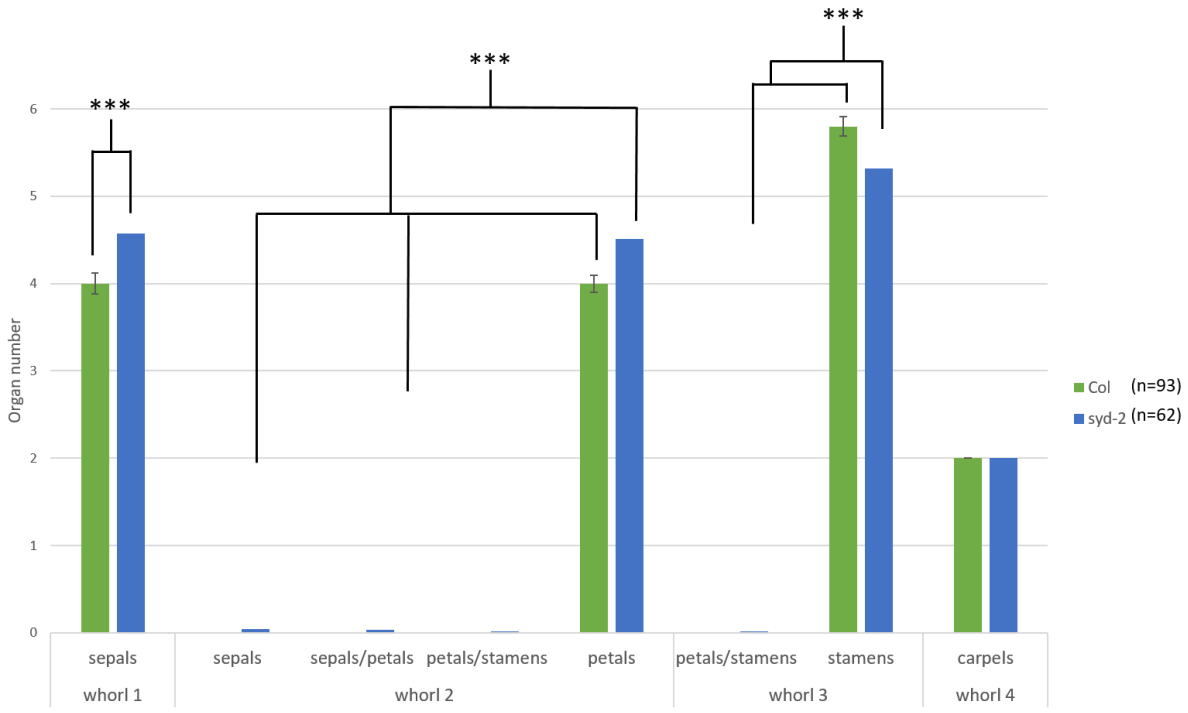

Figure 17: Organ count of *A. thaliana* Col (green) compared to *syd-2* (blue). In whorl 1 sepal number and in whorl 2 petal number averages are significantly elevated in *syd-2* to 4.57 (±0.12) and 4.53 (±0.13) respectively, followed by a significant decrease in stamen number in whorl 3 (Wilcoxon test, p-value ≤ $2.2e^{-16}$). No change in carpel number was observed between the two genotypes. Low number of chimeric organs was found in whorls 2 and 3. 93 Col and 62 *syd-2* flowers were dissected. Statistical significance in whorl 1,2 and 3 is depicted with 3 asterisks, indicating that the p-value ≤ 0.001.

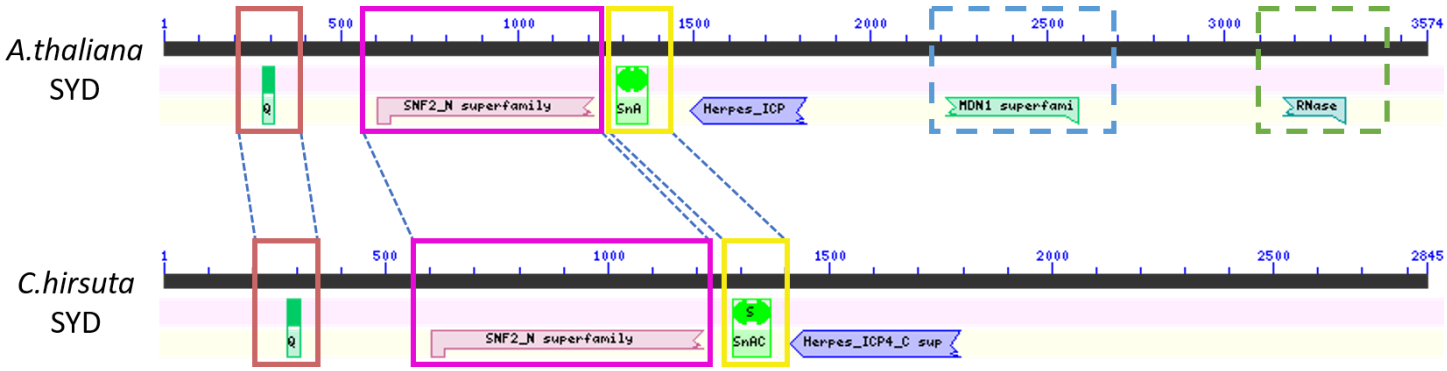

Figure 18: Predicted protein domains in AtSYD and ChSYD. The QLQ domain (red box) is involved in protein-protein interactions. The SNF2_N domain (pink box) contains the DEXDc and the Helicase domain, creating the ATPase subunit. The SnAC domain (yellow box) hydrolyzes ATP, and was shown to bind to nucleosomes. The Herpes_ICP domain is a non-specific domain of viral origin. Two general domains of AtSYD are absent in ChSYD: MDN1 (dashed blue box) and RNase (dashed green box). Size in both sequences in amino-acids.

The floral phenotype of *syd-2* was described to have variable petal and stamen number with stamens splayed outwards (Wagner & Meyerowitz, 2002). To investigate if the floral organ number increase is similar to *exp*, a population of the null mutants was grown and compared to *A. thaliana* Columbia (Col) and Landsberg (Ler) as reference. *syd-2* plants showed significant developmental defects, like reduced growth and smaller leaves (Figure 16b). The flowers of *syd-2* were severely affected as well. The most striking traits were the presence of extra organs and the shorter, broader carpelloid structures in the centre of the flower that had unfused gynoecium tips (Figure 16a). The carpel defects result in female sterile plants, as reported previously (Wagner & Meyerowitz, 2002). Careful examination of the floral organs showed increased petal number in whorl two, but also increased sepal and stamen number. Specifically, sepal number average is increased significantly in whorl 1 (p-value ≤0.001), whereas the significant rise of petal number to 4.5 (p-value ≤0.001) was not connected with presence of chimeric organs in whorl 2, unlike *exp* (Figure 17); additionally, flowers had narrower petal number variation, ranging mainly from 4 to 6 petals. Also, stamens were reduced significantly in *syd-2*, compared to Col and had few chimeric organs (Figure 17). One explanation for the phenotypic differences between *exp* and *syd-2* may be sequence differences between the two orthologs; therefore, I compared the DNA and protein sequences of AtSYD and ChSYD.

The genomic locus of *SYD* in *C. hirsuta*, located in chromosome 4 is 15.2kb long, creating a transcript of 8.8kb. The encoded protein contains 2957 amino acids, slightly smaller than *AtSYD* (3574 aa). A pairwise comparison of the two homolog transcripts reveals a 74.8% similarity, whereas at the protein level the sequences are 66.7% identical. The predicted protein structure of ChSYD shows that all functionally significant domains present in AtSYD are found as well, although two non-specific domains are absent in ChSYD (Figure 18). The

shared QLQ (from the motif QX_3LX_2Q) domain (Figure 18, red box) has been implicated in protein-protein interactions (Van der Knaap, 2000). Both proteins have the two characteristic domains of a chromatin remodelling factor, which are: the SNF2_2 domain (Figure 18, pink box) that contains the DEXDc domain and the Helicase domain, and the SnAC (Snf2 ATP Coupling) domain (Figure 18, yellow box). DEXDc belongs to the DEAD-like helicases and together with the Helicase domain create the ATPase subunit. The SnAC domain is required *in vivo* for transcription regulation by hydrolysing ATP and nucleosome remodelling (Sen, 2011). SNP1, the SNP of interest, is located in the catalytic subunit of the protein, between the SNF2_N and the SnAC domain, whereas SNP2 is in the intronic region of the QLQ domain. One domain missing from ChSYD is called MDN1 (Figure 18, dashed blue box), from the protein Midasin of *S.cerevisiae*, an ATPase with vWA (von Willebrand factor A) domain, involved in ribosome maturation (Marchler-Bauer, 2016). The second domain present only in AtSYD (Figure 18, dashed green box) is part of the ribonuclease E/G family, enzymes that cleave a wide variety of RNAs (Marchler-Bauer, 2016).

The SNF2/SWI2 protein family is present across all three kingdoms of living organisms. In land plants, the SWI2/SNF2 class of chromatin remodelling ATPases is represented by three different genes: homologs of Arabidopsis *BRAHMA* (*BRM*), *SPLAYED* (*SYD*) and *MINUSCULE* (*MINU*) (Sang, 2012). In the annotated genome of *C. hirsuta*, all three genes are present: *ChBRM* (CARHR141280), *ChSYD* (CARHR121200), *ChMINU1* (alternative name: *CHR12* (CARHR80510)) / *ChMINU2* (alternative name: *CHR8* (CARHR265920)) (Gan et al., 2016). The biologically active domains of SNF2/SWI2 proteins display high conservation within land plants (Figures 19a and b) (Flaus, 2006; Knizewski, 2008; Kwon et al., 2007; Sen, 2011). The important amino acid residues for ATP hydrolysis and nucleosome binding have been identified in various organisms, like yeast (for SnAC) (Sen, 2011) and virus strains (for DEXDc) (Champier, 2007).

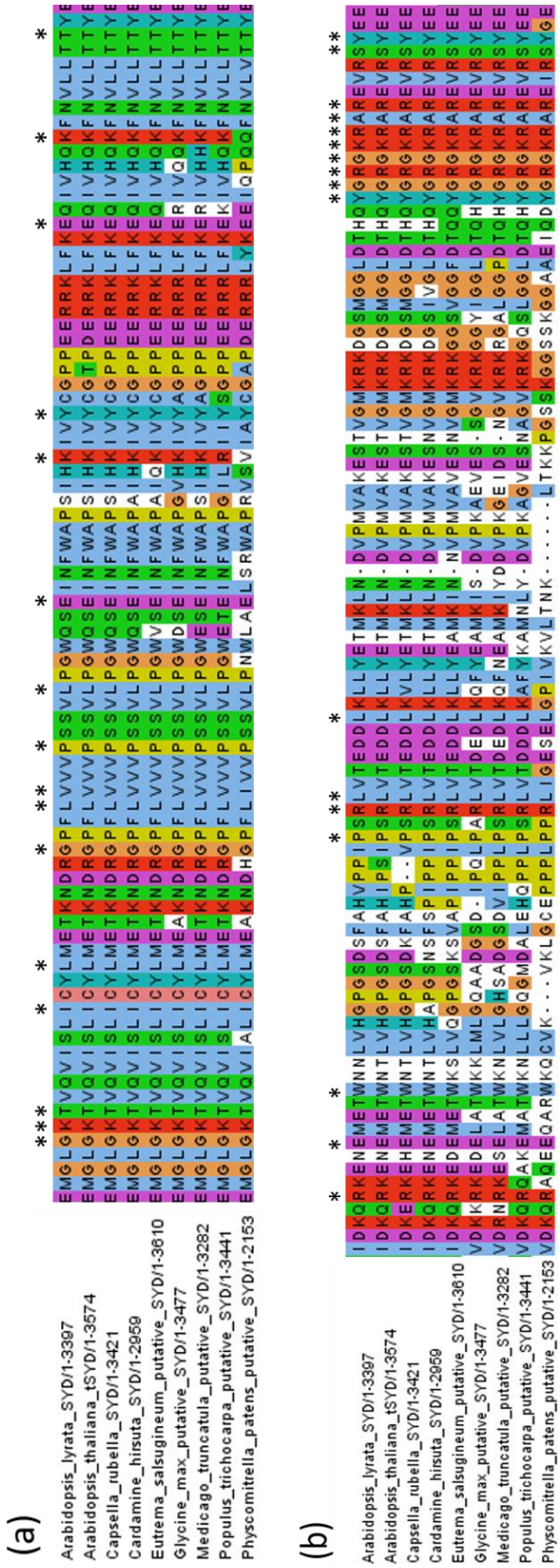

Figure 19: Conserved amino acid residues in two different protein domains of SYD across Angiosperms together with a bryophyte (*Physcomitrella patens*). The conserved amino acids (highlighted with asterisks) are shown in the DEXDc domain (a) and the SnAC domain (b). Multiple sequence alignment (MSA) was performed with the MUSCLE program (Edgar, 2004). Each amino acid is connected to a a color (based on ClustalX colouring), if the amino acid profile of the alignment at that position meets criteria specific for the residue type.

The amino acids for both DEXDc (Figure 19a) and SnAC (Figure 19b) domains are present and conserved within the Brassicaceae family (examples: *Arabidopsis thaliana*, *Capsella rubella*, *Eutrema sasugineum*) and the Fabaceae family (*Glycine max*, *Medicago truncatula*); the amino acid similarity is extended until the division of bryophytes like *Psyscomitrella patens*. Interestingly, the Alanine that SNP1 is affecting remains conserved not only within the plant kingdom but also in the *Drosophila melanogaster SYD* homolog (Figure 20). Moreover, the amino acid presence is extended to *ChBRM* and *AtBRM*, the closest homolog of *SYD* in the SWI2/SNF2 subclade (Figure 20). Therefore, although the mutation is not in a domain of known function, but rather in the linker sequence between two domains, it might be important for the protein conformation. Recent findings about the crystal structure of a SWI2/SNF2 protein from the yeast *Myceliophthora thermophila* has revealed that the SnAC domain flanks the protein core (DEXDc and Helicase domains), playing a key role in stabilization (Xia, 2016); thus, improper connection of the two domains may influence protein functionality.

In conclusion, the floral phenotypes of *syd-2* in *A. thaliana* and *exp* in *C. hirsuta* show similar trends in petal number increase, whereas *syd-2* also showed a significant increase in sepal number and decrease in stamen number. Genomic and protein *SYD* sequence similarity between *A. thaliana* and *C. hirsuta* is relatively high and important residues in biologically active domains are highly conserved. *SPLAYED* contains an ATPase domain and a nucleotide remodeling domain (SnAC), and the exonic SNP1 found in *exp* resides between these two domains. After showing that the *exp* phenotype co-segregates with SNP1 in *SYD* and showing that the amino acid carrying the non-synonymous mutation is conserved, and thus possibly biologically significant, an independent approach targeting specifically the gene of interest is needed to verify the hypothesis that *exp* is a mutant allele of *SYD*.

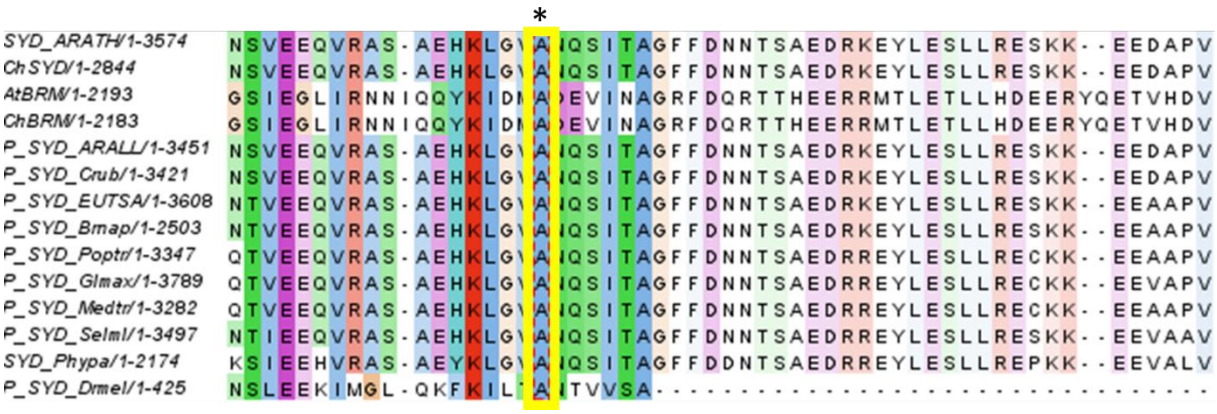

Figure 20: Conservation of the amino acid affected by SNP1. The alanine (in yellow box) is conserved throughout SYD orthologs in flowering plants (examples: *A. thaliana*, *A. lyrata*, *C. rubella*, *P. trichocarpa*, *Gl. max*), lycophytes (P_SYD_Selm: *Selaginella moellendorffii*) and bryophytes (SYD_Phypa: *Physcomitrella patens*) as well in as the fruit fly SYD homolog (P_SYD_Dme). Moreover, the particular amino acid is present in *C. hirsuta* and *A. thaliana* homolog, BRM. Basis of amino acid coloring as in Figure 19.

Figure 21: Inflorescences of wt, *exp* and *amirSYD*. Wt inflorescence seems smaller than *exp* and *amirSYD*, because the flowers in wt remain closed till a later stage, whereas in *exp* and *amirSYD* flowers open prematurely in a similar manner. Scale bars: 1mm

4.5 Artificial miRNAs against *SYD* phenocopy *exp*

The putative causality of SNP1 for the *exp* mutant phenotype and the comparable floral defects of *syd-2*, such as petal number increase, provide a framework to support the claim that *EXP* is *SYD*. Because *exp* is a hypomorphic allele of *SYD*, I expect that silencing *SYD* expression would phenocopy the *exp* mutant. To test this hypothesis, I used a reverse genetics method to silence expression of *SYD* in *C. hirsuta*. During the last decade, a highly successful technique was discovered that uses artificial micro-RNAs (amiRNAs) to target specific genes to cause mRNA cleavage and product degradation, taking advantage of the narrow action spectrum of natural plant miRNAs, compared to the large number of targets of animal miRNAs (Alvarez, J. P. et al., 2006; Schwab, 2006).

It was previously shown that amiRNAs against SWI2/SNF2 chromatin-remodelling ATPases, when broadly expressed in the flower (*pLFY::amiRAtSYD*), phenocopy the *syd* phenotype (Wu et al., 2012). Therefore, I decided to create an amiRNA construct against *SYD* driven by the 35S promoter from the Cauliflower mosaic virus (CamV35S), which is ubiquitously expressed and not subject to auto-regulation, to further support the claim that *SYD* is responsible for the *exp* phenotype. The construct was designed to target a domain necessary for SYD function, the helicase domain, and was created through the WMD3 online tool (http://wmd3.weigelworld.org/cgi-bin/webapp.cgi)(Ossowski, 2008).

For *amiRSYD1- 2*, nine independent lines were generated and seven of them had a single insertion of the construct in the T_2 generation. Between all single insertion lines, I did not observe obvious differences in phenotype, so I selected three of these T_2 lines for my phenotypic analysis. Macroscopic examination of the amiRSYD plants reveals inflorescences that look larger than wt, similar to what was observed in *exp* (Fig. 21). This is not caused by

Figure 22: Flowers of C. hirsuta wt, *exp* and three independent *amiRSYD* lines. *exp* and *amirSYD* flowers show similar floral organ number increase in whorl two compared to wt. Moreover, both have chimeric stamens/petals in whorl three (indicated with red arrows). No phenotypic differences were observed between the independent T_2 lines of *amirSYD*. Scale bars: 100µm

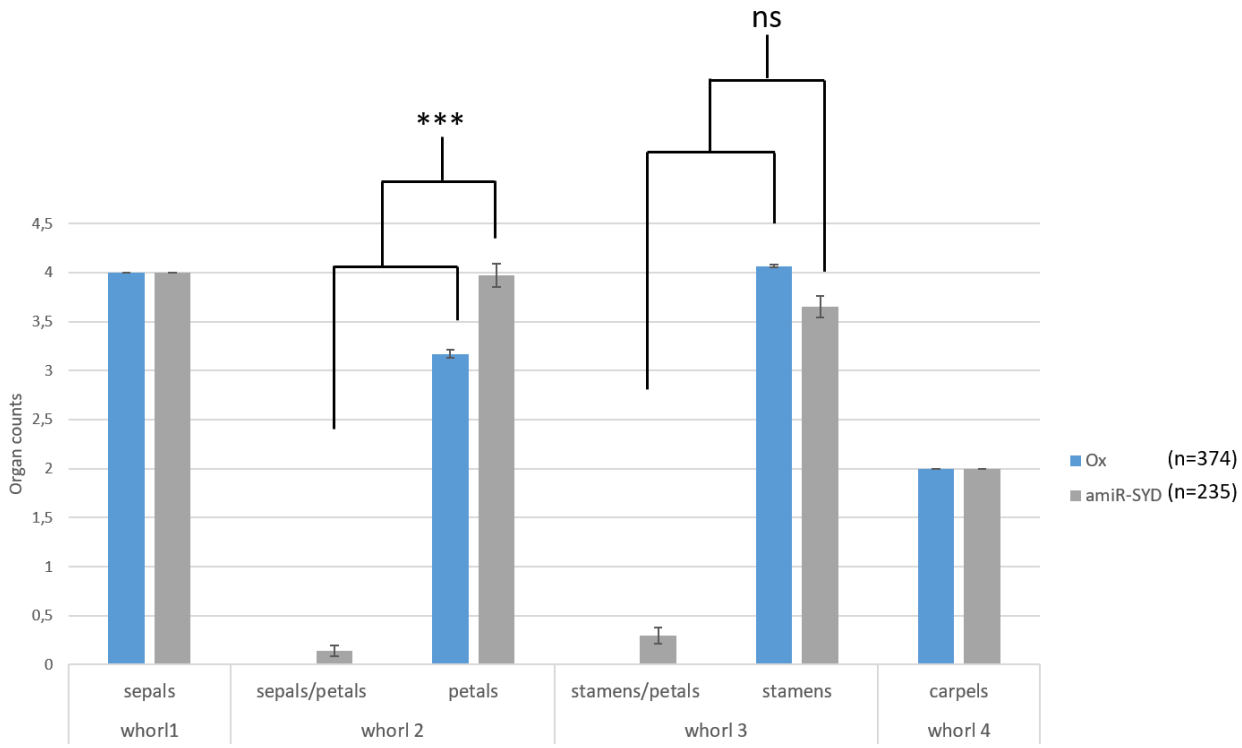

Figure 23: Organ number quantification between C. hirsuta wt Ox (blue) and *amirSYD* flowers (gray) per whorl per floral organ. Sepal number average in whorl 1 is 4 for both wt and *amirSYD*. In whorl 2, *amirSYD* flowers show elevated petal number and chimeric sepals/petals, resulting in a significant increase of floral organ number from 3.17 (±0.04) in wt to 4.14 (±0.11) in *amiRSYD* (Wilcoxon test, p-value ≤ $2.2e^{-16}$). In whorl 3, chimeras between petals and stamens and less stamens were observed in *amirSYD* flowers. The total number of floral organs in whorl 3 shows no significant change compared to wt. Also, there is no change in carpel number average in whorl 4. Number of flowers dissected in *amiRSYD*: 235, in wt: 374. Three asterisks: p-value ≤ 0.001, ns: no significance. Error bars represent SEM.

increased number of flowers present at the IM, but due to premature flower opening and the presence of extra organs that pushes the flowers to open.

Careful phenotyping of three independent *amiRSYD* lines shows similar floral defects as *exp* compared to wt (Figure 22). For illustrative purposes, to highlight the differences between *exp*, *amiRSYD* and wt, I used *C. hirsuta* flowers with four petals to show how extra petals can be generated in the same concentric ring and provide an ideal floral bauplan, indicating that there is enough space in whorl two for extra petals to arise. The flowers of *amirSYD* are characterized by the presence of extra petals and petal-sepal chimeras in whorl two, as well as petal-stamen chimeras in whorl three (Figure 22, red arrows) and occasional unfused gynoecium tips at whorl four. Petal organ number in *amirSYD* shows variability as in *exp* and wt; in the latter, the number varies from 0 to 4, but for both *exp* and *amirSYD* the range is shifted from 3 to 7. The high occurrence of extra organs in whorl two is translated to an average of 4.14 organs in whorl two, which is statistically significant compared to wt (Wilcoxon-test, pvalue: $2.2e\text{-}^{16}$) (Figure 23).

To verify that *amiRSYD* plants have reduced SYD transcription, I measured the expression levels of *SYD* in inflorescences of wt, *exp* and two independent lines of *amiRSYD*. The results in Figure 24 show a significant decrease in *SYD* expression in both *amiRSYD* lines relative to wt (t-test, pvalue ≤ 0.001), and a significant increase in *SYD* expression in *exp* relative to wt (t-test, pvalue ≤ 0.01).

The increase of *SYD* transcript in *exp* background (Figure 24) is contradictive to the results presented so far, since similar phenotypes observed in *exp* and *amiRNA* lines seem to be caused by loss of *SYD* function. Firstly, *exp* was mapped as a SNP on *SYD*, showing to be recessive and the heterozygote plants of the selfed F_2 *exp* population do not show any

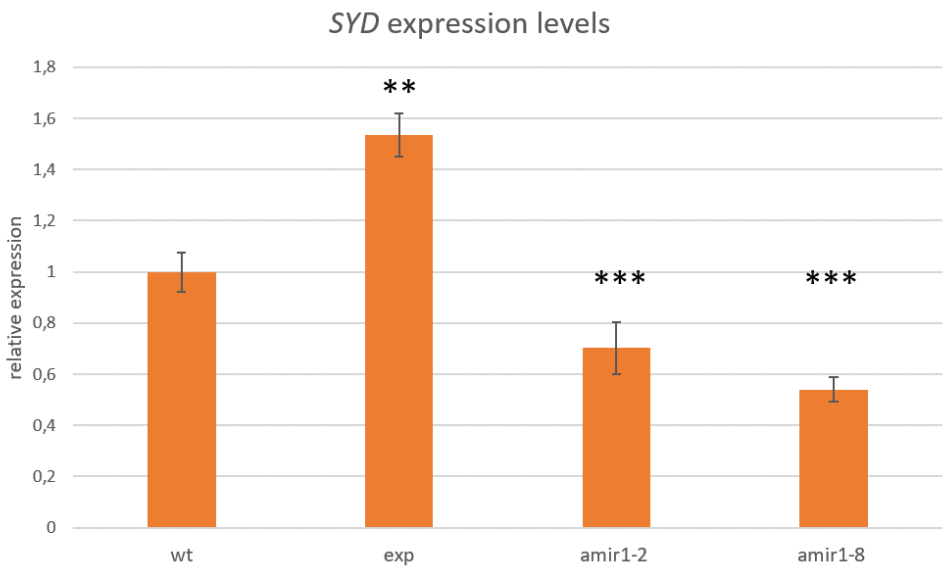

Figure 24: *SYD* relative expression levels in inflorescences of wt, *exp* and *amiRSYD* lines. Expression of *SYD* in *exp* is significantly increased compared to wt (Student's t-test, pval: 0.006). Conversely, *SYD* transcript is reduced by 1-fold in both independent *amiRSYD* T_2 lines (Student's t-test, pval (amir1-2): $8.18e^{-5}$, pval (amir1-8): $2.17e^{-5}$), indicating that the *amiRNA* construct is targeting *SYD*. Statistical significance threshold for two asterisks: pvalue ≤ 0.01, three asterisks: p-value ≤ 0.001. Error bars represent standard error in fold expression.

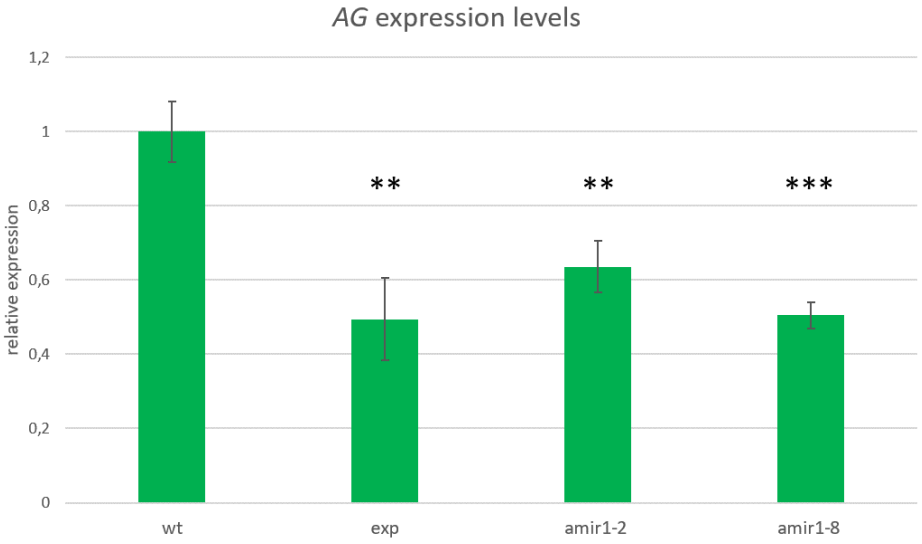

Figure 25: Relative expression levels of *AG* in inflorescences tissues of wt, *exp* and two *amiRSYD* lines. In both *exp* and *amiRSYD* backgrounds, *AG* has significantly reduced transcript levels. In *exp* and *amiRSYD1-8 AG* expression is halved, whereas in *amiRSYD1-2* the reduction is smaller, but still statistically significant (Student's t-test, pval (exp): 0.001, pval (amir1-2): 0.0015, pval (amir1-8): 0.0001). Expression of *AG* in *exp* indicates that *exp* has partial *SYD* loss of function, since *SYD* activates *AG* expression. Statistical significance threshold for two asterisks: pvalue ≤ 0.01, three asterisks: p-value ≤ 0.001. Error bars represent standard error in fold expression

phenotype. Secondly, amiRNA constructs, that are designed to be allele-specific knockouts (Schwab, 2006), have *exp*-like phenotype and reduced *SYD* expression, supporting that *amirSYD* are indeed *SYD*-specific.

To endorse the idea that *SYD* function is reduced in both *exp* and *amirSYD*, despite increased expression of *SYD* in *exp*, I analysed the expression of *AG* in inflorescence tissues of *C. hirsuta* wt, *exp* and *amiRSYD* T_2 lines (Figure 25). *AG*, a direct target of SYD in *A. thaliana*, has reduced expression in *A. thaliana syd* mutants (Wagner & Meyerowitz, 2002; Wu et al., 2012).

The relative expression of *AG* is decreased significantly in *exp* and both independent *amiRSYD* lines compared to wt (t-test, p-values for *exp* and *amir1-2* ≤ 0.01, p-value for *amir1-8* ≤ 0.001). *AG* transcription is reduced by half in *exp* and *amirSYD1-8* background, whereas the *amiRSYD1-2* line showed 40% expression decrease relative to wt. Confirming that *AG* expression is reduced in both *C. hirsuta* and *A. thaliana syd* mutants, indicates functional conservation of SYD between species. Moreover, expression of both *SYD* and *AG* in the *exp* background reveals that the increased level of *SYD* transcript does not cause a gain of *SYD* function in *exp*, since its downstream target has decreased transcription.

In this section I was able to mimic the *exp* phenotype by silencing *SYD* expression, suggesting that a reduction in *SYD* function is responsible for the *exp* phenotype. Multiple independent lines of *amiRSYD* present the same floral organ defects, such as extra petals and petal-sepal chimeras in whorl two, suggesting that *SYD* is indeed *EXP*. I showed that *amiRSYD* causes decreased expression of *SYD*, whereas *SYD* expression is elevated in *exp*. Finally, I provided further support that *exp* is a partial loss-of-function *SYD* allele by showing that a predicted target of *SYD* is downregulated in both *exp* and *amiRSYD* backgrounds.

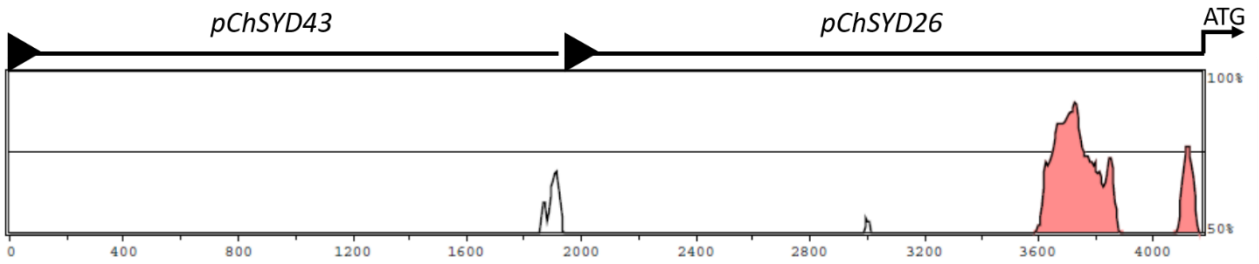

Figure 26: Comparative mVISTA analysis of *pChSYD26* and *pChSYD43* using *pAtSYD* as reference. Two *pAtSYD* sequence elements are highly (75%) conserved in the promoter *ChSYD*, located in the proximal to translation start codon. A third element, further upstream in *pSYD43* also shows high conservation (more than 50%).

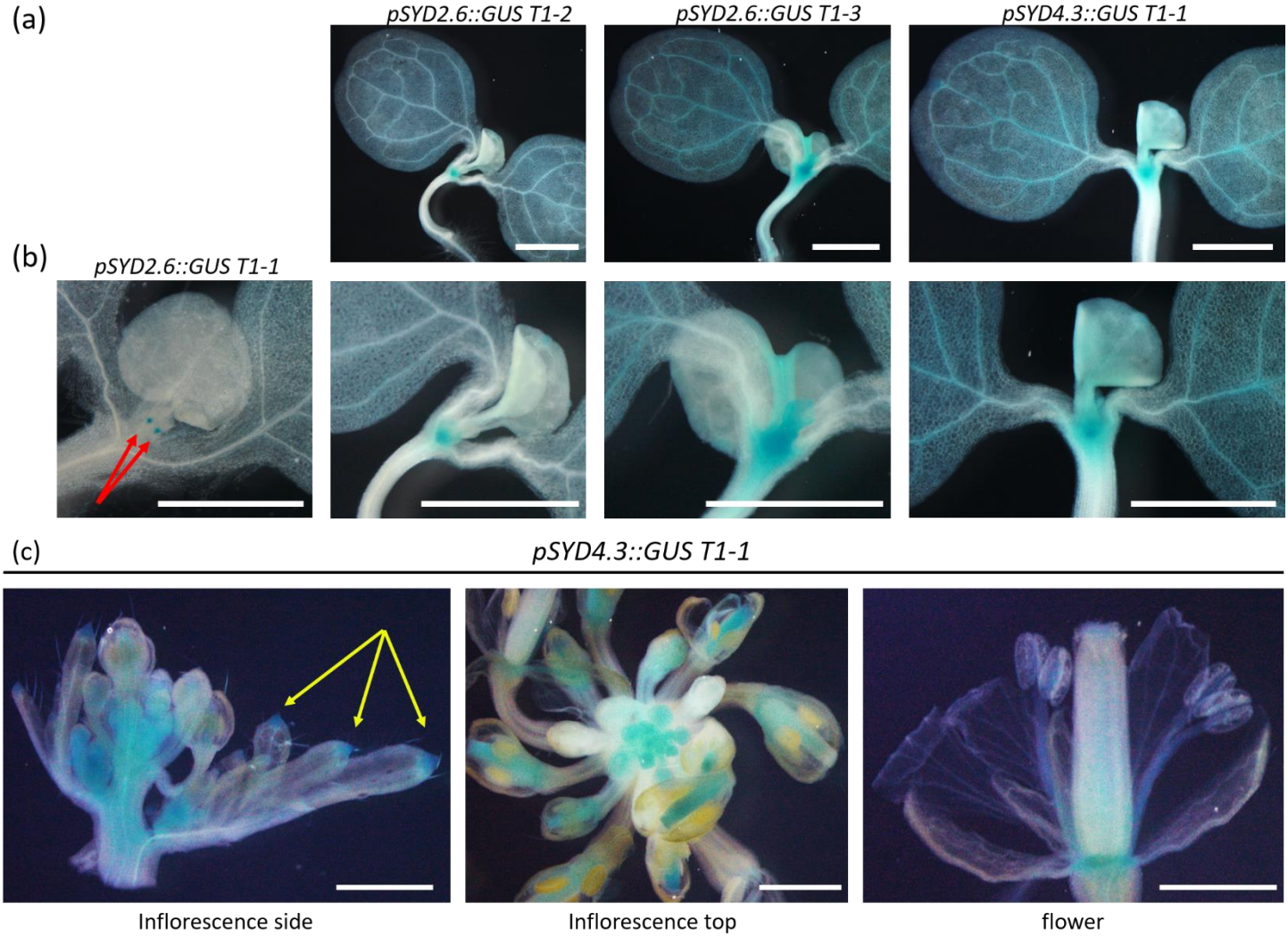

Figure 27: Expression of *pSYD26::GUS* and *pSYD43::GUS* in wt Ox seedlings. (a) 2-week old seedlings showing GUS expression in the cotyledons, shoot apex and SAM. The shoot apices are magnified in (b) to show that the expression pattern of *pSYD* varies from mild and highly specific in the shoot apex flanks (left panel, red arrows) to strong expression across the whole apex. No differences in expression were observed between the two promoters. Additionally, in (c) the expression of *pSYD43* in inflorescences is shown. GUS stain was found on the tops of cauline leaves (inflorescence side, yellow arrows) and in the IM (inflorescence top). Furthermore, *pSYD* is active in early-stage flowers (inflorescence top) that is suddenly lost and is expressed again in petals, stamens and carpels after floral organ outgrowth (inflorescence top, flower). Scale bar: 1mm

4.6 Expression analysis of *SYD* reporters

In this section, I investigate the expression pattern of *SYD* in different parts of the plant and during different developmental stages. A detailed expression analysis of *SYD* in *A. thaliana*, had previously localised *SYD* to rapidly dividing tissues throughout development; *SYD* is highly expressed in all plant meristems, but also in young leaf and flower primordia. During flower development, *SYD* is expressed in all whorls of stage 1 through to stage 3 flowers, and is later restricted to petals, stamens and carpels (Wagner & Meyerowitz, 2002).

The promoter sequence of *A. thaliana SYD* is 2.3kb long, and this sequence is sufficient to recapitulate the described mRNA expression of *SYD* (Su et al., 2006; Wagner & Meyerowitz, 2002). In *C. hirsuta,* the intergenic region between *SYD* and the previous gene is 4.3kb long (Gan et al., 2016). Sequence alignment between the promoters of *AtSYD* and *ChSYD* revealed high conservation of two regions proximal to the translation start codon of *SYD* (Figure 26). To analyse the expression pattern of *SYD* in *C. hirsuta*, I introduced both 4.3kb and 2.6kb promoters into wt *C. hirsuta* background as GUS (β-glucuronidase) reporters. In this way, I could compare the expression conferred by these different lengths of *SYD* promoter sequence to check whether one additional conserved region in the longer promoter sequence affected expression (Figure 26). T_1 transgenic plants containing the *pSYD::GUS* transgenes were subjected to histochemical staining for GUS activity. GUS expression was detected at the seedling stage with strongest expression in the shoot apex, weaker expression in the cotyledons, and no expression in the hypocotyl (Figure 27a,b). The most restricted expression domain, found in *pSYD2.6::GUS T1-1*, was limited to two spots at the shoot apex, possibly flanking the shoot apical meristem or young leaf primordia (Figure 27b). There was little discernable difference between the promoter activity of *pSYD2.6* and *pSYD4.3* at the seedling stage, so *pSYD4.3::GUS* was used to analyse expression in reproductive organs (Figure 27c).

There, GUS expression was detected in inflorescence shoots with strongest expression in the shoot apex, young floral primordia, axillary shoots, and the leaflet tips of cauline leaves (Figure 27c). In flowers, *ChSYD* expression shows both temporal and spatial specificity. It is expressed in early developing flowers (stage 1-3), similar to *AtSYD* (Wagner & Meyerowitz, 2002), but then the signal is lost in older flowers (stage 4-6), reappearing as floral organs grow out (Figure 27c). In these flowers, GUS expression was strongest in carpels, weaker in stamens and petals, and not detected in sepals. In summary, *ChSYD* is expressed in both vegetative and reproductive stages of development, and shows temporal and spatial specificity in *C.hirsuta* flowers, thus connecting the floral organ defects of *exp* with *SYD* expression in wild-type. Moreover, no differences in expression were observed between the short and long *pSYD* promoters.

4.7 Transgenic complementation of *exp with SYD* constructs

The *exp* mutant has a floral phenotype that includes extra petals in whorl two, floral organ identity defects in whorls two and three resulting in chimeric organs, and unfused carpel tips in whorl four. The co-segregation of the phenotype with a SNP located in an exon of *SYD*, together with the similar floral phenotype of plants with reduced *SYD* expression in *C. hirsuta* and *SYD* knockouts in *A. thaliana,* indicate that *exp* may be a mutant allele of *SYD* in *C. hirsuta*. In this section, I complement *exp* with two different *SYD* constructs to prove that *SYD* is *EXP*.

For transgenic complementation of *exp*, I designed different *SYD* constructs to test various hypotheses about *exp*. First, I investigated whether the genomic sequence of *ChSYD* fully complemented *exp*. Second, I investigated if SNP1 was responsible for the *exp* phenotype by introducing the *ChSYD* cDNA sequence, which contained the wild-type sequence for SNP1

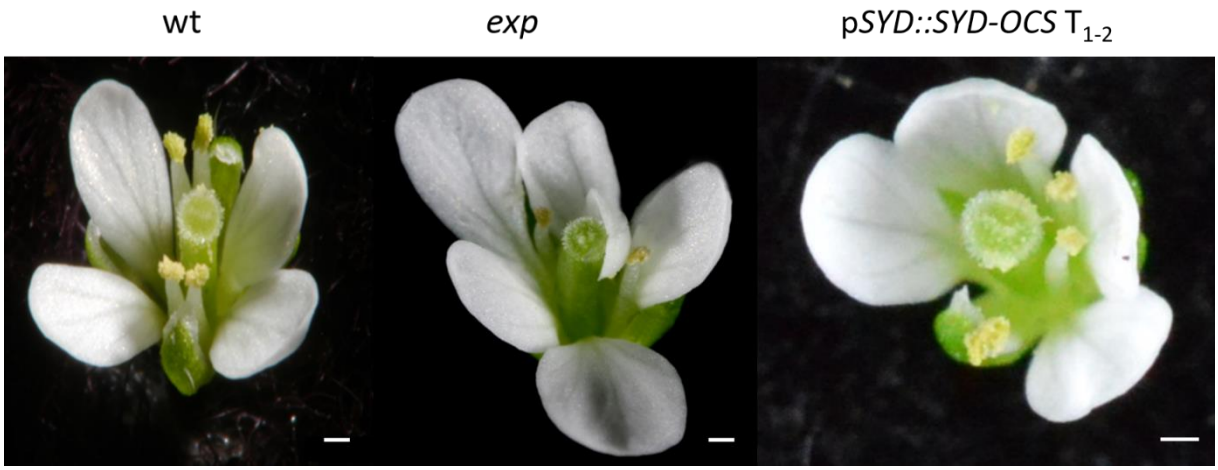

Figure 28: Flowers of *C. hirsuta* wt, *exp* and a transgene line carrying *pSYD::SYD-OCS* in *exp* background. The line shows wt-like characteristics, as no extra petals, no chimeric organs and no unfused carpel tips were present. Scale bar in all three panels is 100µm.

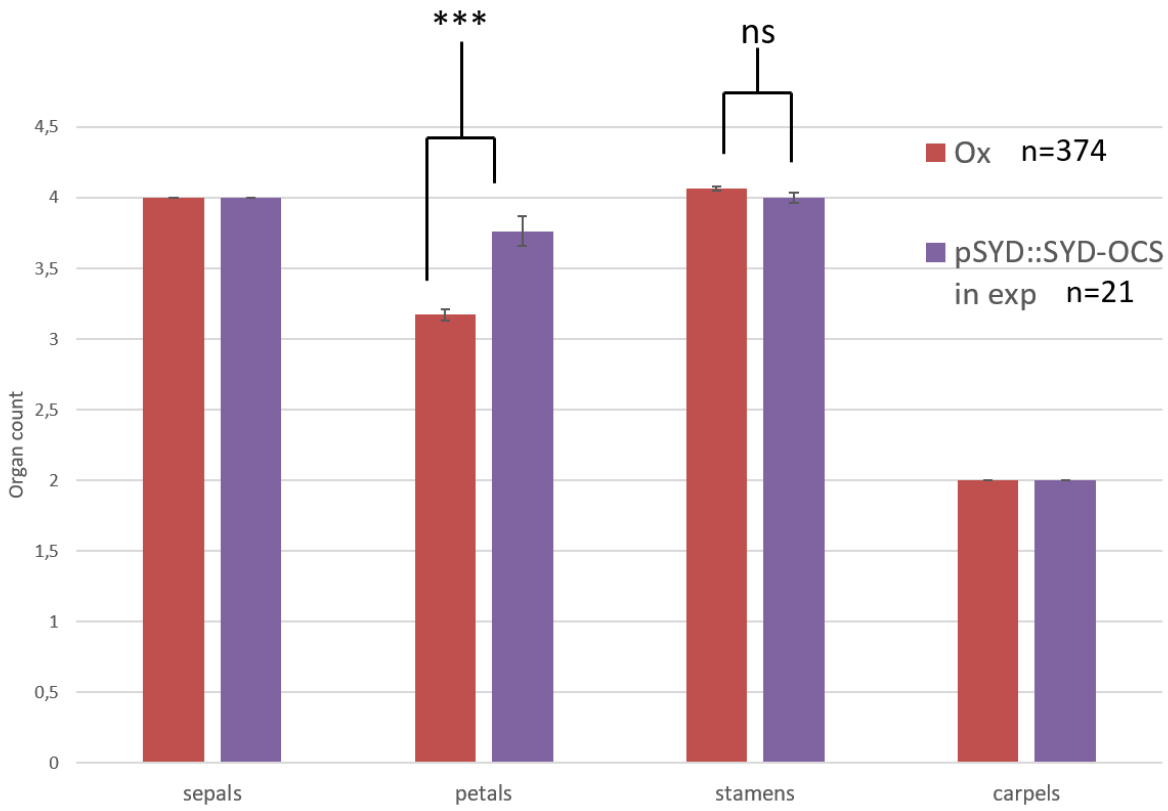

Figure 29: Floral organ count of *C. hirsuta* wt (in red) compared to a transgenic line carrying *pSYD::SYD-OCS* in *exp* background (in purple). In whorl one, sepal number remains stable in both wt and the transgene. In the second whorl, an average petal number below four was observed in the transgenic line, showing a similar trend as wt. Whorl three organ number do not differ significantly from wt. Flowers dissected in wt: 374, in *pSYD::SYD-OCS*: 21. Error bars indicate SEM. Statistical significance: three asterisks: p-value ≤ 0.001, ns: no significance.

but no intronic sequence. I used a truncated version of the *ChSYD* cDNA sequence as this had been shown to be sufficient to complement *syd* mutants in *A. thaliana* (Su et al., 2006).

For the first construct, a genomic *SYD* sequence was cloned from a *C. hirsuta* BAC clone (Hay, A. S. et al., 2014) into the the binary pPCV812 vector containing a mini-RK2 replicon (Koncz, C. et al., 1994; Koncz, C. & Schell, 1986). The *SYD* sequence contained the endogenous 2.6kb promoter containing all functionally conserved elements found in the *A. thaliana SYD* promoter (Figure 26) (Su et al., 2006). I obtained four independent transgenic lines expressing this construct. It is possible that the decreased transformation efficiency of *C. hirsuta* compared to *A. thaliana* (Hay, A. S. et al., 2014) together with the large construct size (approx. 28kb) contributed to this low number of transgenic lines. Three of the plants did not show any complementation, since their flowers were indistinguishable from the *exp* mutant. The floral phenotype of the fourth plant (*pSYD::SYD-OCS* $T_{1\text{-}2}$) resembled *C.hirsuta* wild-type (Figure 28). Careful examination of the flowers confirmed the absence of floral organ identity defects, extra petals, and unfused carpels found in *exp* (Figure 28). The flowers of *pSYD::SYD-OCS* $T_{1\text{-}2}$ contained an indistinguishable number of sepals, stamens and carpels to wild type flowers (Figure 29). In the second whorl, average petal number was less than four (3.76±0.11) and petal number per flower varied between 0 and 4, similar to wild-type flowers (Figure 29). The *pSYD::SYD-OCS* T1 plants were genotyped for a 1500bp region spanning between the genomic region of *SYD* and the OCS terminator to confirm the transgene presence. Only the wild-type looking plant carried the transgene (Figure 30). Also, the wt-looking plant was genotyped for SNP1, to confirm the *exp* background. However, the genotyping primers that I used could not distinguish between the endogenous *SYD* locus and the *SYD* transgene. This genotyping confirmed that the plant carried (at least) one mutant allele and (at least) one copy of the transgene (Figure 31). Assuming that the plant is homozygous for the *exp* mutation, this result

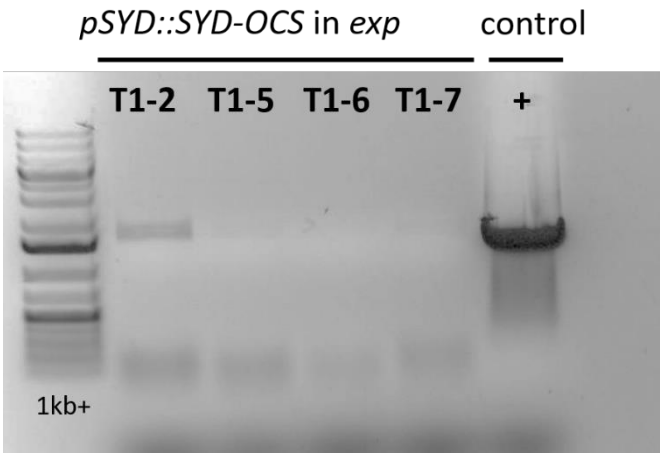

Figure 30: Genotyping of transgenic plants generated for *pSYD::SYD-OCS* construct in *exp* background. Expected is a 1.5kb fragment amplified between *SYD* and the *OCS* terminator sequence. The control sample was the generated vector. T1-2 was the only line that showed amplification of the sequence. As ladder, the GeneRuler 1kb+ was used.

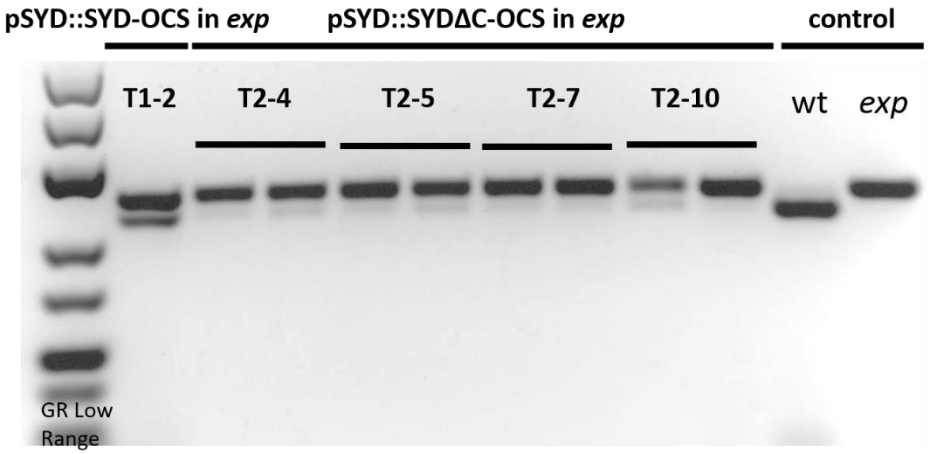

Figure 31: Genotyping for SNP1 mutation in all transgenes generated. The plant carrying *pSYD::SYD-OCS* (T1-2) and showed wt-like floral phenotype showed a digestion pattern similar to a plant heterozygous for *exp*, because it carries one *exp* allele and at least one copy of the transgene. The eight plants carrying the truncated *SYD* version (*pSYD::SYDΔC-OCS*) in the *exp* background exhibit mutant digestion profile because the forward primer used for genotyping anneals in an intron, so the transgene is not amplified and the mutant sequence remains by default undigested. As ladder, the GeneRuler Low Range was used.

shows that a genomic clone of *SYD* is sufficient to complement the *exp* mutant phenotype. The genotype of this plant will be confirmed by examining its selfed progeny to confirm that individuals not carrying the transgene are *exp* mutant. Therefore, *SYD* is very likely to be the gene responsible for the *exp* phenotype.

Although the previous result pinpoints the causal gene, the causal SNP still remains an open question due to the presence of two SNPs in the *SYD* locus in *exp*. To answer this, I used the cDNA sequence of *ChSYD* to create a truncated version (ChSYDΔC) that contained the wild-type version of SNP1, which is in exon 27, but not the wild-type version of SNP2, which is intronic. It was previously shown that two *SYD* transcripts are produced in *A. thaliana*, one full length and one containing only the biologically active N-terminus, which is around 5kb long (Su et al., 2006). Both versions, when introduced into *syd-2* null mutants, rescued the mutant phenotype, suggesting that the C-terminus is not required for activity but might have a negative regulatory role in *SYD* expression by controlling protein self-accumulation (Su et al., 2006).

Based on this information, I used 5kb of the *C. hirsuta SYD* cDNA expressed under the same 2.6kb promoter as before. I generated six independent transgenic lines, with four carrying a single copy of the transgene, which were then analyzed in the T2 generation. Plants were genotyped for both the presence of the truncated *SYD* version and for SNP1. All four lines carried the transgene and showed a homozygous *exp* digestion pattern for SNP1 (Figures 31 and 32). Because the forward primer anneals in an intron and the truncated SYD transgene is cDNA-based, it cannot be amplified. To phenotype these transgenic lines, flowers of three plants were scored per line. Each had wt-looking flowers, showing no obvious increase in petal number, floral organ identity defects, or unfused carpels (Figure 33). The flowers of *pSYD::SYDΔC* lines contained an indistinguishable number of sepals, stamens and carpels to

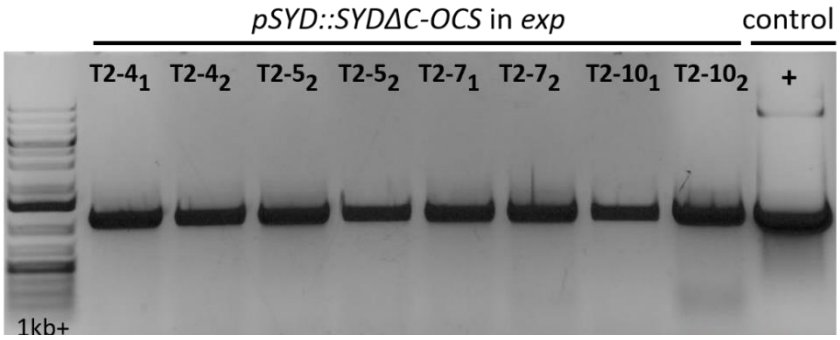

Figure 32: Amplification of transgenic *pSYD::SYDΔC-OCS* sequence introduced in *exp* plants. All transgenic lines showing wt-like phenotype had also the construct (four lines, two individuals per line checked). Expected amplicon size: 1.4kb. Positive control is the vector carrying *pSYD::SYDΔC-OCS*. As ladder, GeneRuler 1kb+ was used.

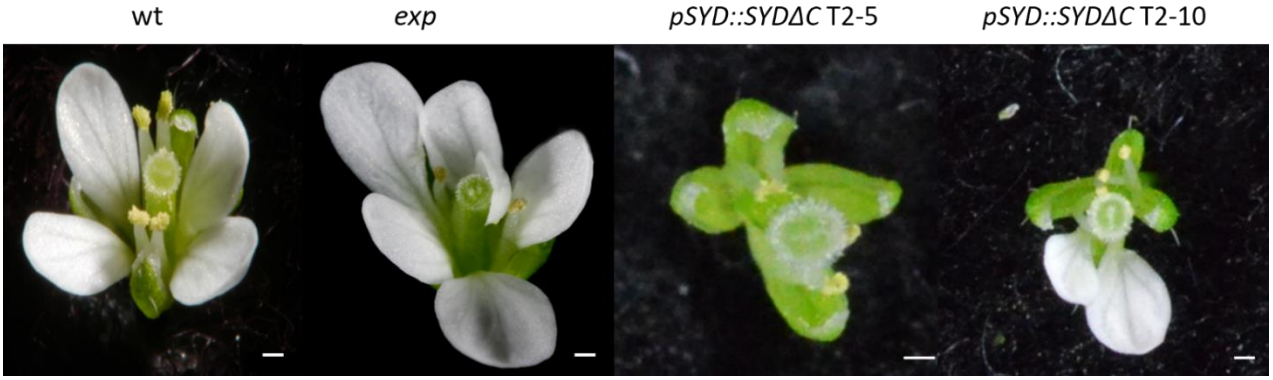

Figure 33: Comparison of floral characteristics between wt, *exp* and two independent lines of *pSYD::SYDΔC* in *exp* background. Both lines carrying the transgene show wt-like floral organization with no mutant floral characteristics. Moreover, plants in all lines have wt-like variable petal number in whorl 2. Scale bar: 100µm.

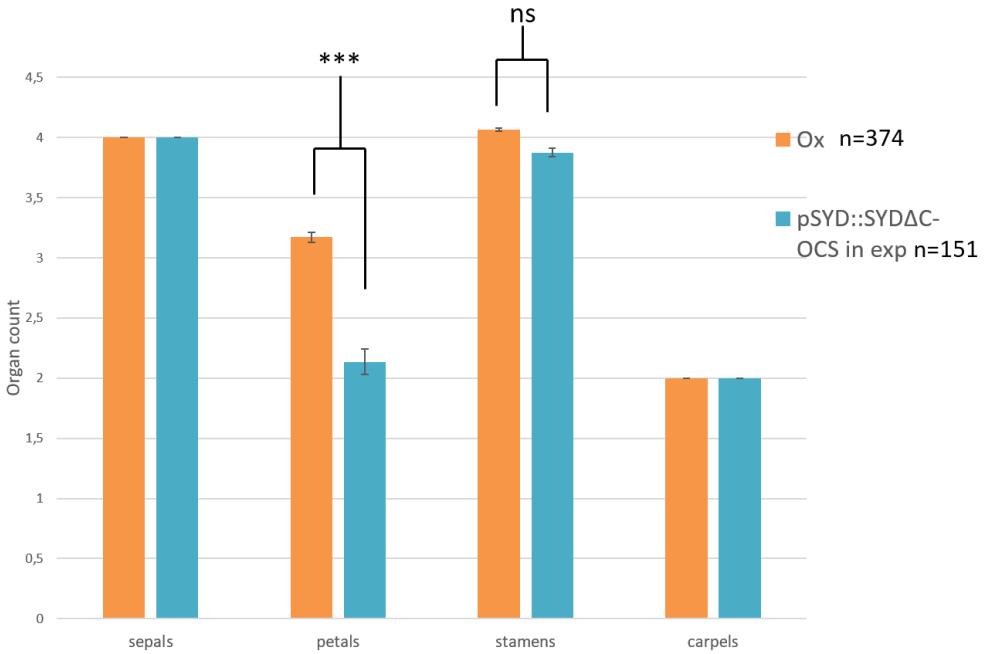

Figure 34: Floral organ count in *C. hirsuta* wt (Ox, in orange) and T_2 lines carrying *pSYD::SYDΔC-OCS* in *exp* background (in blue). Sepal number in both groups remains stable, whereas petal number average in the transgenic lines is reduced to 2.14 (±0.10). In whorl 3 and whorl 4 stamen and carpel number, respectively, show no significant change between wt and the transgenes.

wild type flowers (Figure 34). In the second whorl, average petal number was less than four (2.14±0.1) and petal number per flower varied between 0 and 4, similar to wild-type flowers (Figure 34). Moreover, petal number per flower decreased as plants aged in a similar manner to wild type (Monniaux et al., 2016; Pieper et al., 2016).

In summary, I discovered that *exp* is a mutant allele of *SYD*. This is supported by the presence of a SNP in the gene that co-segregates with the *exp* phenotype. Moreover, when *SYD* is mutated in both *A. thaliana* and *C. hirsuta*, plants tend to show a similar phenotype to *exp* mutants. Furthermore, the expression pattern of *SYD* supports the floral phenotypes observed in the *exp* mutant. Adding back *SYD* to *exp* reverts the phenotype back to wt. Finally, the complementation of *exp* by the *SYDΔC* construct establishes two important facts. First, it strongly suggests that SNP1 in exon 27 of *SYD* is the causal mutation for the *exp* phenotype. Second, it shows that the N-terminus of SYD is the functional part of the protein, similar to *A. thaliana*, and is sufficient to complement *exp*.

Chapter 5

General discussion

5.1 Is *exp* a *SYD* mutant?

The project had as a main goal to characterize the recessive *exp* mutant in *C.hirsuta*. In the two chapters of results, have presented evidence that SYD, an ATP-dependent chromatin remodelling factor, is the causal gene underlying the *exp* phenotype. The *exp* flowers showed a variety of floral organ defects, such as extra organs in whorl two, presence of organ chimeras in whorls two and three, and unfused carpel tips. To understand the molecular basis of *exp*, plants were sequenced to identify point mutations linked to the *exp* allele. Two linked SNPs mapped to the annotated homolog of *AtSYD*. SNP1, located in exon 27, co-segregated with the *exp* phenotype in a segregating population. Additionally, expression of amiRNA against *SYD* produced floral phenotypes similar to *exp*. A comparable phenotype was also observed in *syd-2*, a null mutant in *A. thaliana*¸ indicating that SYD function may be conserved between species. To confirm that a mutated allele of *SYD* is responsible for *exp*, I re-introduced *ChSYD* in the *exp* background, resulting in flowers with wt-like characteristics. Moreover, a truncated version of *ChSYD* that contained only the functional N-terminal of the protein, including the wt amino acid affected by SNP1, was sufficient to rescue the *exp* phenotype, suggesting that SNP1 is the causal mutation underlying the *exp* phenotype. Here, I will discuss the evidence supporting this claim and interpret the extra petals found in *exp* in the context of SYD function in chromatin remodelling.

The *exp* mutant was discovered in a genetic screen for *C. hirsuta* plants with extra petals and the causal SNP responsible for this phenotype was identified using a NGS mapping strategy (Hartwig, 2012; James et al., 2013; Schneeberger et al., 2009). For this purpose, the mutant was backcrossed to its non-mutagenized progenitor (*C. hirsuta* Ox genotype) and then selfed, followed by sequencing of bulked *exp* and Ox plants. These F_2 individuals form an isogenic mapping population in which only EMS-induced mutations are segregating (Hartwig,

2012). The causal mutation and linked SNPs are expected to be fixed in the mutant DNA pool because plants have been selected for the *exp* mutation (James et al., 2013). This approach usually requires approximately 50 plants in each bulked sample and 50x sequence coverage to produce good mapping results in *A. thaliana* (James et al., 2013). However, by using only 35 plants in each bulked sample from a twice backcrossed population, we achieved highly accurate mapping results in *C. hirsuta* with a custom algorithm analysis by X. Gan, since the SNP with the highest p-value was found to be causal for the *exp* phenotype.

The claim that *exp* is caused by a mutation in *SYD* was further supported by recapitulating the *exp* phenotype in *amiR-SYD* plants. *SYD* transcript was partially silenced in four individual T_2 lines expressing *amiRSYD* and each line showed similar floral defects. Similar to *exp* mutants, these plants had extra organs arising from whorl two, no significant difference in organ number in whorl three, chimeric organs in whorls two and three and unfused carpel tips in whorl four (Figures 9,23). The fact that floral phenotypes in *amiRSYD* lines were no more severe that *exp*, together with approximately a 50% reduction in *SYD* transcript in these lines (Figure 24), indicates a weak silencing of *SYD*. Moreover, *exp* appears to be a weak allele of *SYD*, not only due to phenotypic similarities with *amiRSYD* lines, but also since SNP1 causes an amino acid change rather than a premature stop codon. Examining the protein levels of SYD in both *exp* and *amiRSYD* backgrounds to confirm whether SYD levels are reduced compared to wild type, would be one way to validate whether SYD activity is reduced in these genotypes. Moreover, this experiment might help us to understand why the loss-of-function *exp* allele has elevated *SYD* expression. A possible explanation for increased expression may be the overaccumulation of non-functional transcript or the presence of an inactive protein conformation due to the *exp* mutation. For example, a mechanism was discovered for *Rhp26* autoregulation, a member of SWI2/SNF2 subfamily in *S. pombe*, whereby specific interactions

between conserved N-terminal motifs with the core ATPase domains autoinhibit *Rhp26* activity (Wang, 2014). In conclusion, phenocopying *exp* by silencing *SYD* expression in *amiRSYD* transgenics provides additional evidence that *SYD* loss of function causes the *exp* phenotype, but also indicates that *exp* is probably a weak allele of *SYD*. Further phenotypic comparisons with a null allele of *SYD* may be informative regarding the regulation of petal number by SYD in *C. hirsuta*.

Complementation of the *exp* phenotype by constructs expressing both the truncated and full-length version of SYD, validated that an exonic SNP in *SYD* caused the *exp* phenotype in *C. hirsuta*. Comparison with the well-characterized *SYD* locus in *A. thaliana* suggested a high degree of conservation of *SYD* function between *A. thaliana* and *C. hirsuta*. For example, *exp* and *syd-2* flowers had many shared characteristics (extra organs in whorl two, chimeras in whorls two and three, unfused carpels) and only diverged significantly in the increased sepal number found in *syd-2* (Figures 6, 7, 16a). Moreover, the reduced level of *AG* transcripts in *exp* (Figure 13b), suggest that this direct target of *SYD*, functioning with *LFY*, in *A. thaliana*, may be shared in *C. hirsuta* (Wagner & Meyerowitz, 2002; Wu et al., 2012). Thus, *SYD* gene function seems to be conserved between *A. thaliana* and *C. hirsuta*.

Chromatin remodeling is a process controlled by many genes and therefore affects many developmental pathways. In eukaryotic organisms, every somatic cell carries one or multiple copies of its whole genome; to achieve such dense DNA “packaging”, the sequence is wrapped around an octamer of proteins called histones (H2A, H2B, H3 and H4), that is then folded into higher order chromatin fibers. Apart from condensing DNA, chromatin creates mechanistic and biochemical restrictions that influence the access of regulatory proteins that activate gene expression or other processes such as replication, recombination and repair (Kadam et al., 2002). These attributes are controlled by different categories of nucleosome-

modifying and -remodelling complexes (Saha et al., 2006). The latter category includes SWItch/Sucrose Non Fermentable (SWI/SNF) -related ATP-dependent chromatin remodelers that work in multiprotein complexes and use the energy of ATP hydrolysis to alter the chromatin conformation in the cell (Vignali, 2000). In *A. thaliana*, four ATPases have been identified: SYD, BRM, MINU1 and MINU2 (Farrona et al., 2004; Sang, 2012; Wagner & Meyerowitz, 2002). Previous research into SYD and BRM function has shown that these chromatin remodelers interact with various components influencing floral development (Figure 35) (Bezhani et al., 2007; Han, 2015; Kwon et al., 2005; Kwon et al., 2006; Wagner & Meyerowitz, 2002; Wu et al., 2012; Wu et al., 2015). These interactions suggest that chromatin remodeling factors may coordinate pathways that direct floral meristem formation and floral organ initiation, including petals. However, the regulation of petal number by SYD and BRM was not well characterized in previous work.

These two SNF2 ATPases in *A. thaliana*, *SYD* and *BRM*, show high functional redundancy, despite their low overall sequence similarity (approximately 40%) (Bezhani et al., 2007; Sarnowska et al., 2016; Wu et al., 2012). Therefore, it is interesting that some of the floral phenotypes of *exp* in *C. hirsuta*, such as chimeric petal/sepal organs and gynoecium defects, were also found in *syd-2* (this study and (Wagner & Meyerowitz, 2002)) and *brm* alleles (Farrona et al., 2004) in *A. thaliana*. However, the floral phenotypes of *syd* and *brm* mutants in *A. thaliana* also differ, indicating that these paralogous genes have some distinct functions during flower development (Hurtado et al., 2006; Wagner & Meyerowitz, 2002). In particular, the hypomorphic allele, *syd-1*, and the null allele, *syd-2*, were both reported to show elevated petal number (Wagner & Meyerowitz, 2002), similar to *exp* and *amiRSYD*, whereas the hypomorphic allele, *brm-1,* and the null allele, *brm-2*, had normal petal number but reduced petal size (Hurtado et al., 2006). Mutant alleles of *brm* were recently isolated in

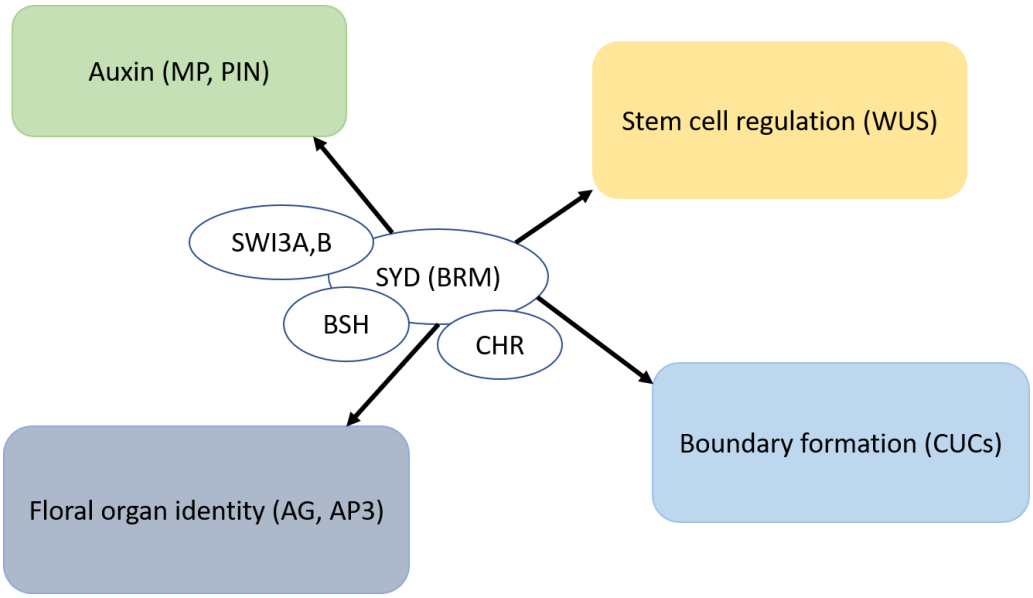

Figure 35: *SYD* and *BRM* interactions with pathways connected to petal number. *SYD* and *BRM* were shown to be necessary for auxin-responsive gene expression as key regulators in flower primordia initiation (Wu et al., 2015). Moreover, *SYD* was identified as directly activating WUS, maintaining proper WUS transcript levels in its expression domain (Kwon et al., 2005). BRM and SYD were also found to promote expression of *CUC* genes, regulators of boundary formation (Kwon et al., 2006). The importance of chromatin remodeling in flowers was highlighted by *SYD*-mediated activation of BC genes via *LFY* (Wu et al., 2012). *SWI3A/B*, *BSH* (*BUSHY*) and *CHR* (*CHROMATIN REMODELING*) are chromatin remodeling co-factors essential for complex activity (Sarnowska et al., 2016).

C. hirsuta by the Tsiantis group (personal communication), which will allow a direct comparison of SYD and BRM functions both within *C. hirsuta* and between *C. hirsuta* and *A. thaliana*. In particular, it will be interesting to compare the role of these SWI2/SNF2 ATPases in regulating petal number between species.

Multiple pathways influence petal number in *A. thaliana*, including stem cell regulation (Brand, 2000; Fletcher, 2001; Fletcher et al., 1999), auxin distribution (Lampugnani 2013), regulators of *AG* (Das et al., 2009; Maier et al., 2009; Running & Meyerowitz, 1996), and organ boundary formation (Baker et al., 2005; Huang et al., 2012). Interestingly, *SYD* has been implicated with most of these pathways in *A. thaliana* as part of chromatin complexes (Figure 35). Therefore, understanding the functional conservation of SYD in *C. hirsuta* would require identifying the protein complexes in which SYD acts, comparing the homology of these interaction partners with those in *A. thaliana.* To investigate the possibility that *SYD* contributes to the difference in petal number between *C. hirsuta* and *A. thaliana*, it would be useful to not only validate known SYD partners in *C. hirsuta*, but also to identify novel interactions by Y2H screens or other proteomic techniques.

5.2 Genetic machinery controlling petal number in *C. hirsuta*

Comparative genetic studies between the related species, *A. thaliana* and *C. hirsuta*, have proved to be a useful approach to understand morphological evolution (Gan et al., 2016; Hofhuis et al., 2016; Vlad et al., 2014). Moreover, exploiting the variation in petal number within natural *C. hirsuta* populations (Monniaux et al., 2016; Pieper et al., 2016) and between *C. hirsuta* and *A. thaliana*, provides a unique opportunity to study the genetic basis of petal number variation both within and between species. For example, recent findings have shown that temporal plant ageing together with multiple QTLs have an effect on average petal number in *C. hirsuta* (Monniaux et al., 2016; Pieper et al., 2016) and that *ChAP1* activation is fully dependent on *LFY*, compared to *A. thaliana*, possibly due to mutations in the *AP1* CArG box sequence (Monniaux et al., 2017). Consequently, comparison of closely related species, combining genomic and morphological differences, may provide insights to understand phenotypic diversity.

Petal number is a robust phenotype in *A. thaliana*, but in *C. hirsuta* this robustness is lost and petal number varies in response to genetic, environmental, and stochastic variation (Monniaux et al., 2016; Pieper et al., 2016). Characterization of the *exp* mutant in this project, establishes a function for SYD chromatin remodelling complexes in petal number control in *C. hirsuta*. Strict control of petal number may have reduced significance in predominantly selfing species such as *A. thaliana* and *C. hirsuta* (Hay, A. S. et al., 2014), allowing for the possibility that pathways controlling petal number could have diverged as part of the selfing syndrome in *C. hirsuta*. The generation and characterization of null alleles of *SYD* in *C. hirsuta* will be important to fully understand the effect of eliminating *SYD* function in the *C. hirsuta* flower. For example, extra petals may be a more obvious feature of the less pleiotropic *exp* allele, than of the null *syd-2* allele in *A. thaliana*, which has a more pleiotropic phenotype. In

conclusion, SYD chromatin remodelling complexes may provide a “structural” component of floral development pathways that provides a degree of both conservation and divergence during floral evolution.

Variability of floral form in angiosperms was previously examined mostly under a comparative and phylogenetic prism, mainly focused on the evolution of floral bauplan between and within families, but also on tracing back morphological characteristics of modern angiosperms to ancestral flowers (Endress, 1987, 1992, 1994; Endress et al., 2009; Ronse De Craene, 2010). More recent studies are directed towards understanding the genomic evolution of master regulators, for example ABCE genes (Kramer, 2007; Kramer et al., 1998; Lee, 2011; Liu, C. J. et al., 2010; Parenicova, 2003), to uncover connections leading to evolution of floral form (Chanderbali et al., 2016; Chanderbali et al., 2010). Comparative studies of trait differences between related species, such as petal number variation between *C. hirsuta* and *A. thaliana*, combined with intensive genomics studies within the Brassicaceae family, provides a context to understand trait diversity within the larger context of the Brassicaceae.

References

Aida, M., Ishida, T., Fukaki, H., Fujisawa, H., & Tasaka, M. (1997). Genes lnvolved in Organ Separation in Arabidopsis: An Analysis of the cup-shaped cotyledon Mutant. *Plant Cell, 9*, 841-857.

Aida, M., Tasaka, M. (2006). Genetic control of shoot organ boundaries. *Curr Opin Plant Biol, 9*, 72-77.

Al-Shehbaz, I. A. (2010). *Flora of North America North of Mexico, Volume 7: Magnoliophyta: Dilleniidae, Part 2*. New York: Oxford University Press.

Alvarez, J., Guli, C. L., Yu, X. H., & Smyth, D. R. (1992). *terminal flower*: a gene affecting inflorescence development in *Arabidopsis thaliana*. *The Plant Journal, 2*, 103-116.

Alvarez, J., Smyth, D. R. (1999). *CRABS CLAW* and *SPATULA*, two *Arabidopsis* genes that control carpel development in parallel with *AGAMOUS*. *Development, 126*, 2377-2386.

Alvarez, J. P., Pekker, I., Goldshmidt, A., Blum, E., Amsellem, Z., & Eshed, Y. (2006). Endogenous and synthetic microRNAs stimulate simultaneous, efficient, and localized regulation of multiple targets in diverse species. *Plant Cell, 18*, 1134-1151.

Andrés, F., & Coupland, G. (2012). The genetic basis of flowering responses to seasonal cues. *Nat Rev, 13*, 627-639.

Bainbridge, K., Guyomarc'h, S., Bayer, E., Swarup, R., Bennett, M., Mandel, T., & Kuhlemeier, C. (2008). Auxin influx carriers stabilize phyllotactic patterning. *Genes & Development, 22*(810-823).

Baker, C. C., Sieber, P., Wellmer, F., & Meyerowitz, E. M. (2005). The *early extra petals1* mutant uncovers a role for microRNA *miR164c* in regulating petal number in *Arabidopsis*. *Curr Biol, 15*(4), 303-315. doi:10.1016/j.cub.2005.02.017

Barkman, T. J., Chenery G., McNeal J. R., Lyons-Weiler J., Elisens W.J., Moore G., Wolfe, A. D., & dePamphilis, C. W. (2000). Independent and combined analyses of sequences from all three genomic compartments converge on the root of flowering plant phylogeny. *Proc Natl Acad Sci U S A, 97*, 13166 - 13171.

Barkoulas, M., Hay, A., Kougioumoutzi, E., & Tsiantis, M. (2008). A developmental framework for dissected leaf formation in the *Arabidopsis* relative *Cardamine hirsuta*. *Nat Genet, 40*, 1136-1141.

Bateman, R. M., Hilton, J., & Rudall, P. J. (2006). Morphological and molecular phylogenetic context of the angiosperms: contrasting the 'top-down' and 'bottom-up' approaches used to infer the likely characteristics of the first flowers. *J Exp Bot, 57*, 3471-35003.

Baum D. A., & Hileman, L. C. (2006). *A developmental genetic model for the origin of the flower.* . Sheffield, UK: Blackwell.

Benková, E., Michniewicz, M., Sauer, M., Teichmann, T., Seifertová, D., Jürgens, G., & Friml, J. (2003). Local, Efflux-Dependent Auxin Gradients as a Common Module for Plant Organ Formation. *Cell, 115*, 591-602.

Bennett, M. J., Marchant, A., Green, H. G., May, S. T., Ward, S. P., Millner, P. A., Walker, A. R., Schulz, B., & Feldmann, K. A. (1996). *Arabidopsis AUX1* Gene: A Permease-Like Regulator of Root Gravitropism. *Science, 273*, 948-950.

Bennett, S. R. M., Alvarez, J., Bossinger, G., & Smyth, D. R. (1995). Morphogenesis in pinoid mutant of *Arabidopsis thaliana*. *The Plant Journal, 8*, 505-520.

Bergonzi, S., Albani, M. C., Ver Loren van Themaat, E., Nordstrom, K. J., Wang, R., Schneeberger, K., Moerland, P. D., & Coupland, G. (2013). Mechanisms of age-dependent response to winter temperature in perennial flowering of *Arabis alpina*. *Science, 340*, 1094-1097.

Bezhani, S., Winter, C., Hershman, S., Wagner, J. D., Kennedy, J. F., Kwon, C. S., Pfluger, J., Su, Y., & Wagner, D. (2007). Unique, shared, and redundant roles for the Arabidopsis SWI/SNF chromatin remodeling ATPases *BRAHMA* and *SPLAYED*. *Plant Cell, 19*(2), 403-416. doi:10.1105/tpc.106.048272

Blein, T., Pulido, A., Vialette-Guiraud, A., Nikovics, K., Morin, H., Hay, A., Johansen, I. E., Tsiantis, M., & Laufs, P. (2008). A Conserved Molecular Framework for Compound Leaf Development. *Science, 322*, 1835-1839.

Bossinger, G., & R., S. D. (1996). Initiation patterns of flower and floral organ development in *Arabidopsis thaliana*. *Development, 122*, 1093-1102.

Bowman, J. L. (1994). *An atlas of morphology and development* (1st ed.). New York, USA: Springer-Verlag.

Bowman, J. L., Alvarez, J., Weigel, D., Meyerowitz, E. M., & Smyth, D. R. (1993). Control of flower development in Arabidopsis thaliana by APETALA1 and interacting genes. . *Development, 119*, 721-743.

Bowman, J. L., Drews, G. N., & Meyerowitz, E. M. (1991). Expression of the Arabidopsis Floral Homeotic Gene *AGAMOUS* Is Restricted to-Specific Cell Types Late in Flower Development. *The Plant Cell, 3*, 749-758.

Bowman, J. L., & Smyth, D. R. (1999). *CRABS CLAW*, a gene that regulates carpel and nectary development in *Arabidopsis*, encodes a novel protein with zinc finger and helix-loop-helix domains. *Development, 126*, 2387-2396.

Bowman, J. L., Smyth, D. R., & Meyerowitz, E. M. (1989). Genes Directing Flower Development in *Arabidopsis*. *The Plant Cell, 1*, 37-52.

Bradley, D. (1997). Inflorescence Commitment and Architecture in *Arabidopsis*. *Science, 275*(5296), 80-83. doi:10.1126/science.275.5296.80

Brand, U., Fletcher, J. C., Hobe, M., Meyerowitz, E. M., Simon, R. (2000). Dependence of Stem Cell Fate in Arabidopsis on a Feedback Loop Regulated by *CLV3* Activity. *Science, 289*, 617-619.

Brewer, P. B., Howles, P. A., Dorian, K., Griffith, M. E., Ishida, T., Kaplan-Levy, R. N., Kilinc, A., & Smyth, D. R. (2004). *PETAL LOSS*, a trihelix transcription factor gene, regulates perianth architecture in the *Arabidopsis* flower. *Development, 131*(16), 4035-4045. doi:10.1242/dev.01279

Causier, B., Schwarz-Sommer, Z., & Davies, B. (2010). Floral organ identity: 20 years of ABCs. *Semin Cell Dev Biol, 21*(1), 73-79. doi:10.1016/j.semcdb.2009.10.005

Champier, G., Hantz, S., Couvreux, A., Stuppfler, S., Mazeron, M.C., Bouaziz, S., Denis, F., Alain, S. (2007). New functional domains of human cytomegalovirus pUL89 predicted by sequence analysis and three-dimensional modelling of the catalytic site DEXDc. *Antiviral therapy, 12*, 217.

Chanderbali, A. S., Berger, B. A., Howarth, D. G., Soltis, P. S., & Soltis, D. E. (2016). Evolving Ideas on the Origin and Evolution of Flowers: New Perspectives in the Genomic Era. *Genetics, 202*(4), 1255-1265. doi:10.1534/genetics.115.182964

Chanderbali, A. S., Yoo, M.-J., Zahn, L. M., Brockington, S. F., Wall, P. K., Gitzendanner, M. A., Albert, V. A., Leebens-Mack, J., Altman, N. S., Ma, H., dePamphilis, C. W., Soltis, D. E., & Soltis, P. S. (2010). Conservation and canalization of gene expression during angiosperm diversification accompany the origin and evolution of the flower. *Proc Natl Acad Sci U S A, 107*, 22570–22575.

Chen, L., Cheng, J. C., Castle, L., & Sung, Z. R. (1997). *EMF* Genes Regulate Arabidopsis lnflorescence Development. *The Plant Cell, 9*, 2011-2024.

Chen, X. (2004). A microRNA as a translational repressor of APETALA2 in Arabidopsis flower development. *Science, 303*(5666), 2022-2025. doi:10.1126/science.1088060

Cheng, Y., Dai, X., & Zhao, Y. (2006). Auxin biosynthesis by the YUCCA flavin monooxygenases controls the formation of floral organs and vascular tissue in *Arabidopsis*. *Genes & Development, 20*, 1790-1799.

Chuang, C. F., Running, M. P., Williams, R. W., & Meyerowitz, E. M. (1999). The *PERIANTHIA* gene encodes a bZIP protein involved in the determination of floral organ number in *Arabidopsis thaliana*. *Genes & Development, 13*, 334-344.

Clark, S. E., Jacobsen, S. E., Levin, J. Z., & Meyerowitz, E. M. (1996). The CLAVATA and SHOOT MERISTEMLESS loci competitively regulate meristem activity in Arabidopsis. *Development, 122*, 1567-1575.

Cnops, G., Jover-Gil, S., Peters, J. L., Neyt, P., De Block, S., Robles, P., Ponce, M. R., Gerats, T., Micol, J. L., & Van Lijsebettens, M. (2004). The rotunda2 mutants identify a role for the LEUNIG gene in vegetative leaf morphogenesis. *Journal of Experimental Botany, 55*, 1529-1539.

Coen, E. S., & Meyerowitz, E. M. (1990). The war of the whorls: genetic interactions controlling flower development. *Nature, 353*, 31-37.

Crane, P. R. (1985). Phylogenetic analysis of seed plants and the origin of angiosperms. *Ann Missouri Bot Gard, 72*, 716-793.

Crewal, S. I., & Elgin, S. C. (2002). Heterochromatin: new possibilities of the inheritance of structure. *Curr Opin Genet Dev, 12*, 178-187.

Darwin, C. R. (1859). *On the origin of species by means of natural selection, or the preservation of favoured races in the struggle for life*. London, UK: John Murray.

Das, P., Ito, T., Wellmer, F., Vernoux, T., Dedieu, A., Traas, J., & Meyerowitz, E. M. (2009). Floral stem cell termination involves the direct regulation of *AGAMOUS* by *PERIANTHIA*. *Development, 136*(10), 1605-1611. doi:10.1242/dev.035436

Daum, G., Medzihradszky, A., Suzaki, T., & Lohmann, J. U. (2014). A mechanistic framework for noncell autonomous stem cell induction in *Arabidopsis*. *Proc Natl Acad Sci U S A, 111*, 14619–14624.

Davies, B., Egea-Cortines, M., de Andrade Silva, E., Saedler, H., & Sommer, H. (1996). Multiple interactions amongst floral homeotic MADS box proteins. *The EMBO Journal, 15*, 4330-4343.

Dinneny, J. R., Yadegari, R., Fischer, R. L., Yanofsky, M. F., & Weigel, D. (2004). The role of JAGGED in shaping lateral organs. *Development, 131*, 1101-1110.

Ditta, G., Pinyopich, A., Robles, P., Pelaz, S., & Yanofsky, M. F. (2004). The SEP4 gene of Arabidopsis thaliana functions in floral organ and meristem identity. *Curr Biol, 14*(21), 1935-1940. doi:10.1016/j.cub.2004.10.028

Dodd, M. E., Silvertown, J., & Chase, M. W. (1999). Phylogenetic analysis of trait evolution and species diversity variation among angiosperm families. *Evolution, 53*, 732-744.

Doyle, J. A. (2008). Integrating Molecular Phylogenetic and Paleobotanical Evidence on Origin of the Flower. *International Journal of Plant Sciences, 169*(7), 816-843. doi:10.1086/589887

Doyle, J. A., & Donoghue, M. J. (1986). Seed plant phylogeny and the origin of angiosperms: an experimental cladistic approach. *Bot Rev, 52*, 321-431.

Drews, G. N., Bowman, J. L., & Meyerowitz, E. M. (1991). Negative regulation of the Arabidopsis homeotic gene AGAMOUS by the APETALA2 product. *Cell, 65*, 991-1002.

Edgar, R. C. (2004). MUSCLE: multiple sequence alignment with high accuracy and high throughput. *Nucleic Acids Res, 32*, 1792-1797.

Edrizzi, K., Moussian, B., Haecker, A., Levin, J. Z., & Laux, T. (1996). The SHOOT MERISTEMLESS gene is required for maintenance of undifferentiated cells in Arabidopsis shoot and floral meristems and acts at a different regulatory level than the meristem genes WUSCHEL and ZWILLE. *The Plant Journal, 10*, 967-979.

Edwards, k. J., Mogg, R. (2001). Plant Genotyping by Analysis of Single Nucleotide Polymorphisms. In H. R. Wallingford (Ed.), *Plant Genotyping: The DNA Fingerprinting of Plants.*: CABI Publishing.

Endress, P. K. (1987). Floral phyllotaxis and floral evolution. *Bot Jahrb Syst, 108*, 417-438.

Endress, P. K. (1990). Patterns of floral construction in ontogeny and phylogeny. *Biological Journal of the Linnean Society, 39*, 153-175.

Endress, P. K. (1992). Evolution and Floral Diversity: The Phylogenetic Surroundings of Arabidopsis and Antirrhinum. *Int J Plant Sci, 153*, 106-122.

Endress, P. K. (1994). Floral structure and evolution of primitive angiosperms: recent advances. *Pl. Syst. Evol., 192*, 79-97.

Endress, P. K. (2011). Evolutionary diversification of the flowers in Angiosperms. *American Journal of Botany, 98*, 370-396.

Endress, P. K., & Doyle, J. A. (2009). Reconstructing the ancestral angiosperm flower and its initial specializations. *Am J Bot, 96*(1), 22-66. doi:10.3732/ajb.0800047

Eshed, Y., Baum, S. F., & Bowman, J. L. (1999). Distinct Mechanisms Promote Polarity Establishment in Carpels of *Arabidopsis*. *Cell, 99*, 199-209.

Eshed, Y., Baum, S. F., Perea, J. V., & Bowman, J. L. (2001). Establishment of polarity in lateral organs of plants. *Curr Biol, 11*, 1251-1260.

Eshed, Y., Izhaki, A., Baum, S. F., Floyd, S. K., & Bowman, J. L. (2004). Asymmetric leaf development and blade expansion in *Arabidopsis* are mediated by KANADI and YABBY activities. *Development, 131*, 2997-3006.

Fan, H. Y., Tudor, M., & Ma, H. (1997). Specific interactions between the K domains of AG and AGLs, members of the MADS domain family of DNA binding proteins. *The Plant Journal, 12*, 999-1010.

Farrona, S., Hurtado, L., Bowman, J. L., & Reyes, J. C. (2004). The Arabidopsis thaliana SNF2 homolog *AtBRM* controls shoot development and flowering. *Development, 131*(20), 4965-4975. doi:10.1242/dev.01363

Feinberg, A. P., & Irizarry, R. A. (2010). Stochastic epigenetic variation as a driving forece of development, evolutionary adaptation, and disease. *Proc Natl Acad Sci U S A, 107*, 1757-1764.

Fenster, C. B., Armbruster, W. S., Wilson, P., Dudash, M. R., & Thomson, J. D. (2004). Pollination Syndromes and Floral Specialization. *Annu Rev Ecol. Evol. Syst., 35*, 375-403.

Ferrandiz, C., Gu, Q., Martienssen, R., & Yanofsky, M. F. (2000). Redundant regulation of meristem identity and plant architecture by *FRUITFULL, APETALA1* and *CAULIFLOWER*. *Development, 127*, 725-734.

Flaus, A., Martin, D., Barton, G. .J. and Owen-Hughes, T. (2006). Identification of multiple distinct Snf2 subfamilies with conserved structural motifs. *Nucleic Acids Res, 34*, 2887.

Fletcher, J. C. (2001). The *ULTRAPETALA* gene controls shoot and floral meristem size in *Arabidopsis*. *Development, 128*, 1323-1333.

Fletcher, J. C., Brand, U., Running, M. P., Simon, R., & Meyerowitz, E. M. (1999). Signaling of Cell Fate Decisions by CLAVATA3 in *Arabidopsis* Shoot Meristems. *Science, 283*, 1911-1914.

Franks, R. G., Liu, Z., & Fischer, R. L. (2006). *SEUSS* and *LEUNIG* regulate cell proliferation, vascular development and organ polarity in *Arabidopsis* petals. *Planta, 224*, 801-811.

Franks, R. G., Wang, C., Levin, J. Z., & Liu, Z. (2002). *SEUSS*, a member of a novel family of plant regulatory proteins, represses floral homeotic gene expression with *LEUNIG*. *Development, 129*, 253-263.

Fransz, P., De Jong, J. H., Lysak, M., Castiglione, M. R., & Schubert, L. (2002). Interphase chromosomes in Arabidopsis are organized as well defined chromocenters from which euchromatin loops emanate. *Proc Natl Acad Sci U S A, 99*, 14584-14589.

Franzke, A., Lysak, M. A., Al-Shehbaz, I. A., Koch, M. A., & Mummenhoff, K. (2011). Cabbage family affairs: the evolutionary history of Brassicaceae. *Trends in Plant Science, 16*, 1360-1385.

Friml, J. (2003). Auxin transport - shaping the plant. *Curr Opin in Plant Biol, 6*, 7-12.

Friml, J., Benková, E., Blilou, I., Wisniewska, J., Hamann, T., Ljung, K., Woody, S., Sandberg, G., Scheres, B., Jürgens, G., & Palme, K. (2002a). AtPIN4 Mediates Sink-Driven Auxin Gradients and Root Patterning in *Arabidopsis*. *Cell, 108*, 661-673.

Friml, J., Vieten, A., Sauer, M., Weijers, D., Schwarz, H., Hamann, T., Offringa, R., & Jürgens, G. (2003). Efflux-dependent auxin gradients establish the apical-basal axis of Arabidopsis. *Nature, 426*, 147-153.

Friml, J., Wiśniewska, J., Benková, E., Mendgen, K., & Palme, K. (2002b). Lateral relocation of auxin efflux regulator PIN3 mediates tropism in Arabidopsis. *Nature, 415*, 806-809.

Frohlich, M. W., & Chase, M. W. (2007). After a dozen years of progress the origin of angiosperms is still a great mystery. *Nature, 450*(7173), 1184-1189. doi:10.1038/nature06393

Frohlich, M. W., & Parker, D. S. (2000). The Mostly Male Theory of Flower Evolutionary Origins: From Genes to Fossils. *Systematic Botany, 25*(2), 155. doi:10.2307/2666635

Galliot, C., Stuurman, J., & Kuhlemeier, C. (2006). The genetic dissection of floral pollination syndromes. *Curr Opin Plant Biol, 9*, 78-82.

Gan, X., Hay, A., Kwantes, M., Haberer, G., Hallab, A., Dello Ioio, R., Hofhuis, H., Pieper, B., Cartolano, M., Neumann, U., Nikolov, L. A., Song, B., Hajheidari, M., Briskine, R., Kougioumoutzi, E., Vlad, D., Broholm, S., Hein, J., Meksem, K., Lightfoot, D., Shimizu, K., Shimizu-Inatsugi, R., Imprialou, M., Kudrna, D., Wing, R., Sato, S., Huijser. P., Filatov, D., Mayer, K. F. X., Mott, R., & Tsiantis, M.

(2016). The *Cardamine hirsuta* genome offers insight into the evolution of morphological diversity. *Nat Plants, 2*, 1-6.

Ganal, M. W., Altmann, T., Röder, M. S. (2009). SNP identification in crop plants. *Curr Opin Plant Biol, 12*, 211-217.

Goethe, J. W. (1790). *Versuch die Metamorphose der Pflanzen zu erklären*. Gotha: Ettingersche Buchhandlung.

Goodrich, J., Puangsomlee, P., Martin, M., Long, D., Meyerowitz, E. M., & Coupland, G. (1997). A Polycomb-group gene regulates homeotic gene expression in Arabidopsis. *Nature, 386*, 44.

Goto, K., Kyozuka, J., & Bowman, J. L. (2001). Turning floral organs into leaves, leaves into floral organs. *Curr Opin Genet Dev, 11*, 449-456.

Goto, K., & Meyerowitz, E. M. (1994). Function and regulation of the *Arabidopsis* floral homeotic gene *PISTILLATA*. *Genes & Development, 8*, 1548-1560.

Grüne, T., Brzeski, J., Eberharter, A., Clapier, C. R., Corona, D. F. V., Becker, P. B., & Müller, C. W. (2003). Crystal structure and functional analysis of a nucleosome recognition module of the remodeling factor ISWI. *Mol Cell, 12*, 449-460.

Graham , S. W., & G., O. R. (2000). Utility of 17 plastid genes for inferring the phylogeny of the basal angiosperms. *American Journal of Botany, 87*, 1712-1730.

Griffith, M. E., da Silva Conceicao, A., & Smyth, D. R. (1999). *PETAL LOSS* gene regulates initiation and orientation of second whorl organs in the Arabidopsis flower *Development, 126*, 5635-5644.

Gu, Q., Ferrandiz, C., & Yanofsky, M. F. (1998). The *FRUITFUL* MADS-box gene mediates cell differentiation during *Arabidopsis* fruit development. *Development, 125*, 1509-1517.

Guo, Y.-L., Bechsgaard, J. S., Slotte, T., Neuffer, B., Lascoux, M., Weigel, D., & Schierup, M. H. (2009). Recent speciation of *Capsella rubella* from *Capsella grandiflora*, associated with loss of self-incompatibility and an extreme bottleneck. *Proc Natl Acad Sci U S A, 106*, 5246-5251.

Gustafson-Brown, C., Savidge, B., & Yanofsky, M. F. (1994). Regulation of the arabidopsis floral homeotic gene *APETALA1*. *Cell, 76*, 131-143.

Han, S. K., Wu, M. F., Cui, S., Wagner, D. (2015). Roles and activities of chromatin remodeling ATPases in plants. *The Plant Journal, 83*, 62-77.

Harder, L. D., & Johnson, S. D. (2009). Darwin's beautiful contrivances: evolutionary and functional evidence for floral adaptation. *New Phytol, 183*, 530-545.

Hartwig, B., James, G. V., Konrad, K., Schneeberger, K., Turck, F. (2012). Fast isogenic mapping-by-sequencing of ethyl methanesulfonate-induced mutant bulks. *Plant Physiol, 160*(2), 591-600. doi:10.1104/pp.112.200311

Hay, A., & Tsiantis, M. (2006). The genetic basis for differences in leaf form between *Arabidopsis thaliana* and its wild relative *Cardamine hirsuta*. *Nat Genet, 38*, 942-947.

Hay, A., & Tsiantis, M. (2016). Cardamine hirsuta: a comparative view. *Curr Opin Genet Dev, 39*, 1-7.

Hay, A. S., Pieper, B., Cooke, E., Mandakova, T., Cartolano, M., Tattersall, A. D., Ioio, R. D., McGowan, S. J., Barkoulas, M., Galinha, C., Rast, M. I., Hofhuis, H., Then, C., Plieske, J., Ganal, M., Mott, R., Martinez-Garcia, J. F., Carine, M. A., Scotland, R. W., Gan, X., Filatov, D. A., Lysak, M. A., & Tsiantis, M. (2014). *Cardamine hirsuta*: a versatile genetic system for comparative studies. *Plant J, 78*(1), 1-15. doi:10.1111/tpj.12447

Hayes, J. J., & Hansen, J. C. (2001). Nucleosomes and the chromatin fiber. *Curr Opin Genet Dev, 11*, 124-129.

Hayes, T. E., Sengupta, P., & Cochran, B. H. (1988). The human c-fos serum response factor and the yeast factors GRM/PRTF have related DNA-binding specificities. *Genes & Development, 2*, 1713-1722.

Heinz, E. (1928). Das heterochromatin der moose. *I Jahrb Wiss Botanik, 69*, 762-818.

Heisler, M. G., Ohno, C., Das, P., Sieber, P., Reddy, G. V., Long, J. A., & Meyerowitz, E. M. (2005). Patterns of auxin transport and gene expression during primordium development revealed by live imaging of the Arabidopsis inflorescence meristem. *Curr Biol, 15*(21), 1899-1911. doi:10.1016/j.cub.2005.09.052

Hellens, R. P., Edwards, E. A., Leyland, N. R., Bean, S., & Mullineaux, P. M. (2000). pGreen: a versatile and flexible binary Ti vector for Agrobacterium-mediated plant transformation. . *Pl Mol Biol, 42*, 819-832.

Hintz, M., Bartholmes, C., Nutt, P., Ziermann, J., Hameister, S., Beuffer, B., & Theissen, G. (2006). Catching a 'hopeful monster': shepherd's purse (*Capsella bursa-pastoris*) as a model system to study the evolution of flower development. *J Exp Bot, 57*, 3530-3542.

Hofhuis, H., Moulton, D., Lessinnes, T., Routier-Kierzkowska, A. L., Bomphrey, R. J., Mosca, G., Reinhardt, H., Sarchet, P., Gan, X., Tsiantis, M., Ventikos, Y., Walker, S., Goriely, A., Smith, R., & Hay, A. (2016). Morphomechanical Innovation Drives Explosive Seed Dispersal *Cell, 166*, 222-233.

Hogan, C., & Varga-Weisz, P. (2007). The regulation of ATP-dependent nucleosome remodelling factors. *Mutat Res, 618*(1-2), 41-51. doi:10.1016/j.mrfmmm.2006.07.010

Honma, T., & Goto, K. (2001). Complexes of MADS-box proteins are suffcient to convert leaves into floral organs. *Nature, 409*, 525-529.

Hsieh, T.-F., & Fischer, R. L. (2005). Biology of Chromatin Dynamics. *Annu Rev Plant Biol, 56*, 327-351.

Huala, E., & Sussex, I. M. (1992). *LEAFY* lnteracts with Floral Homeotic Genes to Regulate *Arabidopsis* Floral Development. *The Plant Cell, 4*, 901-913.

Huang, T., & Irish, V. F. (2016). Gene networks controlling petal organogenesis. *Journal of Experimental Botany, 67*, 61-68.

Huang, T., Lopez-Giraldez, F., Townsend, J. P., & Irish, V. F. (2012). RBE controls microRNA164 expression to effect floral organogenesis. *Development, 139*(12), 2161-2169. doi:10.1242/dev.075069

Hudson, A., Critchley, J., & Erasmus, Y. (2008). The Genus *Antirrhinum* (Snapdragon): A Flowering Plant Model for Evolution and Development. *COld Spring Harb. Protoc., 3*, 1-7.

Hurtado, L., Farrona, S., & Reyes, J. C. (2006). The putative SWI/SNF complex subunit BRAHMA activates flower homeotic genes in Arabidopsis thaliana. *Plant Mol Biol, 62*(1-2), 291-304. doi:10.1007/s11103-006-9021-2

Illustrations, P. (2017). Inflorescence illustrations. doi:https://doi.org/10.6084/m9.figshare.c.3701041.v4

Irish, V. F. (2009). Evolution of petal identity. *J Exp Bot, 60*(9), 2517-2527. doi:10.1093/jxb/erp159

Irish, V. F., & Sussex, I. M. (1990). Function of the apetala-1 gene during Arabidopsis floral development. *Plant Cell, 2*, 741-753.

Jack, T. (2004). Molecular and genetic mechanisms of floral control. *Plant Cell, 16 Suppl*, S1-17. doi:10.1105/tpc.017038

Jack, T., Brockman, L. L., & Meyerowitz, E. M. (1992). The homeotic gene *APETALA3* of *Arabidopsis thaliana* encodes a MADS box and is expressed in petals and stamens. *Cell, 68*, 683-697.

James, G. V., Patel, V., Nordstrom, K. J., Klasen, J. R., Salome, P. A., Weigel, D., & Schneeberger, K. (2013). User guide for mapping-by-sequencing in Arabidopsis. *Genome Biol, 14*(6), R61. doi:10.1186/gb-2013-14-6-r61

Jansen, R. K., Cai, Z., Raubeson, L.A., Daniell, H., Leebens-Mack, J., Müller, K.F., Guisinger-Bellian, M., Haberle, R.C., Hansen, A.K., Chumley, T.W., Lee, S.B. (2007). Analysis of 81 genes from 64 chloroplast genomes resolves relationships in angiosperms and identifies genome-scale evolutionary patterns. *Proc Natl Acad Sci U S A, 104*, 19369-19374.

Jenik, P. D., & Irish, V. F. (2000). Regulation of cell proliferation patterns by homeotic genes during *Arabidopsis* floral development. *Development, 127*, 1267-1276.

Jerzmanowski, A. (2007). SWI/SNF chromatin remodeling and linker histones in plants. *Biochim Biophys Acta - Gene Structure and Expression, 1769*, 330-345.

Jofuku, K. D., den Boer, B. G. W., Van Montagu, M., & Okamuro, J. K. (1994). Control of Arabidopsis Flower and Seed Development by the Homeotic Gene *APETALA2*. *The Plant Cell, 8*, 1211-1225.

Jönsson, H., Heisler, M. G., Shapiro, B. E., Meyerowitz, E. M., & Mjolsness, E. (2006). An auxin-driven polarized transport model for phyllotaxis. *Proc Natl Acad Sci U S A, 103*, 1633-1638.

Josefsson, C., Dilkes, B., & Comai, L. (2006). Parent-dependent loss of gene silencing during interspecies hybridization. *Curr Biol, 16*, 1322-1328.

Kadam, S., & Emerson, B. M. (2002). Mechanisms of chromatin assembly and transcription. *Curr Opin In Cell Biol, 14*, 262-268.

Karley, A. J., Hawes, C., Iannetta, P. P. M., & Squire, G. R. (2008). Intraspecific variation in *Capsella bursa-pastoris* in plant quality traits for insect herbivores. *Weed Research, 48*, 147-156.

Kaufmann, K., Wellmer, F., Muino, J. M., Ferrier, T., Wuest, S. E., Kumar, V., Serrano-Mislata, A., Madueno, F., Krajewski, P., Meyerowitz, E. M., Angenent, G. C., & Riechmann, J. L. (2010). Orchestration of Floral Initiation by APETALA1. *Science, 328*, 85-89.

Kay, K. M., Voelckel, C., Yang, J. Y., Hufford, K. M., Kaska, D. D., & Hodges, S. A. (2006). *Floral characters and species diversification.* New York: Oxford University Press.

Kempin, S. A., Savidge, B., & Yanofsky, M. F. (1995). Molecular basis of the cauliflower phenotype in Arabidopsis. *Science, 267*, 522.

Kerstetter, R. A., Bollman, K., Taylor, R. A., Bomblies, K., & Poethig, S. (2001). *KANADI* regulates organ polarity in *Arabidopsis*. *Nature, 411*, 706-709.

Kim, J., Harter, K., & Theologis, A. (1997). Protein-Protein Interactions Among the Aux/IAA Proteins. *Proc Natl Acad Sci U S A, 84*, 11786-11791.

Kinoshita, A., Betsuyaku, S., Osakabe, Y., Mizuno, S., Nagawa, S., Stahl, Y., Simon, R., Yamaguchi-Shinozaki, K., Fukuda, H., & Sawa, S. (2010). RPK2 is an essential receptor-like kinase that transmits the CLV3 signal in *Arabidopsis*. *Development, 137*, 3911-3920.

Knizewski, L., Ginalski, K., Jerzmanowski, A. (2008). Snf2 proteins in plants: gene silencing and beyond. *Trends in Plant Science, 13*, 557-565.

Koncz, C., Martini, N., Szabados, L., Hrouda, M., Bachmair, A., & Schell, J. (1994). Specialized vectors for gene tagging and expression studies. *Plant Molecular Biology Manual*(B2), 1-22.

Koncz, C., & Schell, J. (1986). The promoter of T_L-DNA gene 5 controls the tissue-specific expression of chimaeric genes carried by a novel type of Agrobacterium binary vector *Mol Gen Genet, 204*, 383-396.

Koncz, C. S. J. (1986). The promoter of TL-DNA gene 5 controls the tissue specific expression of chimaeric genes carried by a novel type of Agrobacterium binary vector. *Mol Gen Genet, 204*, 383-396.

Kramer, E. M. (2007). Understanding the Genetic Basis of Floral Diversity. *Bioscience, 57*, 479-487.

Kramer, E. M., Dorit, R. L., & Irish, V. F. (1998). Molecular Evolution of Genes Controlling Petal and Stamen Development: Duplication and Divergence Within the APETALA3 and PISTILLATA MADS-Box Gene Lineages. *Genetics, 149*, 765-783.

Kramer, E. M., & Hodges, S. A. (2010). *Aquilegia* as a model system for the evolution and ecology of petals. *Phil. Trans. R. Soc., 365*, 477-490.

Krizek, B. (2009). *AINTEGUMENTA* and *AINTEGUMENTA-LIKE6* act redundantly to regulate *Arabidopsis* floral growth and patterning. *Plant Physiol, 150*(4), 1916-1929. doi:10.1104/pp.109.141119

Krizek, B. A., Lewis, M. W., & Fletcher, J. C. (2006). *RABBIT EARS* is a second-whorl repressor of *AGAMOUS* that maintains spatial boundaries in *Arabidopsis* flowers. *Plant J, 45*(3), 369-383. doi:10.1111/j.1365-313X.2005.02633.x

Krizek, B. A., & Meyerowitz, E. M. (1996). The Arabidopsis homeotic genes APETALA3 and PISTILLATA are sufficient to provide the B class organ identity function. . *Development, 122*, 11-22.

Kusaba, M., Dwyer, K., Hendershot, J., Vrebalov, J., Nasrallah, J. B., & Nasrallah, M. (2001). Self incompatibility in the genus *Arabidopsis*: characterization of the S locus in the outcrossing *A. lyrata* and its autogamous relative *A. thaliana*. *Plant Cell, 13*, 627-643.

Kwiatkowska, D. (2006). Flower primordium formation at the Arabidopsis shoot apex: quantitative analysis of surface geometry and growth. *J Exp Bot, 57*(3), 571-580. doi:10.1093/jxb/erj042

Kwon, C. S., Chen, C., & Wagner, D. (2005). WUSCHEL is a primary target for transcriptional regulation by SPLAYED in dynamic control of stem cell fate in *Arabidopsis*. *Genes Dev, 19*(8), 992-1003. doi:10.1101/gad.1276305

Kwon, C. S., Hibara, K., Pfluger, J., Bezhani, S., Metha, H., Aida, M., Tasaka, M., & Wagner, D. (2006). A role for chromatin remodeling in regulation of CUC gene expression in the *Arabidopsis* cotyledon boundary. *Development, 133*(16), 3223-3230. doi:10.1242/dev.02508

Kwon, C. S., & Wagner, D. (2007). Unwinding chromatin for development and growth: a few genes at a time. *Trends Genet, 23*, 403-412.

Lampugnani, E. R., Kilinc, A., & Smyth, D. R. (2012). *PETAL LOSS* is a boundary gene that inhibits growth between developing sepals in Arabidopsis thaliana. *Plant J, 71*(5), 724-735. doi:10.1111/j.1365-313X.2012.05023.x

Lampugnani, E. R., Kilinc, A., & Smyth, D. R. (2013). Auxin controls petal initiation in *Arabidopsis*. *Development, 140*(1), 185-194. doi:10.1242/dev.084582

Längst, G., & Becker, P. B. (2004). Nucleosome remodeling: one mechanism, many phenomena? *Biochim Biophys Acta - Gene Structure and Expression, 1677*, 58-63.

Laufs, P., Peaucelle, A., Morin, H., & Traas, J. (2004). MicroRNA regulation of the CUC genes is required for boundary size control in *Arabidopsis* meristems. *Development, 131*(17), 4311-4322. doi:10.1242/dev.01320

Laux, T., Mayer, K. F. X., Berger, J., & Jurgens, G. (1996). The *WUSCHEL* gene is required for shoot and floral meristem integrity in Arabidopsis. *Development, 122*, 87-96.

Lee, H. L., Irish, V. F. . (2011). Gene duplication and loss in a MADS box gene transcription factor circuit. *Mol. Biol. Evol., 28*, 3367-3380.

Lenhard, M., Bohnert, A., Jürgens, G., & Laux, T. (2001). Termination of Stem Cell Maintenance in Arabidopsis Floral Meristems by Interactions between WUSCHEL and AGAMOUS. *Cell, 105*, 805-814.

Lenhard, M., & Laux, T. (2003). Stem cell homeostasis in the Arabidopsis shoot meristem is regulated by intercellular movement of CLAVATA3 and its sequestration by CLAVATA1. *Development, 130*, 3163-3173.

Leyser, O. (2006). Dynamic Integration of Auxin Transport and Signalling. *Curr Biol, 16*, R424-R433.

Liljegren, S. J., Gustafson-Brown, C., Pinyopich, A., Ditta, G. S., & Yanofsky, M. F. (1999). Interactions among *APETALA1*, *LEAFY*, and *TERMINAL FLOWER1* Specify Meristem Fate. *The Plant Cell, 11*, 1007-1018.

Lippman, Z., Gendrel, A. V., Black, M., Vaughn, M. W., Dedhia, N., McCombie, W. R., Lavine, K., Mittal, V., May, B., Kasschau, K. D., & Carrington, J. C. (2004). Role of transposable elements in heterochromatin and epigenetic control. *Nature, 430*, 471-476.

Liu, C. J., Zhang, J. A., Zhang, N., Shan, H. Y., Su, K. M., Zhang, J. S., Meng, Z., Kong, H. Z., & Chen, Z. D. (2010). Interactions among proteins of floral MADS-box genes in basal eudicots: implications for evolution of the regulatory network for flower development. *Mol. Biol. Evol., 27*, 1598-1611.

Liu, Z., & Meyerowitz, E. M. (1995). *LEUNIG* regulates *AGAMOUS* expression in *Arabidopsis* flowers. *Development, 121*, 975-991.

Livak, K. J., & Schmittgen, T. D. (2001). Analysis of relative gene expression data using real-time quantitative PCR and the 2− ΔΔCT method. . *Methods, 25*, 402-408.

Lohmann, J. U., Hong, R. L., Hobe, M., Busch, M. A., Parcy, F., Simon, R., & Weigel, D. (2001). A Molecular Link between Stem Cell Regulation and Floral Patterning in Arabidopsis. *Cell, 105*, 793-803.

Müller, A., Guan, C., Gälweiler, L., Tänzler, P., Huijser, P., Marchant, A., Parry, G., Bennett, M., Wisman, E., & Palme, K. (1998). AtPIN2 defines a locus of Arabidopsis for root gravitropism control. . *The EMBO Journal, 17*, 6903-6911.

Müller, R., Borghi, L., Kwiatkowska, D., Laufs, P., Simon, R. (2006). Dynamic and compensatory responses of *Arabidopsis* shoot and floral meristems to CLV3 signaling. *Plant Cell, 18*, 1188-1198.

Ma, H., Yanofsky, M. F., & Meyerowitz, E. M. (1991). AGL1-AGL6, an Arabidopsis gene family with similarity to floral homeotic and transcription factor genes. *Genes & Development, 5*(3), 484-495. doi:10.1101/gad.5.3.484

Magallón, S., Gómez-Acevedo, S., Sánchez-Reyes, L. L., & Hernández- Hernández, T. (2015). A metacalibrated time-tree documents the early rise of flowering plant phylogenetic diversity. *New Phytol, 207*, 437-453.

Maier, A. T., Stehling-Sun, S., Wollmann, H., Demar, M., Hong, R. L., Haubeiss, S., Weigel, D., & Lohmann, J. U. (2009). Dual roles of the bZIP transcription factor PERIANTHIA in the control of floral architecture and homeotic gene expression. *Development, 136*(10), 1613-1620. doi:10.1242/dev.033647

Mallory, A. C., Dugas, D. V., Bartel, D. P., & Bartel, B. (2004). MicroRNA regulation of NAC-domain targets is required for proper formation and separation of adjacent embryonic, vegetative, and floral organs. *Curr Biol, 14*(12), 1035-1046. doi:10.1016/j.cub.2004.06.022

Mandel, M. A., Gustafson-Brown, C., Savidge, B., & Yanofsky, M. F. (1992). Molecular characterization of the *Arabidopsis* floral homeotic gene *APETALA1. Nature, 360*, 273-277.

Mandel, M. A., & Yanofsky, M. F. (1995). The Arabidopsis AGL8 MADS box gene is expressed in inflorescence meristems and is negatively regulated by APETALA1. *Plant Cell, 7*, 1763-1771.

Marchler-Bauer, A., Bo, Y., Han, L., He, J., Lanczycki, C.J., Lu, S., Chitsaz, F., Derbyshire, M.K., Geer, R.C., Gonzales, N.R., Gwadz, M. (2016). CDD/SPARCLE: functional classification of proteins via subfamily domain architectures. *Nucleic Acids Res, gkw1129*.

Masters, M. T. (1869). *Vegetable Teratology: An Account of the Principle Deviations from the Usual Construction of Plants*. London, UK: Ray Society.

Mathews, S., Donoghue M. J. (1999). The root of angiosperm phylogeny inferred from duplicate phytochrome genes. *Science, 286*, 947-950.

Mayer, K. F. X., Schoof, H., Haecker, A., Lenhard, M., Jürgens, G., & Laux, T. (1998). Role of WUSCHEL in Regulating Stem Cell Fate in the Arabidopsis Shoot Meristem. *Cell, 95*, 805-815.

McClintock, B. (1951). Chromosome organization and genic expression. *Cold Spring Harb Symp Quant Biol, 16*, 13-47.

McConnell, J. R., Emery, J., Eshed, Y., Bao, N., Bowman, J., & Barton, M. K. (2001). Role of *PHABULOSA* and *PHAVOLUTA* in determining radial patterning in shoots. *Nature, 411*, 709-713.

Melzer, R., & Theissen, G. (2009). Reconstitution of 'floral quartets' in vitro involving class B and class E floral homeotic proteins. *Nucleic Acids Res, 37*(8), 2723-2736. doi:10.1093/nar/gkp129

Mizukami, Y., & Ma, H. (1992). Ectopic expression of the floral homeotic gene AGAMOUS in transgenic Arabidopsis plants alters floral organ identity. *Cell, 71*, 119-131.

Mohrmann, L., & Verrijzer, C. P. (2005). Composition and functional specificity of SWI2/SNF2 class chromatin remodeling complexes. *Biochim Biophys Acta, 1681*(2-3), 59-73. doi:10.1016/j.bbaexp.2004.10.005

Monniaux, M., McKim, S. M., Cartolano, M., Thévenon, E., Parcy, F., Tsiantis, M., & Hay, A. (2017). Conservation vs divergence in LEAFY and APETALA1 functions between *Arabidopsis thaliana* and *Cardamine hirsuta*. *New Phytol*. doi:doi: 10.1111/nph.14419

Monniaux, M., Pieper, B., & Hay, A. (2016). Stochastic variation in Cardamine hirsuta petal number. *Ann Bot, 117*, 881-887.

Moore, M. J., Bell, C. D., Soltis, P. S., Soltis, D. E. (2007). Using plastid genomic-scale data to resolve enigmatic relationships among basal angiosperms. *Proc Natl Acad Sci U S A, 104*, 19363-19368.

Morao, A. K., Bouyer, D., & Roudier, F. (2016). Emerging concepts in chromatin-level regulation of plant cell differentiation: timing, counting, sensing and maintaining. *Curr Opin Plant Biol, 34*, 27-34.

Murashige, T., Skoog, F. (1962). A revised medium for rapid growth and bioassays with tobacco tissue culture. *Physiol. Plant., 15*, 473-497.

Neff, M. M., Neff, J. D., Chory, J., & Pepper, A. E. (1998). dCAPS, a simple technique for the genetic analysis of single nucleotide polymorphisms: experimental applications in Arabidopsis thaliana genetics. *Plant J, 14*(3), 387-392.

Ni, J., & Clark, S. E. (2006). Evidence for Functional Conservation, Sufficiency, and Proteolytic Processing of the CLAVATA3 CLE Domain. *Plant Physiol, 140*, 726-733.

Nole-Wilson, S., & Krizek, B. E. (2006). AINTEGUMENTA Contributes to Organ Polarity and Regulates Growth of Lateral Organs in Combination with YABBY Genes1. *Plant Physiol, 141*, 977-987.

Ogawa, M., Shinohara, H., Sakagami, Y., & Matsubayashi, Y. (2008). Arabidopsis CLV3 Peptide Directly Binds CLV1 Ectodomain. *Science, 319*, 294.

Ohno, C. K., Reddy, G. V., Heisler, M. G. B., & Meyerowitz, E. M. (2004). The Arabidopsis JAGGED gene encodes a zinc finger that promotes leaf tissue development. *Development, 131*, 1111-1122.

Oka, M., Miyamoto, K., Okada, K., & Ueda, J. (1999). Auxin polar transport and flower formation in *Arabidopsis thaliana* transformed with indoleacetamide hydrolase (*iaaH*) gene. *Plant Cell, 40*, 231-237.

Okada, K., Ueda, J., Komaki, M. K., Bell, C. J., & Shimura, Y. (1991). Requirement of the Auxin Polar Transport System in Early Stages of *Arabídopsis* Floral Bud Formation. *The Plant Cell, 3*, 677-684.

Ossowski, S., Schwab, R., Weigel, D. (2008). Gene silencing in plants using artificial microRNAs and other small RNAs. *The Plant Journal, 53*, 674-690.

Otsuga, D., DeGuzman, B., Prigge, M. J., Drews, G. N., & Clark, S. E. (2001). *REVOLUTA* regulates meristem initiation at lateral organs. *The Plant Journal, 25*, 223-236.

Ouellet, F., Overvoorde, P. J., & Theologis, A. (2001). IAA17/AXR3: biochemical insight into an auxin mutant phenotype. *The Plant Cell, 13*, 829-842.

Pajoro, A., Biewers, S., Dougali, E., Leal Valentim, F., Mendes, M. A., Porri, A., Coupland, G., Van de Peer, Y., van Dijk, A. D., Colombo, L., Davies, B., & Angenent, G. (2014). The (r)evolution of gene regulatory networks controlling Arabidopsis plant reproduction: a two-decade history. *J Exp Bot, 65*, 4731-4745.

Palomino, C., Fernandez-Romero, M. D., Rubio, J., Torres, A., Moreno, M. T., & Millan, T. (2009). Integration of new CAPS and dCAPS-RGA markers into a composite chickpea genetic map and their association with disease resistance. *Theor Appl Genet, 118*(4), 671-682. doi:10.1007/s00122-008-0928-7

Parcy, F., Nilsson, O., Busch, M. A., Lee., I., & Weigel, D. (1998). A genetic framework for floral patterning. *Nature, 395*, 561-566.

Parenicova, L. (2003). Molecular and Phylogenetic Analyses of the Complete MADS-Box Transcription Factor Family in Arabidopsis: New Openings to the MADS World. *The Plant Cell Online, 15*(7), 1538-1551. doi:10.1105/tpc.011544

Parkinson, C. L., Adams, K. L., & Palmer, J. D. (1999). Multigene analyses identify the three earliest lineages of extant fl owering plants. *Curr Biol, 9*, 1485-1488.

Pekker, I., Alvarez, J. P., & Eshed, Y. (2005). Auxin response factors mediate *Arabidopsis* organ asymmetry via modulation of KANADI activity. *Plant Cell, 17*(11), 2899-2910. doi:10.1105/tpc.105.034876

Pelaz, S., Ditta, G. S., Baumann, E., Wisman, E., & Yanofsky, M. F. (2000). B and C floral organ identity functions requiore *SEPALLATA* MADS-box genes. *Nature, 405*, 200-203.

Pieper, B., Monniaux, M., & Hay, A. (2016). The genetic architecture of petal number in *Cardamine hirsuta*. *New Phytol, 209*(1), 395-406. doi:10.1111/nph.13586

Prigge, M. J., Otsuga, D., Alonso, J. M., Ecker, J. R., Drews, G. N., & Clark, S. E. (2005). Class III homeodomain-leucine zipper gene family members have overlapping, antagonistic, and distinct roles in Arabidopsis development. *The Plant Cell, 17*, 61-76.

Prusinkiewicz, P., Erasmus, Y., Lane, B., Harder, L. D., & Coen, E. (2007). Evolution and Development of Inflorescence Architectures. *Science, 316*, 1452-1456.

Przemeck, G. K., Mattsson, J., Hardtke, C. S., Sung, Z. R., & Berleth, T. (1996). Studies of the role of the Arabidopsis gene MONOPTEROS in vascular development and plant cell axialization. *Planta, 200*, 229-237.

Qiu , Y.-L., Lee J., Bernasconi-Quadroni F., Soltis D. E., Soltis P. S., Zanis M., Zimmer E. A., Chen Z., Savolainen V., & Chase, M. W. (1999). The earliest angiosperms: Evidence from mitochondrial, plastid and nuclear genomes. . *Nature, 402*, 404-407.

Rast, M. I., & Simon, R. (2008). The meristem-to-organ boundary: more than an extremity of anything. *Curr Opin Genet Dev, 18*, 287-294.

Ratcliffe, O. J., Bradley, D. J., & Coen, E. S. (1999). Separation of shoot and floral identity in *Arabidopsis*. *Development, 126*, 1109-1120.

Reddy, G. V., Heisler, M. G., Ehrhardt, D. W., & Meyerowitz, E. M. (2004). Real-time lineage analysis reveals oriented cell divisions associated with morphogenesis at the shoot apex of Arabidopsis thaliana. *Development, 131*, 4225-4237.

Reinhardt, D., Mandel, T., & Kuhlemeier, C. (2000). Auxin Regulates the Initiation and Radial Position of Plant Lateral Organs. *The Plant Cell, 12*, 507-518.

Reinhardt, D., Pesce, E.-R., Stieger, P., Mandel, T., Baltensperger, K., Bennett, M., Traas, J., Friml, J., & Kuhlemeier, C. (2003). Regulation of phyllotaxis by polar auxin transport. *Nature, 426*, 255-260.

Renner, S. S. (1999). Circumscription and phylogeny of the Laurales: Evidence from molecular and morphological data. . *American Journal of Botany, 86*, 1301-1315.

Riechmann, J. L., Krizek, B. A., & Meyerowitz, E. M. (1996). Dimerization specificity of Arabidopsis MADS domain homeotic proteins APETALA1, APETALA3, PISTILLATA, and AGAMOUS. *Proc Natl Acad Sci U S A, 93*, 4793-4798.

Riechmann, J. L., & Meyerowitz, E. M. (1998). The AP2/EREBP family of plant transcription factors. *Biological Chemistry, 379*, 633-646.

Ronse De Craene, L. P. (2007). Are Petals Sterile Stamens or Bracts? The Origin and Evolution of Petals in the Core Eudicots. *Annals of Botany, 100*, 621-630.

Ronse De Craene, L. P. (2010). *Floral diagrams: An aid to understand floral morphology and evolution.* New York: Cambridge University Press.

Running, M. P., & Meyerowitz, E. M. (1996). Mutations in the *PERIANTHIA* gene of *Arabidopsis* specifically alter floral organ number and initiation pattern. *Development, 122*, 1261-1269.

Sablowski, R. (2007). Flowering and determinacy in *Arabidopsis*. *J Exp Bot, 58*(5), 899-907. doi:10.1093/jxb/erm002

Saha, A., Wittmeyer, J., & Cairns, B. R. (2006). Chromatin remodelling: the industrial revolution of DNA around histones. *Nat Rev Mol Cell Biol, 7*, 437-447.

Sambrook, J., Russell, D.W. (2001). *Molecular cloning. A laboratory manual.* . New York: Cold Spring Harbor Laboratory Press.

Sang, Y., Silva-Ortega, C. O., Wu, S., Yamaguchi, N., Wu, M. F., Pfluger, J., Gillmor, C. S., Gallagher, K. L., Wagner, D. (2012). Mutations in two non-canonical Arabidopsis SWI2/SNF2 chromatin remodeling ATPases cause embryogenesis and stem cell maintenance defects. *Plant J, 72*(6), 1000-1014. doi:10.1111/tpj.12009

Sarnowska, E., Gratkowska, D. M., Sacharowski, S. P., Cwiek, P., Tohge, T., Fernie, A. R., Siedlecki, J. A., Koncz, C., & Sarnowski, T. J. (2016). The Role of SWI/SNF Chromatin Remodeling Complexes in Hormone Crosstalk. *Trends in Plant Science, 21*, 594-608.

Sarnowski, T. J., Ríos, G., Jásik, J., Świeżewski, S., Kaczanowski, S., Li, Y., Kwiatkowska, A., Pawlikowska, K., Koźbiał, M., Koźbiał, P., & Koncz, C. (2005). SWI3 Subunits of Putative SWI/SNF chromatin-remodeling complexes play distinct roles during Arabidopsis development. *Plant Cell, 17*, 2454-2472.

Sauret-Güeto, S., Schiessl, K., Bangham, A., Sablowski, R., & Coen, E. (2013). *JAGGED* controls *Arabidopsis* petal growth and shape by interacting with a divergent polarity field. *PLoS Biol, 11*(4), e1001550. doi:10.1371/journal.pbio.1001550

Sawa, S., Ito, T., Shimura, Y., & Okada, K. (1999a). *FILAMENTOUS FLOWER* Controls the Formation and Development of *Arabidopsis* Inflorescences and Floral Meristems. *The Plant Cell, 11*, 69-86.

Sawa, S., Watanabe, K., Goto, K., Liu, Y.-G., Shibata, D., Kanaya, E., Morita, E. H., & Okada, K. (1999b). FILAMENTOUS FLOWER, a meristem and organ identity gene of Arabidopsis, encodes a protein with a zinc Wnger and HMG-related domains. *Genes & Development, 13*, 1079-1088.

Schiessl, K., Kausika, S., Southam, P., Bush, M., & Sablowski, R. (2012). JAGGED controls growth anisotropy and coordination between cell size and cell cycle during plant organogenesis. *Curr Biol, 22*, 1739-1746.

Schneeberger, K., Ossowski, S., Lanz, C., Juul, T., Petersen, A. H., Nielsen, K. L., Jorgensen, J. E., Weigel, D., & Andersen, S. U. (2009). SHOREmap: simultaneous mapping and mutation identification by deep sequencing. *Nat Methods, 6*(8), 550-551. doi:10.1038/nmeth0809-550

Schoof, H., Lenhard, M., Haecker, A., Mayer, K. F. X., Jürgens, G., & Laux, T. (2000). The Stem Cell Population of Arabidopsis Shoot Meristems IsMaintained by a Regulatory Loop between the CLAVATA and WUSCHEL Genes. *Cell, 100*, 635-644.

Schultz, E. A., & Haughn, G. W. (1991). LEAFY, a Homeotic Gene That Regulates lnflorescence Development in Arabidopsis. *The Plant Cell, 3*, 771-781.

Schwab, R., Ossowski, S., Riester, M., Warthmann, N., Weigel, D. (2006). Highly specific gene silencing by artificial microRNAs in *Arabidopsis*. *Plant Cell, 18*, 1121-1133.

Schwarz-Sommer, Z., Huijser, P., Nacken, W., Saedler, H., & Sommer, H. (1990). Genetic control of flower development by homeotic genes in Antirrhinum majus. *Science, 250*, 931-936.

Sen, P., Ghosh, S., Pugh, B. F., Bartholomew, B. (2011). A new, highly conserved domain in Swi2/Snf2 is required for SWI/SNF remodeling. *Nucleic Acids Res, 39*, 9155-9166.

Sessions, A., Nemhauser, J. L., McCall, A., Roe, J. L., Feldmann, K. A., & Zambryski, P. C. (1997). *ETTIN* patterns the *Arabidopsis* floral meristem and reproductive organs. *Development, 124*, 4481-4491.

Sessions, A., Yanofsky, M. F., & Weigel, D. (2000). Cell-Cell Signaling and Movement by the Floral Transcription Factors LEAFY and APETALA1. *Science, 289*, 779-781.

Shannon, S., & Meeks-Wagner, D. R. (1991). A Mutation in the *Arabidopsis TFL1* Gene Affects Inflorescence Meristem Development. *The Plant Cell, 3*, 877-892.

Sicard, A., Stacey, N., Hermann, K., Dessoly, J., Neuffer, B., Baurle, I., & Lenhard, M. (2011). Genetics, evolution, and adaptive significance of the selfing syndrome in the genus *Capsella*. *Plant Cell, 23*, 3156-3171.

Sieber, P., Wellmer, F., Gheyselinck, J., Riechmann, J. L., & Meyerowitz, E. M. (2007). Redundancy and specialization among plant microRNAs: role of the MIR164 family in developmental robustness. *Development, 134*(6), 1051-1060. doi:10.1242/dev.02817

Siegfried, K. R., Eshed, Y., Baum, S. F., Otsuga, D., Drews, G. N., & Bowman, J. L. (1999). Members of the *YABBY* gene family specify abaxial cell fate in *Arabidopsis*. *Development, 126*, 4117-4128.

Smaczniak, C., Immink, R. G., Angenent, G. C., & Kaufmann, K. (2012a). Developmental and evolutionary diversity of plant MADS-domain factors: insights from recent studies. *Development, 139*(17), 3081-3098. doi:10.1242/dev.074674

Smaczniak, C., Immink, R. G., Muino, J. M., Blanvillain, R., Busscher, M., Busscher-Lange, J., Dinh, Q. D., Liu, S., Westphal, A. H., Boeren, S., Parcy, F., Xu, L., Carles, C. C., Angenent, G. C., & Kaufmann, K. (2012b). Characterization of MADS-domain transcription factor complexes in Arabidopsis flower development. *Proc Natl Acad Sci U S A, 109*(5), 1560-1565. doi:10.1073/pnas.1112871109

Smith, R. S., Guyomarc'h, S., Mandel, T., Reinhardt, D., Kuhlemeier, C., & Prusinkiewicz, P. (2006). A plausible model of phyllotaxis. *Proc Natl Acad Sci U S A, 103*, 1301-1306.

Smyth, D. R., Bowman, J. L., & Meyerowitz, E. M. (1990). Early Flower Developement in *Arabidopsis*. *The Plant Cell, 2*, 755-767.

Soltis, D. E., Bell, C. D., Kim, S., & Soltis, P. S. (2008). Origin and early evolution of angiosperms. . *Ann NY Acad. Sci., 1133*, 3-25.

Soltis , D. E., Soltis P. S., Chase M. W., Mort M. E., Albach D. C., Zanis M., Savolainen, V., Hahn, W. H., Hoot, S. B., Fay, M. F., Axtell, M., Swensen, S. M., Prince, L. M., Kress, W. J., Nixon, K. C., & Farris, J. S. (2000). Angiosperm phylogeny inferred from 18S rDNA, rbcL , and atpB sequences. . *Botanical Journal of the Linnean Society, 133*, 381-461.

Soltis, P. S., Soltis, D. E., & Chase, M. W. (1999). Angiosperm phylogeny inferred from multiple genes as a tool for comparative biology. *Nature, 402*, 402-404.

Specht, C. D., & Bartlett, M. E. (2009). Flower Evolution: The Origin and Subsequent Diversification of the Angiosperm Flower. *Annual Review of Ecology, Evolution, and Systematics, 40*(1), 217-243. doi:10.1146/annurev.ecolsys.110308.120203

Sprengel, C. K. (1793). *Das Entdeckte Geheimniss der Natur Im Bau und in der Befruchtung der Blumen*. New York, USA: Weldon & Wesley.

Sridhar, V. V., Surendrarao, A., Gonzalez, D., Conlan, R. S., & Liu, Z. (2004). Transcriptional repression of target genes by LEUNIG and SEUSS, two interacting regulatory proteins for *Arabidopsis* flower development. *Proc Natl Acad Sci U S A, 101*, 11494-11499.

Steeves, T. A., Sussex, I. M. . (1989). *Patterns in Plant Development.* Cambridge: Cambridge University Press.

Su, Y., Kwon, C. S., Bezhani, S., Huvermann, B., Chen, C., Peragine, A., Kennedy, J. F., & Wagner, D. (2006). The N-terminal ATPase AT-hook-containing region of the Arabidopsis chromatin-remodeling protein SPLAYED is sufficient for biological activity. *Plant J, 46*(4), 685-699. doi:10.1111/j.1365-313X.2006.02734.x

Sun, F. L., Cuaycong, M. H., & Elgin, S. C. (2001). Long-range nucleosome ordering is associated with gene silencing in Drosophila melanogaster pericentric heterochromatin. *Mol Cell Biol, 21*, 867-879.

Takeda, S., Matsumoto, N., & Okada, K. (2004). RABBIT EARS, encoding a SUPERMAN-like zinc finger protein, regulates petal development in *Arabidopsis thaliana*. *Development, 131*(2), 425-434. doi:10.1242/dev.00938

Takhtajan, A. (1997). *Diversity and classification of flowering plants*. New York, USA: Columbia University Press.

Theissen, G., Becker, A., Di Rosa, A., Kanno, A., Kim, J. T., Münster, T., Winter, K.-U., & Saedler, H. (2000). A short history of MADS-box genes in Plants. *Plant Molecular Biology, 42*(1), 115-149. doi:10.1023/a:1006332105728

Theissen, G., Becker, A., Winter, K. U., Munster, T., Kirchner, C., & Saedler, H. (2002). *How the land plants learned their floral ABCs: the role of MADS-box genes in the evolutionary origin of flowers.* . London: Taylor and Francis.

Theissen, G., & Saedler, H. (2001). Plant Biology. Floral quartets. *Nature, 409*, 469-471.

Theophrastus. (350 BC- 287 BC). *Enquiry into Plants* (A. F. Hort, Trans.). London, UK: Heinemann, W.

Thompson, J. N. (2005). *The geographic mosaic of coevolution*. Chicago, IL, USA: University of Chicago Press.

Tsukiyama, T. (2002). The in vivo functions of ATP-dependent chromatin-remodelling factors. *Nat Rev Mol Cell Biol, 3*(6), 422-429. doi:10.1038/nrm828

Tsukiyama, T., Daniel, C., Tamkun, J., & Wu, C. (1995). ISWI, a member of the SWI2/SNF2 ATPase family, encodes the 140 kDa subunit of the nucleosome remodeling factor. *Cell, 83*, 1021-1026.

Ulmasov, T., Hagen, G., & Guilfoyle, T. (1997). ARF1, a transcription factor that binds to auxin response elements. *Science, 276*, 1865-1868.

Van der Knaap, E., Kim, J. H., Kende, H. (2000). A Novel Gibberellin-Induced Gene from Rice and Its Potential Regulatory Role in Stem Growth. *Plant Physiol, 122*, 695-704.

Varga-Weisz, P. (2001). ATP-dependent chromatin remodeling factors: Nucleosome shufflers withmany missions. *Oncogene, 20*, 3076-3085.

Vernoux, T., Besnard, F., & Traas, J. (2010). Auxin at the Shoot Apical Meristem. *Cold Spring Harb Perspect Biol, 2*. doi:a001487

Vernoux, T., Kronenberger, J., Grandjean, O., Laufs, P., & Traas, J. (2000). PIN-FORMED 1 regulates cell fate at the periphery of the shoot apical meristem. *Development, 127*, 5157-5165.

Vignali, M., Hassan, A. H., Neely, K. E., Workman, J. L. (2000). ATP-dependent chromatin-remodeling complexes. *Mol Cell Biol, 20*, 1899-1910.

Vlad, D., Kierzkowski, D., Rast, M. I., Vuolo, F., Dello Ioio, R., Galinha, C., Gan, X., Hajheidari, M., Hay, A., Smith, R. S., Huijser, P., Bailey, D., & Tsiantis, M. (2014). Leaf Shape Evolution Through Duplication, Regulatory Diversification, and Loss of a Homeobox Gene. *Science, 343*, 780-783.

Vroemen, C. W. (2003). The *CUP-SHAPED COTYLEDON3* Gene Is Required for Boundary and Shoot Meristem Formation in *Arabidopsis*. *The Plant Cell Online, 15*(7), 1563-1577. doi:10.1105/tpc.012203

Wagner, D., & Meyerowitz, E. M. (2002). SPLAYED, a Novel SWI-SNF ATPase Homolog, Controls Reproductive Development in Arabidopsis *Curr Biol, 12*, 85-94.

Wagner, D., Sablowski, R. W., & Meyerowitz, E. M. (1999). Transcriptional activation of *APETALA1* by *LEAFY*. *Science, 285*, 582-584.

Waites, R., & Hudson, A. (1995). *phantastica:* a gene required for dorsiventrality of leaves in *Antirrhinum majus*. *Development, 121*, 2143-2154.

Wang, L., Limbo, O., Fei, J., Chen, L., Kim, B., Luo, J., Chong, J., Conaway, R.C., Conaway, J.W., Ranish, J.A., Kadonaga, J.T.,. (2014). Regulation of the Rhp26ERCC6/CSB chromatin remodeler by a novel conserved leucine latch motif. . *Proc Natl Acad Sci U S A, 111*, 18566-18571.

Weigel, D., Alvarez, J., Smyth, D., Yanofsky, M. F., & Meyerowitz, E. M. (1992). LEAFY controls floral meristem identity in Arabidopsis. . *Cell, 69*, 843-859.

Weigel, D., & Nilsson, O. (1995). A developmental switch sufficient for flower initiation in diverse plants. *Nature, 377*, 495-500.

Weijers, D., Schlereth, A., Ehrismann, J. S., Schwank, G., Kientz, M., & Jürgens, G. (2006). Auxin triggers transient local signaling for cell specification in Arabidopsis embryogenesis. *Dev Cell, 10*, 265-270.

Whittall, J. B., & Hodges, S. A. (2007). Pollinator shifts drive increasingly long nectar spurs in columbine flowers. *Nature, 447*, 706-710.

Wollmann, H., Mica, E., Todesco, M., Long, J. A., & Weigel, D. (2010). On reconciling the interactions between *APETALA2*, miR172 and *AGAMOUS* with the ABC model of flower development. *Development, 137*(21), 3633-3642. doi:10.1242/dev.036673

Wu, M. F., Sang, Y., Behzani, S., Yamaguchi, N., Han, S. K., Li, Z., Su, Y., Slewinski, T. L., & Wagner, D. (2012). SWI2-SNF2 chromatin remodeling ATPases overcome polycomb repression and control floral organ identity with the *LEAFY* and *SEPALLATA3* transcription factors *PNAS, 109*, 3576–3581.

Wu, M. F., Yamaguchi, N., Xiao, J., Bargmann, B., Estelle, M., & Wagner, D. (2015). Auxin-regulated chromatin switch directs acquisition of flower primordium founder fate. *eLife, 4*. doi:10.7554/eLife.09269

Xia, X., Liu, X., Li, T., Fang, X., Chen, Z. (2016). Structure of chromatin remodeler Swi2/Snf2 in the resting state. *Nature Structural & Molecular Biology, 23*, 722-729.

Yadav, R. K., Perales, M., Gruel, J., Girke, T., Jönsson, H., & Reddy, G. V. (2011). WUSCHEL protein movement mediates stem cell homeostasis in the *Arabidopsis* shoot apex. *Genes & Development, 25*, 2025-2030.

Yamanaka, S., Nakamura, I., Watanabe, K. N., & Sato, Y. (2004). Identification of SNPs in the waxy gene among glutinous rice cultivars and their evolutionary significance during the domestication process of rice. *Theor Appl Genet, 108*(7), 1200-1204. doi:10.1007/s00122-003-1564-x

Yanagisawa, T., Kiribuchi-Otobe, C., Hirano, H., Suzuki, Y., & Fujita, M. (2003). Detection of single nucleotide polymorphism (SNP) controlling the waxy character in wheat by using a derived cleaved amplified polymorphic sequence (dCAPS) marker. *Theor Appl Genet, 107*(1), 84-88. doi:10.1007/s00122-003-1235-y

Yanofsky, M. F., Ma, H., Bowman, J. L., Drews, G. N., Feldmann, K. A., & Meyerowitz, E. M. (1990). The protein encoded by the *Arabidopsis* homeotic gene *agamous* resembles transcription factors. *Nature, 346*.

Zanis , M. J., E.., S. D., Soltis P. S., Mathews S., & Donoghue, M. J. (2002). The root of the angiosperms revisited. . *Proc Natl Acad Sci U S A, 99*, 6848 - 6853.

Zhang, L., Barrett, S. C. H., Gao, J.-Y., Chen, J., Cole, W. W., Liu, Y., Bai, Z.-L., & Li, Q.-J. (2004). Predicting mating patterns from pollination syndromes: the case of “sapromyiophily” in *Tacca chantrieri* (Taccaceae)[1]. *Am J Bot, 92*, 517-524.

Zhang, Y., Fang, Z., Wang, Q., Liu, Y., Yang, L., Zhuang, M., & Sun, P. (2012). Chloroplast subspecies-specific SNP detection and its maternal inheritance in Brassica oleracea L. by using a dCAPS marker. *J Hered, 103*(4), 606-611. doi:10.1093/jhered/ess006

Zhao, Y., Christensen, S. K., Fankhauser, C., Cashman, J. R., Cohen, J. D., Weigel, D., Chory, J. . (2001). A role for flavin monooxygenase-like enzymes in auxin biosynthesis. *Science, 291*, 306-309.

List of Abbreviations

LFY: LEAFY

SAM: Shoot Apical Meristem

FM: Floral Meristem

IM: Inflorescence Meristem

TFL1: TERMINAL FLOWER 1

QTL: Quantitative Trait Loci

RIL: Recombinant Inbred Lines

Ox: Oxford

fp2: four petals 2

AP1: APETALA1

WUS: WUSCHEL

CLV1/3: CLAVATA1/3

OC: Organizing Centre

CZ: Central Zone

LRR: Leucine-rich receptor

AG: AGAMOUS

SYD: SPLAYED

SNF2: Sucrose Non-Fermenting2

GA: Gibberellin

EMF1/2: EMBRYONIC FLOWER1/2

AP3: APETALA3

PI: PISTILLATA

CAL: CAULIFLOWER

FUL: FRUITFUL

SEP1/4: SEPALLATA1/4

AGL: AGAMOUS-LIKE

MADS box: MCM1, AGAMOUS, DEFICIENS and SRF

MIKC: MADS-box, Intervening, Keratin-like, C-terminal domain

CArG: CC(A/T)6GG

Y2H: Yeast two-hybrid

AP2: APETALA2

mRNA: messenger RNA

miRNA: micro-RNA

kDa: kilo Dalton

REF6: RELATIVE OF EARLY FLOWERING6

CHD: Chromodomain/Helicase/DNA binding domain

PKL: PICKLE

ISWI: Imitation SWItch

CHR4/7/11: CHROMATIN REMODELING 4/7/11

SEU: SEUSS

LUH: LEUNIG-HOMOLOG

IP: Immunoprecipitation

CUC: CUP-SHAPED COTYLEDON

NAC: NAM, ATAF1/2, CUC2

EEP1: EARLY EXTRA PETALS1

PTL: PETAL LOSS

RBE: RABBIT EARS

ERF: Ethylene Response Factor

HD-ZIP: homeodomain/leucine zipper

PHB: PHABULOSA

PHV: PHAVOLUTA

CRN: CORONA

ATHB8: ARABIDOPSIS THALIANA HOMEOBOX 8

REV: REVOLUTA

KAN: KANADI

YAB: YABBY

GARP: (GOLDEN, ARR, Psr1)

FIL: FILAMENTOUS FLOWER

LEU: LEUNIG

ANT: AINTEGUMENTA

ETT: ETTIN

ARF: AUXIN RESPONSE FACTOR

YUC: YUCCA

PIN: PIN-FORMED

AUX: AUXIN RESISTANT

STM: SHOOT MERISTEMLESS

PID: PINOID

JAG: JAGGED

PAN: PERIANTHIA

T-DNA: Transposable element DNA

SWI/SNF: SWItch/Sucrose Non-Fermenting

ATP: Adenosine Triphosphate

BRM: BRAHMA

MINU1/2: MINUSCULE1/2

RNAi: RNA interference

ChIP: Chromatin Immunoprecipitation

CLF: CURLY LEAF

PRC2: Polycomb Repressor Complex2

ARF5/MP: AUXIN RESPONSE FACTOR/MONOPTEROS

BDL: BODENLOS

EXP: EXTRA PETALS

EMS: Ethyl methanesulfonate

SNP: Single Nuclear Polymorphism

MAS: Marker Assisted Polymorphism

SSCP: Single Strand Conformation Polymorphism

CCM: Chemical Cleavage of Mismatches

EMC: Enzyme Mismatch Cleavage

dCAPS: Derived Cleaved Polymorphic Sequences

RE: Restriction Endonuclease

PCR: Polymerase Chain Reaction

BRM: BRAHMA

MINU1/2: MINUSCULE1/2

QLQ: The motif QX_3LX_2Q

SnAC: Snf2 ATP Coupling

vWA: von Willebrand factor A

amiRNA: artificial micro-RNA

wt: wild type

GUS: β-glucuronidase

BAC: Bacterial Artificial Clone

NGS: Next Generation Sequencing

Acknowledgements

First and foremost, I would like to express my gratitude to my supervisor, Angela Hay, for providing me with a stimulating project that I enjoyed a lot. I was lucky to have Angela's guidance; her insight and support was fundamental for the completion of my PhD. Also, I was fortunate to be surrounded by great minds like Miltos, Peter, Xiangchao, Richard, Franziska. Their comments and our discussions in different timepoints of my time in Cologne helped me to sharpen my focus. My scientific and personal advancement was achieved through my interactions with all of them. I would like to thank all the members of my committee as well; their assistance was vital for my degree.

A separate paragraph belongs to the members of Angela's lab: Marie, Anahit, Wolfram and Hugo. Marie, I thank you for putting up with me, through all my questions, my mistakes, and my stress. You were always there to show me the way, even when you didn't have to. Anahit, I thank you for roughing me up. You acted like a compass for me, because sometimes things must be done in a certain way. Wolfram, thank you for your constant assistance. You were there to push the project forward in a very difficult time, without you it would have been almost impossible.

The members of the Tsiantis department are a unique breed. They have always provided a great working place and between them I felt like home. I think I've learned something from all of you, and this will never be forgotten. The PhD group from the MPI, one of the most diverse and dynamic groups I have ever met. Our similar state is a bond that, I think, will stay forever. We shared many moments, not always good, but always tried to make the best out of each situation.

My friends abroad: Aris and Ilias. You are always with me, I am lucky to have you guys.

The three (out of four) musketeers of the department: Francesco, Chidi, Aleksandra. You were the support system on a daily basis, the friends to turn to when in need. Our adventures during this whole time, our discussions, our nights out, our coffees, will always be cherished. You helped me pull through.

I would like to thank my mother, my father, my brother and my aunt for their constant support. Their opinion is always important, and I am grateful to be surrounded by so much love. They were there, day and night, high and low, Greece and Germany and I couldn't have done it without you.

The process of acquiring a PhD degree, is never easy. For this, you need a person to make you feel that everything is going to be OK during this period, and after. To experience something more than a feeling. For me, this person is Rousanna.

This dissertation, to be produced, contains a piece of everyone mentioned in this page.

Erklärung

Ich versichere, dass ich die von mir vorgelegte Dissertation selbständig angefertigt, die benutzten Quellen und Hilfsmittel vollständig angegeben und die Stellen der Arbeit - einschließlich Tabellen, Karten und Abbildungen -, die anderen Werken im Wortlaut oder dem Sinn nach entnommen sind, in jedem Einzelfall als Entlehnung kenntlich gemacht habe; dass diese Dissertation noch keiner anderen Fakultät oder Universität zur Prüfung vorgelegen hat; dass sie - abgesehen von unten angegebenen Teilpublikationen - noch nicht veröffentlicht worden ist sowie, dass ich eine solche Veröffentlichung vor Abschluss des Promotionsverfahrens nicht vornehmen werde. Die Bestimmungen der Promotionsordnung sind mir bekannt. Die von mir vorgelegte Dissertation ist von Dr. Angela Hay betreut worden.

Köln, Juli 2017

_____

Evangelos Kouklas

Lebenslauf

Persönliche Angabe

Name: Evangelos Kouklas

Geburtsdatum: 26.02.1986

Geburtsort: Thessaloniki, Griechenland

Nationalität: Griechisch

Familenstand: Ledig

Ausbildung

Seit 2013 Doktorand-Promotion. Max-Planck-Institut für Pflanzenzüchtungsforschung, Köln Deutschland. Arbeitsgruppe von Dr. Angela Hay, Abteilung für Vergleichende Entwicklungsgenetik.

Oktober 2009 – Mai 2011 Master-Abschluss, Wageningen Universität und Forschungszentrum (WUR), Wageningen, Niederlande. Fakultät: Pflanzenbiotechnologie. Titel der MSc. (Haupt-)Arbeit: "Funktionelle Charakterisierung einer neuartigen bHLH-Transkriptionsfaktorfamilie während der *Arabidopsis*-Embryogenese". Betreuer: Prof. Dr. Dolf Weijers, Dr. Bert De Rybel und Prof. Dr. Sacco de Vries. Titel der MSc. (Zweit)-Arbeit: "Bau einer zytoplasmatischen Bibliothek von *Arabidopsis thaliana*". Betreuer: Dr. ing. Joost Keurentjes, Dr. Padraic Flood, Prof Dr. Hans de Jong.

Oktober 2005 – September 2010 Bacherlor-Abschluss, Universität von Thessaly, Volos, Griechenland. Fakultät: Agrawirtschaft, Pflanzenproduktion und Ländlichen Umgebung. Titel der BSc. Arbeit: " Geschlechtsbestimmung in Kiwipflanzen (*Actinidia deliciosa*) mit der Verwendung von RAPD molekularen Markern". Betreuern: Prof. Dr. Athanasios Mavromatis, Prof. Dr. Avraam Khah, Prof. Dr. Dimitrios Nanos. Abschlussnote: 7,28/10.